UNIVERSITÀ DEGLI STUDI DI MILANO

FACOLTÀ DI MEDICINA E CHIRURGIA

Doctoral Programme in Clinical Research

XXXVI cycle

MORPHOLOGICAL, MOLECULAR AND GENETICAL ASPECTS OF THE ORAL CAVITY IN COVID-19 DISEASE FOR DIAGNOSIS, SURVEILLANCE, AND TISSUE REGENERATION PURPOSES

BIO16

Tutor: Prof. Claudia Dellavia

PhD Coordinator: Prof. Massimo Del Fabbro

Candidate: Dolaji Henin

Identification number: R12828

Academic Year: 2022-2023

Table of contents

Abstract

The oral cavity often displays signs and/or symptoms of systemic conditions, some of which resolve without consequences, while others may leave sequelae. The present thesis connects the results from anatomical, biological and clinical investigations carried out during the COVID-19 pandemic, designed to describe various aspects of the involvement of the oral cavity in COVID-19's pathology, diagnosis and course. The aims of the research project were to i) assess the presence of SARS-CoV-2 in the oral cavity through molecular tests to validate Molecular Salivary Testing (MST) as a reliable diagnostic tool for COVID-19 surveillance; ii) study the morphological and immunohistochemical alterations occurring in the lingual tissues of COVID-19 subjects; (iii) investigate the genetic susceptibility to the infection; (iv) contribute to define the pathogenesis of the disease and (v) explore new methodologies such as the use of nanomaterials for regenerative purposes.

Salivary samples were analysed by MST concerning the presence of SARS-CoV-2 and compared to the gold standard, the nasopharyngeal swab. The findings from our study contributed to validate MST for diagnosis and surveillance in communities such as schools, where MST was employed first in 2020, to surveil 401 children and later in 2021 and 2022, with Dried Blood Spot test, to assess the immunological profile of a sample composed by school personnel. Further, the presence of the virus in the oral cavity was described by comparing by RT-PCR samples of lingual tissues from corpses of individuals with or without a history COVID-19. In the same sample, the morphological and immunohistochemical features of the lingual tissues following COVID-19 were investigated and an inflammatory pattern of the lingual gustatory and non-gustatory papillae was observed.

The genetic and phenotypical evaluation of the bitter receptor TAS2R38 was evaluated in patients with mild and severe COVID-19 and compared to healthy ones. No correlation between disease's severity and TAS2R38 expression was observed regarding disease's susceptibility and gene expression.

In a further development of the project, nanomaterials were studied to explore their regenerative potential as drug delivery systems and as targetable systems for oral tissues' repair processes. Nanofibers loaded with Hyaluronic Acid and Vitamin E (NFE) were produced and their effect on Human Gingival Fibroblasts (HGF) was evaluated. NFE induced HGF proliferation, adhesion, collagen cross-linking and reduction of collagen degradation, thus favouring collagen deposition in gingival connective tissue. Furthermore, molecular imprinted nanoparticles were tested on target cells, showing a good affinity. Considering the consequences of some systemic conditions on the oral cavity, among which the long-term consequences of COVID-19, known as Long-COVID, can be considered, nanofibers might be helpful in tissue regeneration procedures of the oral tissues, that we are currently investigating.

Personal preface

COVID-19 has been a major dramatic event that marked history and left essential signs in many people's lives. Critical challenges suddenly faced the whole world in many areas, specifically in the research field that, in a short and stressful time, had to provide solid and robust responses to a severe and urgent problem and with no supporting literature.

As oral healthcare workers and researchers, we had to face both clinically and academically the transmission and prevention problem of COVID-19. We addressed whether the virus was present in the oral cavity and how to take advantage of it. Hence, we started to work even in the very active phase of the pandemic, sometimes facing directly infected people to sample them, with fear but moved by a deep desire to help and a vast curiosity at the same time.

A great unpredictability and sudden changes characterised these three years of pandemic, so we had to adapt our research to these changes and variations. This thesis project, therefore, saw different adaptations, making planning timing and procedures difficult. Also, the dissemination of COVID-19 discoveries by our research group and other scientists has been dynamic and quick, given the urgent need to answer questions.

Today, three years later, I can affirm that this past period has represented a unique moment for my doctoral experience, allowing me to follow and deepen many clinical, biological and morphological aspects.

Introduction

The early pandemic scenario

In December 2019, Pneumonia broke out in Wuhan, Hubei Province, China, with an unknown aetiology. Many of the initial cases reported to have been exposed to Wuhan's South China Seafood Market, suspecting facts about potential transmission from live animals [1].

At the end of January 2020, WHO declared the severe acute respiratory syndrome coronavirus 2 (SARS-CoV-2) epidemic a public health emergency of international interest. In February, the disease was named COVID-19 (coronavirus disease- 2019). After the rapid spread of the infection, on March 11, WHO officially declared the novel coronavirus outbreak a pandemic.

All the countries that experienced increased infections acted to contain the outbreak. In Italy, the Lombardy region press office issued a list of cities in complete lockdown and around 100,000 people were affected by the travel restrictions.

At the end of March 2020, COVID-19 provoked more than 800,000 total confirmed cases and 40,000 deaths [2]. In the first months of the pandemic, predicting the outbreak's growth was confounded by the lack of available data, the unavailability of diagnostic reagents, changes in surveillance intensity and case definition and overstressed healthcare systems [3]. Initially, in Wuhan, the exponential growth rate of the outbreak was estimated to be 0.1-0.14/day with a doubling time of 6-7 days but lately, the CDC estimates the early growth rate to be 0.21-0.30 per day with a doubling time of 2.3-3.3 days [3].

As of March 2020, 74,386 cases were confirmed in Italy, and 7,503 deaths were reported[4].

Starting from 2020, Italy experienced one of the largest clusters in the world, with a high associated mortality rate, putting a strain on the country's economic and healthcare system [5–7].

The global strategies in response to COVID-19 have been [8]:

- Mobilise all sectors and communities in response to the problem and prevention.
- Control sporadic cases and clusters by preventing community transmission and quickly finding and isolating all cases.
- Contain community transmission through infection prevention and control measures.
- Decrease mortality by offering appropriate clinical care.
- Develop safe and effective vaccines and therapies.

No European country was able to control the transmission of COVID-19 effectively. Italy dealt with the emergency through a national healthcare service and 22 regional/provincial healthcare services. This heterogeneity did not provide uniform and clear guidelines and adequate organisational protocols and resources regarding diagnostic procedures, contact tracing, and therapies at the territorial and hospital levels.

Testing, tracing, tracking, and treating were critical elements of the strategy to contain an infection and aim to identify cases and close contacts as early as possible, thereby interrupting potential chains of transmission and providing appropriate care to the affected individuals. Close contact was defined as exposure, without personal protective equipment (PPE), to a COVID-19-positive individual in a confined space for more than 15 minutes and at less than 2 meters or through close physical contact [9]. Contact with the secretions of a COVID-19 case is also considered a high-risk exposure.

SARS-CoV-2 infection primarily spreads through the respiratory route by producing droplets and aerosols containing viral material by infected individuals. The clinical presentation varies widely: 20% of infected individuals are completely asymptomatic, while the majority have mild flu-like symptoms and characteristic symptoms such as

anosmia and ageusia [10]. 80% of symptomatic individuals experience a mild form of the disease, 15% develop a severe form of infection, and 5% develop a critical form. Only a small percentage of patients develop a severe form, but given the widespread infection, the absolute number of severely ill patients requiring respiratory support, prolonged hospitalisations in specialised wards, or intensive care had significant consequences.

From the beginning of the pandemic until January 2021, the number of positive cases worldwide was approximately 87 million, with nearly 2 million deaths, while in Italy, there were 2.2 million positive cases with 76,000 deaths [11]. Unfortunately, contact tracing was complex. As the number of cases increased, the ability to identify contacts tended to decrease.

In both the first and second waves, the healthcare systems of different countries tried their best to manage the emergency, often relying on the collaboration of citizens to voluntarily self-isolation when there was a simple suspicion of illness during peak periods. At some point, all countries resorted to extreme measures such as lockdowns, social distancing, and restricting individual mobility. Among the emergency measures, the closure of schools and limitations on the opening or access to various workplaces had a significant impact.

School closure

During the first wave, schools in Italy were closed in February and reopened in September. As cases increased, in-person classes were again suspended for students from the second year of middle school by late October and early November. Middle schools resumed in-person classes in early December for a brief period, while high schools never reopened until February 2021. In January 2021, measures included remote learning for all classes starting from the second year of middle school. Until the end of January 2021, only children aged 0 to 12 could attend school in person. Starting from February 2021, as infection rates decreased, all schools gradually reopened and remained open without further closures.

From September 2020 to September 2022, strict safety measures were requested when schools were open. These included mandatory mask-wearing, strict social distancing, and adherence to symptom management protocols outlined by the Italian National Health Institute[12].

The bad consequences of protracted school closure on learning impact and social interaction of disadvantaged children and teenagers well known. Various studies indicate that, in similar circumstances, the gap between students from disadvantaged families and those with favourable cultural and/or socioeconomic backgrounds significantly widened [13–15]. High school dropouts and increased educational poverty were evidenced in Italy after the lockdown periods [16]. Later, after the mandatory vaccination, schools gradually reopened in April 2021.

COVID-19 disease

Pathogenesis

Coronaviruses from the *Coronaviridae* family are known to be animal and human pathogens. In the past decades, coronaviruses infected humans after spilling over from animal reservoirs. In 2003, SARS-CoV originated in China, while MERS-CoV in the Middle East [17].

SARS-CoV-2, the causative agent of COVID-19, revealed to be a new form of Coronavirus. SARS-CoV-2 shares with SARS-CoV 79% of the genetic sequence. The viral RNA encodes structural, non-structural and accessory proteins, which are delivered into the human cell through an enveloped virion.

A coronavirus consists of an envelope (E), a membrane (M), a nucleocapsid (N), and a spike (S) protein. The spike protein forms projections externally, appearing like a crown and, therefore, the name of coronavirus [18].

The surface of the virion is characterised by the spike glycoprotein, which mainly determines the viral tropism [19]. The S protein is structured by two subunits: the S1 subunit, which binds the host entry receptor angiotensin-converting enzyme 2 (ACE2) and the S2 subunit, mediating the membrane fusion.

Wrapp et al. (2020) demonstrated that SARS-CoV-2 has a 10- to 20-fold higher affinity to the ACE2 receptor, compared to SARS-CoV, with a stronger affinity [20].

After binding to ACE2 on the target cell, the S protein is cut by the transmembrane serine protease TMPRSS2 [21–23]. This step activates the S2 subunit to fuse the viral and host lipid membrane, releasing the RNA in the cell. This one seems to be the most corroborated mechanism of virus penetration. Hence, the synergic action of the ACE-2 receptor and TMPRSS2 is essential for the entry of SARS-CoV-2 into the host.

The multiciliate cells in the nasopharynx or trachea and the sustentacular cells in the nasal olfactory mucosa seem to be the first targeted cells by SARS-CoV-2 during human infection. After the virus entry and protein replication, pattern recognition receptors can detect SARS-CoV-2 in the cytoplasm and initiate the signalling cascade to transcribe Interferon (IFN) I and III. IFN and Chemokines are also produced by epithelial cells, neutrophils and macrophages through the Toll-like receptors [24,25]. The cell responds to IFN producing IFN-stimulated genes, which have direct or indirect antiviral functions. Meanwhile, Cytokines promote the growth of B cells and T cells responses. If innate or adaptive responses do not clear the virus, it can spread to the lower respiratory tract via inhalation of viral particles or by dissemination along the tracheobronchial tree.

The initial site of infection can also be the lower respiratory tract. The infection and inflammation of the alveoli limit gas exchange. Many studies reported that alveolar type 2 cells seem to be primarily infected. Alveolar type 1 cells mediate gas exchange, while those type 2 secrete the pulmonary surfactant, reducing the surface tension during respiration in the alveoli[26–28]. Alveolar type 2 cells are also the precursor cells of AT1 in adults[29].

ACE2

The Renin-angiotensin-aldosterone (RAAS) pathway acts as a homeostatic regulator of vascular function. It controls blood flow, blood pressure, natriuresis and trophic responses to many stimuli. Renin released by macula densa upon low intra-tubular sodium concentrations converts angiotensinogen into angiotensin I [18]. ACE converts angiotensin I to angiotensin II (AngII), which has different effects according to which receptor is binding. AngII binding AT1 receptor promotes oxidative stress,

inflammation, fibrosis and vasoconstriction, while binding AT2 stimulates opposite effects. Chronic activation of RAAS is associated with AngII/AT1 with inflammation, apoptosis, and fibrosis[30].

ACE2 was individuated in 2000, and it converts AngII into Ang (1-7), and AngI to Ang (1-9). Ang (1-7) promotes vasodilation, antioxidation and antiproliferative effects. ACE2 also reduces the amounts of Ang II, which protects against inflammation and tissue damage.

The spike protein competes with AngII for ACE2, blocking ACE2 activity and reducing the enzyme expression, promoting RAAS imbalance, and mediating deleterious effects on the body.

ACE2 expression is detected in Alveolar type 1 cells, bronchial transient epithelial secretory cells, respiratory epithelial cells, myocardial cells, endothelial cells and artery smooth muscle cells, oesophagus epithelial cells, neurons and glia, tongue epithelial cells, stomach, cholangiocytes, adipose tissue, pancreatic exocrine glands and islets, renal proximal tubule cells, podocytes, bladder urothelial cells, testis (Leydig and Sertoli cells and spermatogonia), uterus epithelial cells, ovary and breast, maternal–foetal interface, enterocytes from ileum and colon, and rectum cells [18,31]. Zou et al. (2020) reported a connection between ACE2 expression and the potential organ risk of COVID-19 infection, defining a high-risk infection in tissues with a proportion of ACE2 >1%. ACE2 percentages expressed by different organs are reported below:

Lower Respiratory Tract (2%), Lung (> 1%), Heart (> 7.5%), Ileum (30%), Oesophagus (> 1%), Kidney (4%), Bladder (2.4%), Liver (<1%), Stomach (<1%)[30]. The low expression of ACE2 receptors in nasal and pulmonary tissues in young subjects compared to adults, may explain their non-respiratory clinical manifestations. In the oral mucosa, ACE2 is expressed in the epithelia of the tongue, lip and cheek[32].

Inflammation and SARS-CoV-2

In COVID-19, the inflammatory response is highly increased and operates through different mechanisms involving cytokines, in particular, IFNα and IFNγ and through thromboinflammation, in particular in COVID-19 patients, a high level of Factor VIII has been evidenced.

SARS-CoV-2 variants

The genetic code of SARS-CoV-2 underwent continuous mutations, resulting in the emergence and global circulation of various variants [33]. The Pango (Phylogenetic Assignment of Named Global Outbreak Lineages) is a nomenclature system developed in early 2020 to denominate the genetic lineages of the virus specifically [34]. Pango defines two major lineages, A and B, from which descend sub-lineages are named with a numerical value. Pango aims to define epidemiologically relevant phylogenetic clusters. Afterwards, the WHO label, based on the Greek alphabet (Alpha, Beta, Gamma, …), was introduced to facilitate public communications. The Alpha, Beta, Gamma, Epsilon, Eta, Iota, Kappa, and Lambda variants appeared in 2020, Delta, Mu and Zeta in the beginning of 2021 and Omicron in November 2021 [35]. CDC has categorised the virus variants according to their transmissibility, the severity of the disease, the neutralisation capacity by antibodies originating following previous infections or vaccination, the reduction of the efficacy of the treatments or vaccines and the failure of their diagnostic detection [36]. Therefore, variants were classified as "Variants being monitored" (VBM), "Variants of Interest" (VOI), "Variants of Concern" (VOC) and "Variants of high consequence" (VOHC) to identify the prime concern in the global monitoring and research. Alfa and Delta were included in the VBM with other variants (Beta, Gamma, Delta, Epsilon, Eta, Iota, Kappa, Zeta and Mu) as they were associated with more severe disease or increased transmission of the virus, but nowadays are no longer detected. In January 2022, the Omicron variant rapidly replaced Delta globally and was included in the VOC as it is highly transmissible, and the antibodies generated after vaccines or previous infections seemed not to prevent its infection. Omicron is considered 1.6 times more infectious than the Delta variant, with a risk of reinfection even in people who have recovered

from COVID-19. However, the variants caused less severe forms of disease than the original virus, most likely due to the integration of pharmaceutical protocols [37] and the introduction of vaccines worldwide [38].

Clinical characteristics

Transmission

The transmission happens *via* fomites and droplets during close and unprotected contact between an infected and un-infected subject [39]. The virus could spread from the infected person's nose or mouth through little droplets during sneezing, coughing, speaking, singing, or even breathing [40–46]. Another person can be infected if those little droplets are inhaled at a short distance (short-range airborne transmission) or if infected particles come in contact with the eyes, nose, or mouth [47]. Infected particles can range between 0.6 and 100 μm, and the number of droplets increases proportionately with the coughing rate[48]. Asadi et al. (2020) reported that pre-or asymptomatic subjects can produce a large quantity of particles smaller than 1 μm. Droplets can aggregate in nuclei according to size, ambient temperature, and humidity[49]. The transmission can happen through indirect contact. Early studies in Wuhan confirmed the aerosol transmission of SARS-CoV-2, suggesting airborne transmission in healthcare facilities due to aerosol produced by medical procedures[41].

Infection risk

Van Dorelaman et al. (2020) reported that SARS-CoV-2 is viable in the aerosol particles for at least three hours, maintaining their infectious power. Many mathematical models were initially proposed to quantify the infection risk [45]. Wells and Riley's model was the most widely used [50]. Their equation analysed the risk of infection based on infection and susceptible people in a space with a ventilation rate and quantity of infectious material in the air.

$$N_{\mathrm{c}} = S(1 - \mathrm{e}^{-Iqpt/Q})$$

Wells and Riley equation: (new cases infected (Nc), time (t), infective (I) and susceptible (S) people, space with ventilation rate, Q, m^3 /S, and quantity of infectious material in the air, q where the pulmonary ventilation rate of susceptible individuals is p m^3 /S

Wells-Riley equation, successful for measles outbreaks in schools, presented a few limitations, such as the assumption of a uniform distribution of aerosol particles through the space, which is not possible even with a good ventilation system.

Clinical manifestations

The incubation period lasts about 4-5 days before the symptom's onset[51]. The incubation period is variable and involves 25-40% of the viral transmission before the clinical signs[52].

Symptoms can last from 1 to 14 days, with different severity and generally include ageusia/dysgeusia, anosmia, fatigue, migraine, cough, fever, dyspnoea, muscle and joint pain.

Some individuals may experience gastrointestinal symptoms like diarrhoea and nausea. It's essential to note that symptom severity can range from mild to severe, with severe cases potentially leading to pneumonia or acute respiratory distress syndrome (ARDS) [53].

Mason et al. (2020) defined three stages of disease development [54]. The first step is the asymptomatic state, occurring the first two days after the infection: the virus binds to the nasal epithelial cells. It starts replicating, infecting primary ciliated cells, and then involving the conducting airways. No clinical manifestations are shown in this step despite the high infectious power of the virus. At this stage, the virus is detectable by the nasopharyngeal swab (NPS), and it is necessary to prevent the super-spreading phenomenon. In the second stage, the SARS-CoV-2 virus involves the respiratory tract proliferating through the conducting airways. Clinical manifestations of the infection are fever, cough, fatigue, sputum production, and headache. Less frequent dysgeusia, anosmia and gastrointestinal symptoms such as diarrhoea and vomiting may be shown. The third stage occurs in 20% of infected people with a pulmonary disease involving diffuse alveolar damage.

Symptoms have been shown to be milder in the recent variants, such as delta and omicron, however, with high transmissibility, even in vaccinated subjects. COVID-19 variants mainly affect the upper respiratory tract and their clinical manifestations include congestion, sneezing and mild sore throat. Symptoms such as dysgeusia and anosmia seem to be less common. Concerning the duration of the diseases, vaccinated people infected with omicron reported 6.87 days, compared with 8.89 days in delta variant [55].

Asymptomatic cases

However, in some cases, the infection is asymptomatic, and subjects do not experience symptoms throughout the infection. Asymptomatic cases can act as reservoirs of the virus and actively transmit the infection, contributing to the spread of the pandemic. The extent of transmission from asymptomatic individuals remains unknown [56].

COVID-19 and Oral Cavity

Oral tissues as viral target

The oral cavity is covered by a mucous membrane of stratified squamous epithelium. A stratified squamous non-keratinized epithelium covers the internal part of the lips, cheeks, floor of the mouth and ventral surface of the tongue. A stratified squamous keratinised epithelium characterised by the masticatory mucosa lines the hard palate and the gingiva. The dorsum of the tongue is covered by a specialised epithelium, containing nerve endings for general sensory and taste reception. The surface is bathed by saliva produced by major and minor salivary glands. The cellular and tissue heterogeneity of the oral cavity is assumed by Huang et al. (2021) to underline a non-uniform SARSCoV-2 infection across oral sites.

The Tongue

The tongue is a muscular organ characterised by a horizontal part, the body, located in the oral cavity, and a vertical one, the base, that articulates inferiorly with the hyoid bone. Between the two portions, a V-shaped line (sulcus terminalis) is interposed [57]. The mucosa of the ventral surface is smooth and thin, while the mucosa of the dorsum is thick, characterised by the presence of non-gustatory, filiform papillae (FLP) and gustatory papillae, circumvallate (VP), foliate (FP) and fungiform papillae (FGP), that cover the entire surface of the tongue from the sulcus terminalis to the tip.

FLP possess mechanical, tactile and thermal sensitivity, they cover the surface of the dorsum, and they are pyramidal shaped with a superficial cornified epithelium dressing a connective axis.

Gustatory papillae located on the lingual dorsum, have gustatory functions thanks to the presence of taste buds (TB), a goblet-shaped structure, with a 50 μm diameter, composed of 50-120 elongated cells: type I cells, 50-70% (dark-toned), glia-like cells, type II cells,15-30% (light-toned cells) acting as receptors, type III, 5-15% (presynaptic cells) transmit taste signals to sensory afferent fibres, and few type IV cells at the base of the structure [58–60]. Afferent nerve fibres transduce the gustatory stimulus.

FP are located postero-laterally along the lingual margins and are characterised by approximately 20 parallel rows of ridges and valleys. FPs are innervated by the glossopharyngeal nerve (IX) in the posterior portion of the lingual margin and by the chorda tympani (VII) in the anterior portion. VPs are located in the posterior third of the lingual dorsum following the sulcus terminalis. They are surrounded by a vallum, creating a sulcus around the papilla, which contains an average of 250 buds (50% of the tongue). VPs measure between 2 and 8 mm, and their number varies between 4 and 8 in humans. VPs are innervated by a large nerve fibre plexus originating from the IX cranial nerve. Demographical features such as sex, race, and age may influence the number and dimensions of VP [60]. FGPs are scattered on the surface of the dorsum of the tongue anteriorly to the sulcus terminalis and present a fungus morphology. Their number varies between 150 and 400, and their measure varies between 0.5 and 1 mm. FGPs are supplied by gustatory fibres of the chorda tympani. Considering extra-papillary sites, TBs are located in the wall of the epiglottis, oropharynx, soft palate, and glosso-palatine arch and are supplied by the Vagus nerve. Due to such a system's complexity and redundancy, taste disorders were usually uncommon, until the COVID-19 era.

Salivary glands

Salivary glands are exocrine glands producing and secreting saliva into the oral cavity. They are categorised in major and minor, according to their size. Major glands include parotid, submandibular and sublingual glands. The minor salivary glands line the oral mucosa and are scattered throughout the oral cavity[61].

Saliva

Saliva is a clear mucoserous exocrine secretion. The secretion of saliva occurs from salivary glands: parotid, sublingual, submandibular and accessory glands. It is a mix of fluids from salivary glands and gingival crevicular fluid. Saliva has many functions, which can mainly be categorised as follows: lubrication and protection, buffering action and clearance, maintenance of tooth integrity, antibacterial action and taste and digestion. Saliva is composed of various electrolytes (Na, K, Mg, Ca, $HCo3^-$. $PO4^{3-}$) and also contains immunoglobulins, proteins, enzymes, mucins, urea and ammonia. Saliva is a versatile fluid employed in research for local and systemic disease diagnosis, treatment and prevention. Nowadays, saliva is attracting the researcher's

interest in the diagnostic field, but especially in the screening field, being the salivary sample easy to collect, non-invasive and rich in biological information. Saliva can be analysed for emotional, hormonal, immunological, and nutritional and metabolic influences[62]. The presence of biomarkers in the saliva allows disease diagnosis. However, the low concentration of analytes found in saliva compared to blood (100 to 1000-fold lower) is a barrier to making it a first diagnostic choice [63].

SARS-CoV-2 infection of the oral cavity

The cellular and tissue heterogeneity of the oral cavity is assumed by Huang et al. (2021) to underline a non-uniform SARSCoV-2 infection across oral sites. The authors used single-cell RNA sequencing datasets to analyse 50 cell clusters from salivary glands and gingiva [64]. They found that multiple epithelial cell subtypes are susceptible to infection.

However, since the outbreak of the pandemic, the oral cavity has been minimally considered in COVID-19 pathogenesis, considering it as a passive transfer for viral transmission from the respiratory tract. Marchesan et al. (2021) hypothesised the presence of an oral-systemic axis concerning COVID-19, which involves and inter-connects the lungs, nasal cavity, and oral cavity[65]. Offenbacher, in 1980, defined a bidirectional relationship between oral and systemic health, suggesting that the oral cavity could serve as a source of transient bacteriemia and a low-grade systemic inflammation[66]. In fact, the oral microbiome can be distributed more commonly along the respiratory and gastrointestinal tract. However, whether the oral microbiome can influence distant sites is still unknown.

Critical issues concerned whether the oral symptoms in COVID-19 patients were due to a direct SARS-CoV-2 infection or were the manifestation of systemic inflammation. In this scientific scenario, the infectious role of saliva became relevant.

Oral symptoms

Dysgeusia

One of the symptoms most reported by patients is dysgeusia, often coexisting with anosmia, occasionally not discernible from one to another. Taste and smell impairment was commonly reported as an initial symptom.

Ageusia is the loss of the ability to taste, while hypogeusia is a partial loss. Dysgeusia indicates a generic alteration of the sense of taste [67].

Various mechanisms have been proposed as potential causes of the taste impairments associated with COVID-19. Although taste and smell are strictly connected, and taste and olfactory dysfunctions are often concomitant, they seem to have different origins rather than dysgeusia being a consequence of anosmia, also considering that dysgeusia appears to be more frequently reported than anosmia. The hypothesised mechanisms of COVID-19 dysgeusia include (i) damage of the cranial nerves responsible for gustatory transmission, especially cranial nerve VII impairment due to the initial viral colonisation of the nasopharynx structure that eventually reaches the middle ear; (ii) zinc level reduction in COVID-19 patients as zinc is involved in the gustatory function; (iii) SARS-CoV-2 interaction with sialic acid receptors as sialic acid is involved in the taste processing pathway; (iv) direct damage of the oral tissues as taste buds and salivary glands have been proven to have an ACE2 expression [68].

Being ACE2 largely expressed in many structures such as the Vagus nerve, the ventrolateral medulla, the solitary tract nucleus, the nigra substance, the ventricles, the middle temporal gyrus, the olfactory bulb, and the motor cortex and posterior cingulate, dysgeusia was hypothesised to be caused by a central or peripheral nervous dysfunction [69,70]. Autopsies examinations of COVID-19 cadavers showed brain injuries and the presence of viral RNA in the tissues. Elmakaty et al. (2022) evidenced the presence of SARS-CoV-2[71]. Two main mechanisms were hypothesised, the former consists of a hematogenous pathway. SARS-CoV-2 could pass the blood-brain barrier, infecting the cerebral vascular endothelium. The latter hypothesised a neural pathway, in which the virus travels through the olfactory and the trigeminal nerves. Another theory supports the neurotropism of SARS-CoV-2, which could directly

infect the cranial nerves responsible for transmitting taste (VII, IX and X). Also, olfactory dysfunction may cause dysgeusia [72].

Xerostomia

Saliva secretion is commonly impaired after COVID-19, ACE2 and TMPRSS2 are highly expressed in the ductal and acini epithelium in the salivary glands, both mucous and serous [73]. The virus could enter inside epithelial cells through the ACE2 receptor leading to acute sialoadenitis, with a subsequent reparation through fibroblast proliferation and connective tissue formation. However, fibrosis of the salivary gland duct could cause a diminished salivary flow in patients after healing. Many patients reported Long COVID manifestations concerning hyposalivation and dry mouth sensation [74]. Chen et al. (2020) reported a 46% prevalence of xerostomia in patients infected with SARS-CoV-2, with an equal distribution among male and female subjects[74]. Xerostomia patients also experience various symptoms such as a burning feeling, dysgeusia, angular stomatitis, and dysphagia[75,76]. Many authors reported cases of parotitis and sialoadenitis [77–79].

Oral mucosal lesions

Oral mucosal lesions were observed in 20% of COVID-19 patients. A sample of 666 patients was examined in Madrid (Spain), and 25.7% of them evidenced several mucocutaneous manifestations such as lingual papillitis, glossitis, aphthous stomatitis, mucositis, burning sensation and dysgeusia. Iranmanesh et al. (2020), reported in a critical review that the most common oral region involved during SARS-CoV-2 infections were the tongue (38%), labial mucosa (26%) and palate 22(%) and with the following clinical diagnosis: herpetiform lesions, aphthous stomatitis, candidiasis, vasculitis, Kawasaki-like, mucositis, EM-like, necrotising periodontal disease, angina bullosa-like, drug eruption, angular cheilitis, atypical Sweet syndrome and Melkerson-Rosenthal syndrome [80]. Iranmadesh also reported a symptomatic manifestation in 68% of the cases[80]. Cruz Tapia et al. (2020) reported in 4 patients with COVID-19 vascular disorder, angina bullosa hemorragica-like lesion, and nonspecific stomatitis; in one patient, histological analysis proved perivascular reactive lymphocytic infiltrate, focal capillary thrombosis, and haemorrhage[81].

Diagnostic tests

The characteristics a diagnostic test should have

A*ccuracy*

Different statistical measurements can quantify the accuracy of a test.

The most important are sensitivity, specificity, predictive value, and reliability. The sensitivity of a test is the probability that a sick person will test positive, while the specificity is the probability that a healthy person will test negative. A high sensitivity test will have a high probability that a sick subject will test positive and a low probability of testing negative. In contrast, a high specificity test will, therefore, have a high probability that a healthy subject will test negative and a low probability of being positive [82].

$$Sensitivity = \frac{\text{TRUE POSITIVES}}{\text{TOTAL OF SICK INDIVIDUALS}}$$

$$Specificity = \frac{\text{TRUE NEGATIVES}}{\text{TOTAL OF HEALTHY INDIVIDUALS}}$$

The predictive value is an index of the probability that a positive subject to a diagnostic test is ill. Therefore, there is a positive and negative predictive value in the same way. The predictive value, however, does not indicate the goodness of a test but is closely related to the prevalence of the disease in a population.

Reliability or Cohen's κ is a statistical index that measures the grade of agreement between a test and a commonly used test. It is a value between -1 and +1 and quantifies the degree of agreement attributable to chance [82].

Safety and practicality

A diagnostic test should also have characteristics that make it a practical and applicable object:

- Safety for the operator for the collection and processing of biological material.
- Affordability, being inexpensive to be performed for mass screening and to be accessible to the general population.
- Practicality and flexibility of execution, not needing to be performed in organised structures or with specific tools.
- Simplicity, meaning that it's not operator-dependent and does not depend on the probability of finding the virus in a specific anatomical region.
- Availability on the market.
- Speed of execution.

Diagnostic tests available for the detection of SARS-CoV-2

There are three main types of virus detection methods based on the target being investigated[83]:

- Tests for the research of the presence of viral RNA, are molecular investigation techniques that use Real-Time RT-PCR, a technique of amplifying viral genome sequences.
- Test for the detection of viral antigens present on the surface of proteins.
- Test for the detection of antibodies generated against SARS-CoV-2 (not diagnostic)

Test for the detection of viral RNA

The detection of the viral RNA is the technique generally used for diagnosing viral pathologies and was largely used for MERS and SARS-CoV epidemic. It is performed by amplifying the nucleic acids using the reverse transcription polymerase chain reaction (RT-PCR) [84].

Other amplification-based methods are being utilised alternatively to RT-PCR for SARS-CoV diagnosis, such as digital-PCR and isothermal amplification-based assays. To date, RT-PCR is considered the standard for SARS-CoV-2 detection. The development of RT-PCR assays for a new virus requires the sequencing of the viral genome. Thus, numerous RT-PCR assays have been developed sequencing different

genome portions. The different sequencing yielded different sensitivities for the same test [85].

There have been many attempts to develop a valid protocol with good sensitivity and specificity, examining different portions of the viral genome and samples. Some authors in the first pandemic wave attempted to test sample pools to detect the virus, such as faeces.

However, RT-PCR presents different weaknesses in analytical and preanalytical aspects. The probability of achieving false negative results using this method is about 100% on the first day after infection and decreases around the third day to 38% to increase again[86]. Furthermore, a correct interpretation of the RT-PCR is essential since the positivity of this test does not necessarily indicate the subject's infectivity: there are many cases of positive RT-PCR even after the resolution of the symptoms.

The RT-PCR technique has numerous limitations associated with the availability, costs and the need for personnel trained in the use of laboratory equipment. Therefore, cheaper, faster, and more practical diagnostic tools were needed in such a great pandemic.

Molecular Naso-pharyngeal swab (NPS)

The NPS currently constitutes the gold standard test, the choice method for the identification of symptomatic and asymptomatic positive subjects.

The biological material is collected from the upper airways by a cotton swab, rubbing on the respiratory mucous membranes. The test is performed both through the nasopharyngeal and the oropharyngeal route.

NPS is currently the most reliable and recognised method for detecting the Virus in suspected or screened subjects. However, its execution requires facilities and tools, adequate biological safety measures, trained laboratory technicians and significant economic costs. Important issues concern the safety of health personnel collecting biological material[87].

Different factors can cause the risk of obtaining a false negative:

- Bad sample quality
- Sample collection obtained in an advanced stage of the disease
- The sample was taken from a compartment where the virus was absent
- Inappropriate handling of the sample
- Technical reasons related to the test or mutations of the Virus (WHO)

Molecular salivary test (MST)

The sample is analysed with RT-PCR in the same way as NPS. The molecular salivary test requires the direct collection of the saliva produced by the major salivary glands or the collection of the *sputum, a* respiratory secretion produced from the posterior oropharyngeal region.

The collection of the posterior oropharyngeal saliva allows the examination of both bronchopulmonary and nasopharyngeal secretions,+ as reported by many authors.

Tests for antigenic research (rapid tests)

In the past urgent situation, antigenic tests have been developed as rapid tests, which can be performed in out-of-hospital settings, designed to directly detect the proteins of the SARS-CoV-2 virus produced by the replication of the virus in respiratory secretions. The target analyte of the test is the nucleocapsid protein of the virus, abundantly present in nasal secretions. The test is performed through a kit without needing reagents, machinery, special structures, or personnel and can also be performed by non-healthcare workers. This test suffers from a poorer sensitivity and specificity compared to the ones PCR processed. The FDA recommends performing repeat testing indeed. The serial testing, following a negative result, to reduce the risk of false negative results, even in asymptomatic cases, should be three negative results for those without symptoms and 2 for symptomatic subjects [88].

Several studies reported that the antigen test compared with NPS varied in sensitivity from 0 to 94%, always maintaining a specificity higher than 97%. The rapid throat swab seems to be very effective in patients with high viral load which usually appears in the pre-symptomatic (1-3 days before the onset of symptoms) and in patients in the early symptomatic stages (first 5-7 days) [89].

Despite the performance limitations, the Ag-RDTs could play a significant role in patient management in public health decisions and virus surveillance if adequately executed and interpreted.

Serological test: quantitative and qualitative

The serological test investigates the presence of antibodies directed against SARS-CoV-2 in the body. In response to an infectious stimulus, the immune system forms antibodies detectable in the blood, plasma, and serum. Antibodies are specific against a particular pathogen; in this case, they are specific against the SARS-CoV-2 virus, and their presence can be used to diagnose different pathogens. Three types of antibodies are created in response to the infection: IgA, IgG and IgM, whose levels vary throughout the disease stages. IgG levels are often investigated because they most persist inside the body, and their presence reflects long-term immunity, even if they are the last antibodies to be created during infection. Many tests investigate both the presence of IgG and IgM. The level of IgM, detectable 4-5 days after infection, rises quickly with the onset of the disease and declines at the same time as resolution. Alternatively, many tests combine IgA and IgG or all three antibodies to each other. Rather than IgG and IgM, IgA seems detectable in the blood earlier, in the first two days after contagion.

The serological test can be performed in the laboratory or rapidly through the immuno-chromatographic test. Laboratory tests can be qualitative, detecting the presence or absence of Ig or quantitative, performed by immune-enzymatic techniques (ELISA) or indirect immunofluorescence (IFA).

The rapid test is based on immune-chromatographic technique and is performed through devices similar to pregnancy tests. A small amount of blood, about one or two drops, is required to be placed on a strip, and the result is ready within 10-15 minutes by the appearance of visible lines.

However, the rapid test is less accurate than the one performed in the laboratory. Serological testing can help diagnose suspected SARS-CoV-2 infection in symptomatic patients when the molecular test has failed, to determine whether a

person has encountered the virus and developed an immune response. For its simple execution, it can also be used as a screening test.

The collection and handling of the sample in the case of laboratory tests is less risky for the operator and can be performed in numerous analysis laboratories throughout the territory. However, the test performance is limited because antibodies are not detectable in asymptomatic subjects and in the early stages of infection. Serological diagnosis can be made after a large and heterogeneous seroconversion phase, at least 21 days after symptoms onset. Another significant disadvantage is the low sensitivity of the test.

Dried Blood Spot

Dried Blood Spot (DBS) is a technique using a drop of capillary blood dried on a filter paper to analyse through ELISA a ratio value of sample absorbance over a calibrator, classifying the sample as negative (<0.8), inconclusive ($\geq$0.8 and <1.1), and positive ($\geq$1.1). DBS has proven useful as a non-invasive self-sampling methodology for detecting SARS-CoV-2 type G immunoglobulins (IgG)[90]. Amendola et al. (2021) reported that DBS is an acceptable alternative to plasma/serum for SARS-CoV-2 IgG detection, describing a significant concordance between the two tests, from samples collected from 52 Health Care Workers[90]. Morley et al. (2020) highlighted in their work a 98.1% sensitivity and 100% specificity of DBS, compared to matched serum samples [91].

Vaccines

Since 2020, different vaccines against SARS-CoV-2 have been developed, and vaccine campaigns have been integrated over time[92].

Vaccines can be classified as whole virus vaccines (WVV), subunit vaccines (SV), viral vector vaccines (VVV) and gene vaccines (GV). The WVV include inactivated vaccines and live-attenuated vaccines, consisting of virus particles grown in culture and then killed or weakened, in order to stimulate the immune response by humoral immunity. The SV contains only a selected antigenic part of the virus. The VVV are made by a modified version of the virus to deliver the genetic material. Examples of VVV are Ad26.COV2.S (Janssen (Johnson & Johnson) and AZD1222 (Oxford/AstraZeneca, UK). The GV use a specific antigen-coding DNA or mRNA sequence into the organism cells to induce the immune response, such as mRNA-1273 (Moderna, USA) and BNT162b2 (Pfizer/BioNTech)[93].

In Italy, the first available vaccine, BNT162b2 was introduced on December 21, 2020, and was initially reserved for health workers, then extended to the population> 80 and eventually offered to the whole population. The Moderna vaccine followed shortly (early January 2021), with the same targets.

AstraZeneca at the beginning of 2021 was released for the adult population (18-55 years). After few months the target population was changed because of thromboembolic complications and later was completely abandoned. The school staff received AstraZeneca for the first and second doses, while for the third Pfizer or Moderna. The evidence regarding the durability and efficacy levels of these vaccines remains limited [94], nevertheless, Monforte et al. (2022) reported milder symptomatology of hospitalised vaccinated subjects compared to the un-vaccinated ones [94].

Nanomaterials and drug delivery systems

A drug delivery system (DDS) is a device or a formulation carrying drugs or molecules to the tissues with adequate posology and in a targeted manner, reducing adverse effects and improving patient compliance. These technologies could be tablets, or injectables like vaccines. Polymer vehicles have significantly advanced as DDS.

Nanofibers

Nanofibers (NF) are fibres synthesised in nano-scale size, from a wide range of materials, with 3D structures and functionalised surface properties. Nanofibers can be manufactured through the electrospinning technique through a high electrical voltage applied to a polymer solution. The electrospun fibres are obtained in different forms, and sizes. Fibers could be spun as a yarn, membrane or scaffold [95,96].

The excellent thermal, mechanical, chemical and morphological properties make nanofibers ideal for biomedical applications: scaffolds for tissue engineering and antimicrobial devices such as mask filters. The 3D nanostructure can be loaded with proteins, enzymes, and drugs to create biologically active devices that deactivate microorganisms. Nanofibers are easily loaded with several types of molecules, including antibacterial and antiviral agents, in accordance with many studies[97,98]. The release of the loaded molecules can be controlled, meeting the different clinical needs. The prolonged substance release is allowed because the nanofibers, made of biodegradable polymers, break down gradually and in a regulated way. Factors influencing the substance release from NF are the hydrophobicity and the thickness of the fibres. It is also possible to extend the molecules release using core-shell nanofibers made by numerous molecules-loaded layers and an external polymer layer acting as a rate-controlling barrier.

Molecularly Imprinted Polymers (MIPs)

Molecularly Imprinted Polymers (MIPs) could be promising polymeric carriers.
The molecular imprinting allows the production of clever polymers able to recognise a specific target. MIPs present several advantages, such as high stability even in

extreme environmental conditions (pH, temperature, pressure), ease of preparation, cost-effectiveness, drug loading and enantioselectivity. MIPs are prepared following a template made by the targeted molecules, used to produce a complementary binding region through the polymeric matrix[99].

After the polymerisation process, the template is extracted, forming a cavity that matches the template in terms of size, shape, and chemical properties. This cavity is capable of recognising the template's spatial characteristics and can rebind with the template when needed (Fig.1). Thus, MIPs are able to identify their targets with a high sensitivity. The molecular imprinting can be applied to a wide range of targets from small molecules to peptides, proteins and cells. MIPs hence have potential applications as therapeutic agents as they bind targets with an equivalent specificity to antibodies[100].
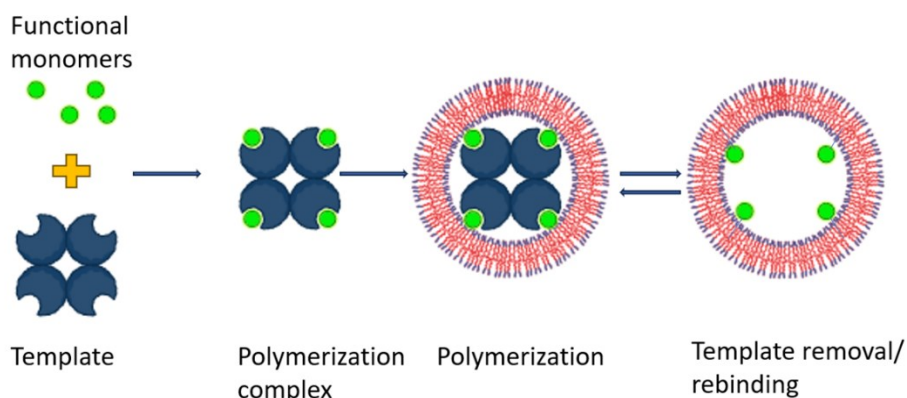

Fig.1 Graphic representation of the the process of molecular imprinting. This image was created with *Biorender.com.*

Nanotechnologies to fight COVID-19

Part of the strategy to fight the virus was to create many devices for individual protection, mainly facial masks. Many researchers took up the work on the improvement of face masks, concerning design and development through appropriate material, aiming at producing multi-functional masks, with different characteristics,

such as reusability, lightweight, comfort and face adaptability. Traditional facial masks, especially at the beginning of the pandemic had many limitations:

- inability to inactivate the virus;
- discomfort for those who is wearing it;
- imperfect adherence to the face, allowing little droplets to pass through the mask;
- slipping caused by the head movement.

Electrospun nanofibers have been explored mainly for their air filtration applications. The high surface-to-volume ratio, the low resistance and the high filtration performance make nanofibers ideal for healthcare air filtration. The incorporation of antimicrobial agents with nanofibers for filter production is known to possess antimicrobial properties. Neeta et al. (2007) reported the antimicrobial activity of polyvinyl chloride and polyacrylonitrile nanofibers containing Silver nanoparticles[101]. Muniz et al. (2023) produced a filtering electrospun membrane loaded with biocidal agent from polyvinyl alcohol nanofibers loaded with benzalkonium chloride, resulting biocidal against *E. Coli*, *S. aureus* and SARS-CoV-2 (HCoV-229E)[102], proposing it for facial mask design.

Additionally, nanomaterials, compared with traditional small molecules or antibodies, offer drug developers virus binders, cell-membrane decoys and viral-envelope inhibitors. During the pandemic, many researchers put their efforts to use nanotechnologies to fight SARS-CoV-2. Specifically, Pfizer-BioNtech and Moderna vaccines were both lipid nanoparticle-based, carrying mRNA into cells.

Nanoparticles are also a promising vehicle for small antiviral agents. Nanoparticles were also designed to be a therapeutic tool rather than just a carrier for drugs, attempting to make them bind to the virus directly[103]. Antiviral materials target chemically and physically many types of viruses differently from the traditional specific antiviral therapies. Sigl et al. (2021), described a "programmable icosahedral canvas for the self-assembly of icosahedral shells" that have viral trapping and antiviral properties [104]. Those block products obtained from DNA assembly have internal cavities up to 280 nm. Zhang et al. (2020) reported cellular nanosponges made of plasma membranes from human lung epithelial type II cells, presenting SARS-CoV-2 entry receptors and able to decoy the virus [105].

Many "nano-strategies" are still in development, even after the COVID-19 emergency is gone, because of the need to prepare for future possible viral pandemics. Many funding programs are thus supporting new research to be ready with solutions for emerging viruses.

Among nanotechnologies, MIPs were also described to be able to recognize small virus particle. In fact, those kinds of MIPs are generally prepared using viral particles as templates. Parisi et al. (2021) described MIPs against SARS-CoV-2 as able to inhibit in vitro the virus infection, creating the idea of "monoclonal type" antibodies able to recognise the virus and to block its binding to ACE2[106].

MIPs were largely investigated to produce sensors able to detect the presence of SARS-CoV-2. This MIP-diagnostic is based on the recognition of the spike-protein using the receptor-binding domain as a template[96].

Aims of the thesis project

The aims of the present project were to

- Assess the presence of SARS-CoV-2 in the oral cavity through **molecular** tests to validate the Molecular Salivary Test (MST) as a reliable **diagnostic** tool for COVID-19 **surveillance** of fragile and controlled settings.
- Explore new methodologies for the use of nanomaterials for **regenerative solutions**, starting from
    - The **morphological and immunohistochemical** alterations occurring in lingual tissues of COVID-19 subjects;
    - The investigation of the **genetical** susceptibility to the infection;
    - The definition of the **pathogenesis** of the disease.

The validation of the Molecular Salivary Test (MST)

Background

The Nasopharyngeal swab considered the gold standard for virus detection, presented several disadvantages and limitations, especially for its invasiveness and tolerability among fragile individuals. SalivaDirect™ protocol developed by Vogels et al. (2020) demonstrates the reliability of saliva as a sample for COVID-19 diagnosis[87].

Aim

The present work aimed at optimising a protocol for saliva collection, able to guarantee a correct self-sampling or caregiver-guided sampling, designed for fragile subjects such as children.

Methods

The optimisation of the protocol

The FDA emergency approved SalivaDirect ™ protocol of Yale University, based on the use of saliva as a sample for COVID-19 diagnosis. Our research group optimised the sample collection method to allow a correct self-collection of the saliva. This method uses a sterile cotton roll kept under the tongue close to the Wharton duct for two minutes and in the lower vestibular space for two minutes. The cotton roll properly soaked is preserved in a sterile 50 ml tube. Saliva is recovered through a sterile syringe squeezing the roll. Saliva is then processed as recommended by Vogels et al. (2020) [87], with a modification of the thermal cycler profile: 5′ at 95 °C followed by 5′ at 4 °C. from which 5 μl were used for qPCR. N1 (FAM, BHQ-1 labelled probe) and RP (Cy5, BHQ-1) primers/probes as described by the protocol of Centers for Disease Control, were used [107] with Applied Biosystem 7500 Fast instrument. Samples were considered positive upon detection of N1 (Ct<40). Invalid samples were assessed by RP (Ct>35).

Comparison with the Nasopharyngeal Swab (NPS)

This work aimed to test the reliability of MST, comparing it with the gold standard NPS, in both a sample of adults and children. The concordance between the two tests was assessed using the Kappa statistic (Cohen's unweighted Kappa, k). In table 1 are described the values of k (Tab.1).

k value	Concordance
0	poor
0.01 < k < 0.20	slight
(0.21 < k < 0.40)	Fair
0.41 < k < 0.60	Moderate
0.61 < k < 0.80	Substantial
0.81 < k < 1.00	Almost perfect
k=1	Perfect

Tab.1 Values of Cohen k and the correspondent concordance.

This part of the project was conducted in accordance with the recommendations of the Comitato Etico Interaziendale Milano Area A, protocol approval numbers N. 31554 (adults) and N. 0050308 (children). All subjects/caregivers gave written informed consent in accordance with the Declaration of Helsinki.

The reliability of the method was first tested on 192 adults in the San Paolo Hospital in Milan and later, the two tests were coupled in a paediatric sample, analysing 109 children[108].

Results

The present work allowed the production of a scientific publication[108].

First, 192 adults were tested, with ages ranging from 18 to 85, 52.2% were female.

The concordance between MST and NPS resulted in a 0.85 concordance and a k=0,69. The concordance increased in asymptomatic subjects with a 0.96 concordance and k=0.83, indicating almost perfect concordance.

Later, the two tests were coupled in a paediatric sample, analysing 109 children, (age: 0-17, 46.4 % females). The concordance resulted in 0.94 with a k=0.81.

COVID-19 surveillance of fragile and controlled settings

Surveillance of two primary schools in Milan (2020-2021)

Background
COVID-19 outbreak was faced through many urgent interventions, such as school closure, with no evidence that it could reduce SARS-CoV-2 transmission.

Aim
The part of the project aimed at surveilling the children of two primary schools weekly through the Molecular Salivary Test.

Methods
A school surveillance program started in November 2020 in two primary schools in Milan (Italy) and was conducted for 6 weeks. The principal informed by email the pupils' families and teachers by email about the project design. Participation was voluntary. The study was conducted in accordance with the Declaration of Helsinki and was approved by the Ethical Committee (C.E Interaziendale Milano Area A, N. 0050308).

All the participants/ legal guardian signed an informed consent, according to the Declaration of Helsinki. All the participants school students and teachers) received detailed information on how to collect saliva (Fig.2) [109].
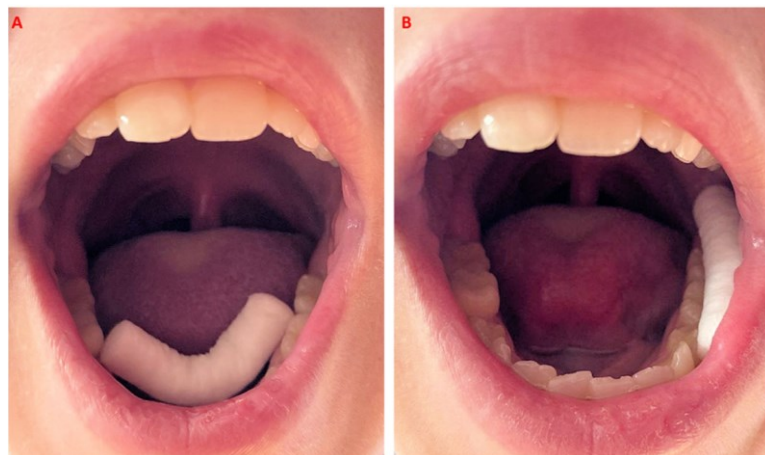

Fig.2 Picture showing the cotton roll, A) positioned under the tongue beneath the Warton duct and B) in the lower vestibular space to correctly collect the salivary sample.

The saliva collection was first guided by the research group at school and then an explicative movie was administered to the participants.

After vaccines were given to the adult's population, our research group decided to surveil a school staff introducing a new test to detect the SARS-CoV-2 IgG using a semi-quantitative method, the dried blood spot (DBS).

Results

The results of this work were published by Carmagnola et al. (2021)[109].

The study was conducted for 6 weeks and surveilled 401 children (mean age 8, 6 to 11, 49% were female) and 12 teachers.

	T1	T2	T3	T4	T5	T6
Total adhesions (2 schools)	333	361	373	389	401	401
Analysed (%)	203 (61)	271 (75)	290 (77)	297 (76)	310 (77)	248 (64)
Not detectable MST %	8	11	11	9	11	8
Positive MST (%)	1 (0.5)	2 (0.7)	2 (0.7)	0 (0)	0 (0)	0 (0)

Tab 2. The table shows the number of participants for each time point, the percentage of analysed sample, the not detectable ones and the positive for SARS-CoV-2 detection.

At the beginning of the study, two classes were in quarantine and were released after 14 days, therefore we can appreciate a higher number of participants after the first two weeks of surveillance. The last week of the surveillance corresponded to the last day before the Christmas vacation and many families anticipated their departures to their holiday location due to a stay-at-home measure announced by the Italian government.

Overall, 1619 MSTs were analysed during the surveillance period. The 10% of the samples were not processable due to the inadequate amount of saliva collected by the cotton roll (Tab.2).

During the study, 5 positive children in 5 different classes were detected (one in the first week, two in the second week and two in the third week). All the teachers resulted always negative. Any positive symptoms did not underline the positive MST results. The 5 classes were quarantined after these finding.

COVID-19 monitoring of school personnel through Molecular Salivary Test and Dried Blood Spot (2021-2022)

Background

The vaccinal plan started in December 2020 and first was addressed to healthcare workers and fragile subjects, such as immunocompromised and old individuals. In March 2021, school personnel underwent vaccination, and students not vaccinated were admitted to school. In this period, the response to the vaccines and the effects of non-strict contact between vaccinated and non-vaccinated individuals still had to be investigated.

Aim

This study aimed to test the validity and efficacy of the association of MST and DBS for communities' surveillance by investigating the immunological profile of a group of school staff during and following the phases of COVID-19 vaccine introduction and administration.

Methods

This school surveillance program was set in a school in Milan composed of 813 pupils (6 to 18 years), 103 teachers, 21 administrative staff and janitors, targeting only the vaccinated adults since the children at the time were not allowed to receive vaccination.

Therefore, the criteria for being included in the study were the following:

- Age 18-65 years
- Being vaccinated with Astrazeneca

Participation was voluntary. The study was conducted according to the Declaration of Helsinki and was approved by the local ethical committee (UNIMI- Number 108/20, 17/11/2020). Participants were requested to fill out and sign the informed consent.

The study lasted for 14 months, from April 2021 to June 2022. Figure 3 illustrates the timeline of the study that followed the present scheme:

- T1, W1: collection of MST and DBS samples (1 month after the first vaccine dose)

- W2-W6: weekly collection of MST samples + collection of DBS on T2, W6
- T3: collection of MST+ DBS samples (1 month after the second dose)
- T4: collection of MST+ DBS samples (4 months after the second dose)
- T5: collection of MST+ DBS samples (7 months after the second dose)
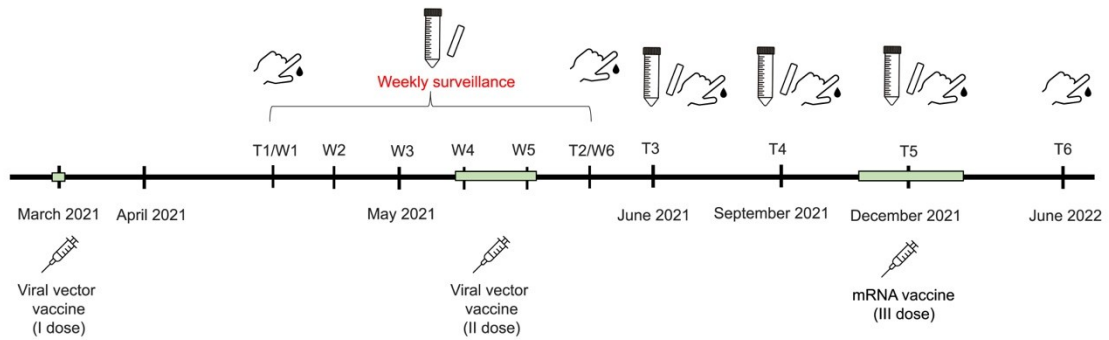- T6: : collection of MST+ DBS samples(1 year after T3)

Fig. 3 Timeline of anti-SARS-CoV-2 vaccinations and sample collection during the surveillance period from March 2021 to June 2022.

In the period from W1 to W6, participants provided weekly their MST samples to individuate rapidly COVID-19 cases, as reported by the CDC, between the two doses the immunity could not have been obtained yet [110]. The program timeline was set according to the school's logistical needs, such as holidays and school breaks, since at the time defined guidelines about the correct surveillance timing were not available.

Before T1, the COVID-19 and vaccination history of the participants was investigated through a questionnaire. Participants also received instructions for the self-collection of both samples. At T6 a second questionnaire about the recent COVID-19 history was administered.

Samples collection

Each participant received a pouch with a tube containing a dental roll for saliva collection and a Guthrie card with a lancing device for DBS collection. On scheduled days, saliva was self-collected according to Borghi et al. (2020) protocol [108]. DBS was self-obtained by applying capillary forefinger blood, obtained by a lancet needle, on a Guthrie Card [90]. The samples were placed back in the pouch and taken to school, where they were collected and delivered to our lab for analysis.

Molecular investigation

The molecular analysis of MST samples was performed using a Real Time RT-PCR according to the protocol of Borghi et al. (2020).

Serological investigation

DBS samples were considered adequate if at least one circular spot (4.76 mm diameter) was fully blood-soaked. Disks were punched out of the card and incubated for 1 hour at 37 °C in 250 µL of ELISA Sample Buffer (Euroimmun, Lübeck, Germany) to elute antibodies from the paper. Eluates were analysed for anti-SARS-CoV-2 IgG using the semi-quantitative anti-SARS-CoV-2 ELISA test (Euroimmun, Lübeck, Germany), following the manufacturer's instructions. A ratio value was calculated as the sample's absorbance ratio to the calibrator's absorbance value (ODs/Cal). The ratio value was interpreted as follows: <0.8 negative, ≥0.8 to <1.1 borderline and ≥1.1 positive. Samples collected from subjects who provided at least 3 samples out of the 6 requested were also analysed by a quantitative anti-SARS-CoV-2 ELISA test. Elutes used for the semi-quantitative analysis were further diluted using ELISA Sample Buffer according to the following ratio values:

1. samples with a 3.5 ratio value, tested as is
2. samples with a 3.5<ratio<5, diluted 1:10
3. samples with a ratio value equal/higher than 5, diluted 1:50

The diluted samples were then tested according to the manufacturer's instructions. Results expressed as relative units - RU/mL were converted to Binding Antibody Unity/mL (BAU/mL) using the conversion factor 3.2 [19]. Antibody trends of subjects who had previously contracted SARS-CoV-2 infection or who showed unexpectedly high values not associated with recent vaccinations, were further investigated through a semi-quantitative analysis of anti-SARS-CoV-2 antibody against nucleocapsid protein (Anti-SARS-CoV-2 NCP ELISA-IgG, Euroimmun, Lübeck, Germany) according to the manufacturer's instructions.

Results

Subjects

Sixty subjects among the school staff (46 teachers, 14 administrative, technical, and auxiliary staff) agreed to participate in the study. The sample was composed by 7 males and 53 females, median age 46 years, range 24-64 years).

Samples

A total of 327 saliva samples (327/540 expected, 60.56%) and 251 DBS (251/360 expected, 69.72%) were collected (Tab.3). Only 5 participants complied to collect a saliva sample at each set time point (8.33%), while 11 (18.33%) collected all the capillary blood samples required. An average of 5.5 saliva samples and 3.2 DBS were collected for each participant. The highest participation rate for saliva surveillance was observed at week 3, with 71.7% (43/60) of the expected samples, whereas for the serological surveillance, the highest compliance was observed at the first time point.

	T1 (W1)	W2	W3	W4	W5	T2 (W6)	T3	T4	T5	T6
MST samples	39	35	43	36	35	40	26	36	37	
DBS	55					53	33	39	37	34

Tab.3 The number of MST samples and DBS collected at each time point. Empty boxes indicate that samples were not collected.

The 4.59% of saliva samples were inadequate because of the low amount of saliva collected (15/327). As the study progressed, participants provided increasing numbers of well-collected samples (from 82.1% at W1 to 100% in W5, followed by a decline in December with 91.9%).

Concerning DBS, 222 samples were considered adequate, 80% of which at T1, 77.36% at T2, 96.97% at T3, 94.88% at T4, 91.88% at T5 and 100% at T6.

COVID-19 history

All participants received the first (March 2021) and second dose (May 2021) of AstraZeneca (full vaccination). Among them, 86% also received the third dose (booster) with an mRNA vaccine between December and January 2022.

Fifteen subjects had a COVID-19 history before the first vaccine dose (BV), while nine reported to have been infected after the third dose (AV). Three of them had COVID-19 before the first and after the third dose. All AV cases happened from January 2022. In total, 21 subjects (24 episodes) experienced COVID-19.

Symptoms reported AV were milder than those reported BV, which included fever, respiratory distress, and ageusia/ dysgeusia with a duration that ranged from 5 to 180 days with a mean of 34.37±55,93 days. The AV group reported mild influenza-like symptoms with 5.85 ±3.27 average days of symptoms (Tab.5). Among AV subjects, only one subject reported to have been infected at school.

Symptoms	BV	AV	Infected Twice	
			BV	AV
Cold	3/12	4/6	2/3	3/3
Sinusitis	2/12	0/6	1/3	0/3
Fever	5/12	3/6	0/3	1/3
Anosmia/dysosmia	5/12	1/6	3/3	1/3
Ageusia/dysgeusia	5/12	2/6	3/3	1/3
Dyspnoea	3/12	0/6	0/3	0/3
Cough	4/12	2/6	0/3	0/3
Muscular and joint pain	1/12	1/6	0/3	1/3
Renal pain	1/12	0/6	0/3	0/3
Conjunctivitis	1/12	0/6	0/3	0/3
Lethargy	3/12	2/6	0/3	0/3
Headache	1/12	1/6	0/3	0/3
Gastro-intestinal symptoms	2/12	1/6	0/3	0/3

Tab.5 Symptoms declared by subject infected by SARS-CoV-2.

Molecular surveillance

The 312 adequate MST samples resulted negative for SARS-CoV-2 RNA detection.

Serological surveillance

Regarding DBS, 90.54% out of 222 adequate samples, resulted positive for the IgG semi-quantitative analysis. Only at the first two time points, negative DBS were verified, 20.45% at T1 and 14.63% at T2.

Borderline results were found at T1 (2/44, 4.55%), T2 (3/41, 7.32%), and at T4 (1/37, 2.70%). At T6 all tests resulted positive, with an increase of the ratio in all the samples.

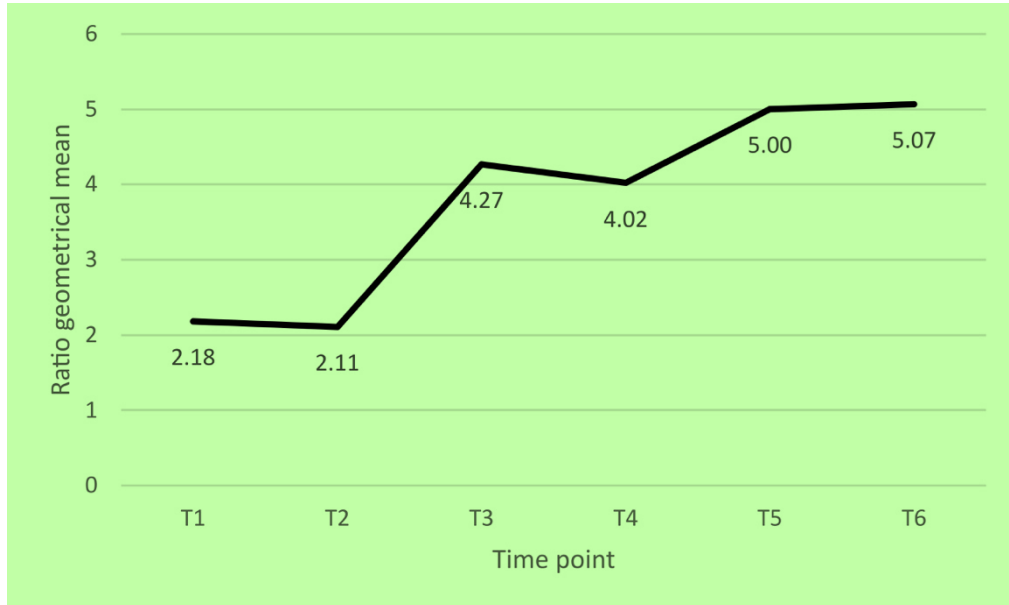Figure 4 shows the geometric mean of the SARS-CoV-2 IgG ratio observed at each time point.

Fig.4 Anti SARS-CoV-2 antibody ratio trend represented as geometrical mean of ratio at each time point.

A comparable curve was observed also evaluating the antibody titre of 33 participants who contributed to the project with 3 or more DBS during the study period (Fig. 5).
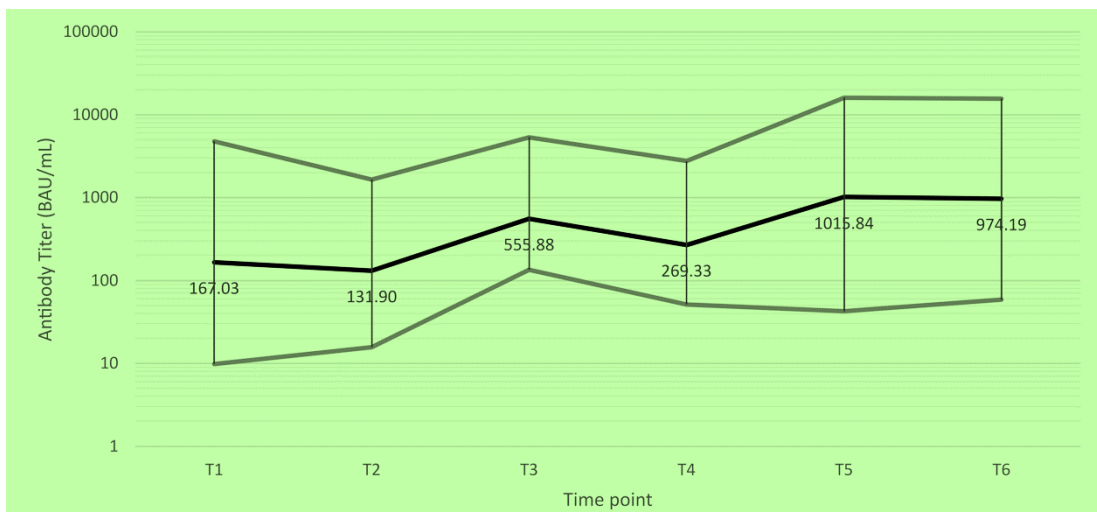

Fig.5 The trend of anti-SARS-CoV-2 antibody titres expressed as geometrical mean of a single subject's antibody titres at each time point (black line) and 95% CI (grey lines).

Samples collected from five participants who reported having been infected with SARS-CoV-2 before the start of the study were tested for the presence of SARS-CoV-2 IgG antibody against NCP, indicating that an infection had occurred. Only two subjects showed the presence of these antibodies at T1 (Tab.6).

Subject ID	T1	T3	T4	T5
#1	0.4	0.3	0.3	0.4
#14	0.3		0.2	0.2
#17	**1.3**	**1**	**1.1**	
#21	**1.2**	**0.8**		0.5
#37	0.5		0.4	0.3

Tab.6 Anti-SARS-CoV-2 antibodies against NCP protein ratio in five subjects with previous COVID-19 experience. The ratio was evaluated in subjects who reported to have experienced SARS-CoV-2 infection before the administration of the first vaccine dose. Empty boxes indicate that the sample was not collected.

The same test was conducted on samples collected from 4 subjects who showed an abnormal increase in their antibody values three months after the administration of the second dose of vaccine (T4) (Tab.7).

Subject ID	Antibody test	T1	T2	T3	T4	T5	T6
#5	Anti-S (BAU/mL)	27.552	16.32	280	828.8	2256	988.8
	Anti-NCP (ratio)			**2.1**	**1.3**	**1**	
#9	Anti-S (BAU/mL)	4784	1664	1572.8	1943.2	841.6	1089.6
	Anti-NCP (ratio)			0.2	0.2	0.3	

#26	Anti-S (BAU/mL)	128.96		1444.8	5360	692.8	
	Anti-NCP (ratio)			0.2	0.2	0.2	
#45	Anti-S (BAU/mL)	2352	1600	792	1616		2128
	Anti-NCP (ratio)			**3.1**	**2.1**		

Tab.7 Anti SARS-CoV-2 antibodies against NCP protein in subjects with abnormal increase in the antibody values.

Investigation of the morphological and immunopathological alterations occurring in lingual tissues of COVID-19 subjects

Background

SARS-CoV-2 is found in the oral cavity during infection, primarily in saliva used for diagnosing COVID-19 [63,64]. The virus enters cells through ACE2, notably present in areas like the lingual dorsum and lingual papillae. Host antiviral defences, involving chemokines, cytokines, and interferon, are activated upon viral entry. Inflammation triggered by factors like IFN-γ might impact taste function [65-67]. SARS-CoV-2's inflammatory cascade includes thrombo-inflammation, with increased factor VIII levels linked to severe outcomes in COVID-19 patients [68].

Aim

The present study aimed to assess the presence of SARS-CoV-2 inside the lingual tissue using RT-PCR and to describe the lingual dorsum micro- and macro-anatomy in COVID-19 positive subjects by means of histology and immunohistochemistry.

Methods

Sixteen deceased subjects were collected in the Institute of Forensic Medicine of Milan. The subjects were classified as COVID-19 positive (COVID-19 +) and COVID-19 negative (COVID-19 -). Data about COVID-19 status were gathered from clinical files for subjects who underwent NPS in the days before death. For subjects passed for sudden death, Antibody testing for SARS-CoV-2 IgM was performed by means of Serological sampling. The bodies were stored at -3 ° C temperature from the day of discovery/death up to 1-2 days before the autopsy. Unfreezing was performed at a temperature of 15 ° C for about 24 hours.

First all the macro-anatomy of the tongues of the subjects was observed and circumvallata (VP), Foliata and Filiform Papillae were recognized.

VP number and size were evaluated, being simple to identify compared to other papillae and susceptible to alterations **(Fig.6).** Minimally invasive punch biopsies (4-6 mm) of all the papillae were executed (Biopsy Punch, Kai Medical, Japan).

Fig.6 Picture of excised human tongue from a cadaver. A) Foliata papilla B) Vallata papilla C) filiform papilla
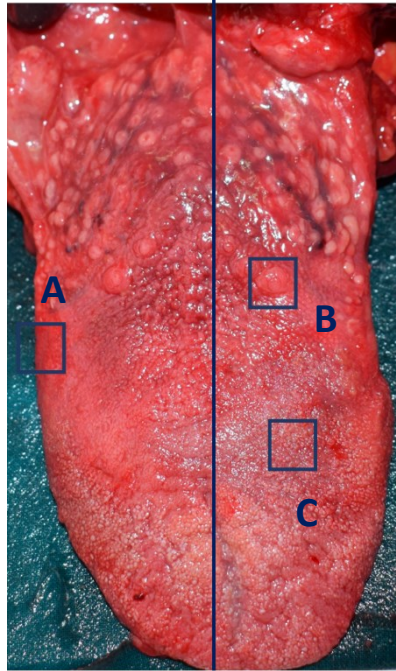
The three types of papillae were collected bilaterally, performing 6 biopsies for each tongue. The obtained samples were then halved longitudinally, the first half was fixed in 10% formalin/0.1 M phosphate buffer saline (PBS) (pH 7.4) at room temperature for histological and immunohistochemical analysis, the second half was fixed in RNAlater® (Quiagen, Düsseldorf, Germany) for molecular analysis for SARS-CoV-2 extraction.

The biopsies were harvested from tissues included in the standard functional dissection procedure, were minimal in number and dimensions, and were performed in such a way that the aesthetic features of the cadaver could be maintained, as requested by the law (art. 37 of Regolamento Polizia Mortuaria). Concerning privacy issues, an anonymisation procedure was applied, which makes it impossible to trace the identity of the corpses.

Histological processing and morphological analysis

Samples were fixed, dehydrated in ethanol (from 70% to 100%), clarified in xylol, and embedded in paraffin. Serial 6 µm sections were obtained to detect the TB position

and then mounted on 3-aminopropyl-trietoxi-xilane coated slides. Sections were then hydrated in decreasing concentrations of xylol and ethanol.

The papillae general morphology was evaluated through Hematoxylin and Eosin (HE) and Silver Impregnation (SI) (Bielschowsky method modified by Gless-Marsland). ACE2, IFNɣ and Factor VIII expression were evaluated through immunostaining.

The recovery of the antigen was performed with Proteinase K solution at 37°C in a humidified chamber for 20 minutes. Slides were incubated for 50 minutes at room temperature with the following antibodies: ACE2 (BIOSS Antibodies code bs-1004R), INFɣ and the Factor VIII. The sections were washed with PBS solution three times for 5 minutes, treated with the polymer labelling kit (Ultravision Quanto DetectionSystem HRP, Thermo Scientific, Loughborough, Leicestershire, UK), and revealed with diaminobenzidine (Ultravision DAB, ThermoScientific). The sections were counterstained with Mayer's hematoxylin, dehydrated, coverslipped, and captured by a high-resolution digital scanner (NanoZoomer S60, Hamamatsu Japan ©) and whole slide images were browsed using NanoZoomerDigitalPathology © software NDP.view2 (Hamamatsu Photonics KK).

Molecular processing

Upon removal of the RNA later solution, the samples were sliced into small pieces using a No. 21 blade. 20 µL of Proteinase K 800U/ml (New England BioLabs) and 500 µL of phosphate-buffered saline without Ca/Mg (Promo Cell) were added to 100µg of each sample, vortexed, and then left overnight at 56°C, 800rpm to degrade proteins. Nucleic acids were extracted from the supernatant by centrifugation at 1200g for 5 minutes using the NucliSENS® easyMAG™ automated platform (BioMérieux Benelux B.V.), following the specific B2.0 protocol with off-board lysis and a final elution volume of 55 µL. The quality of extraction was evaluated by amplifying the human RNase P gene, and appropriately prepared samples were subjected to SARS-CoV-2 testing using Real-Time PCR targeting the N1 and N2 regions, following the CDC's diagnostic protocol [CDC. Research Use Only 2019-Novel Coronavirus (2019-nCoV) Real-time RT-PCR Primers and Probes. Available from: https://www.cdc.gov/coronavirus/2019-ncov/lab/rt-pcr-panel-primer-probes.html].

Each Real-Time PCR test included negative controls (DNase and RNase free water) and positive controls (2019-nCoV_N Positive Control, IDT).

Results

These findings are reported in a paper published by Henin et al. (2022)[111].

Study population

8 COVID-19+ (males, mean age 52,75) and 8 COVID-19- subjects (6 males and 2 females, 68), diagnosed through NPS and immune tests were examined. The mean time distance between death and autopsy date was 16,75 days in the COVID-19+ and 9,75 days in the COVID-19- group (Tab.8).

Morphological analysis: Macroscopic analysis

The anatomy of the tongue was well maintained in all the COVID-19- subjects and in 7 out of 8 in the COVID-19+ group. The tongue of ID1 (Tab.8), deceased in a traffic accident, was intensely traumatised and didn't provide any adequate sample to be examined. In the macroscopic analysis, the FGP were not identifiable in all the subjects, most likely due to tissue wrinkling due to the formalin fixation. Therefore, FGP were excluded from the analysis. The other gustatory and non-gustatory papillae were identified in 15 subjects, in subject ID1 only FLP were identifiable.

Subject ID	Age (years)	Gender	Death-autopsy time lapse (days)	Pre-death history	Cause of death
COVID-19- +					
1	41	M	9	Unknown	Traffic accident
2	65	M	17	Influenza-like symptoms	Bilateral pneumonia
3	67	M	7	Unknown	Cardiac arrest
4	73	M	7	Previous hospitalisation for COVID-19 related respiratory symptoms	Cardiac arrest
5	57	M	57	Influenza-like symptoms	Pulmonary oedema
6	47	M	10	Influenza-like symptoms	Pulmonary oedema
7	25	M	11	Influenza-like symptoms	Cardiac arrest
8	47	M	16	Influenza-like symptoms	Cardiac arrest
COVID-19 -					
9	68	M	6	Influenza-like symptoms in HIV+	Cardiac arrest

10	50	M	8	Influenza-like symptoms	Cardiac arrest
11	85	M	5	Unknown	Stroke
12	77	F	30	Unknown	Cardiac arrest
13	51	M	8	Influenza-like symptoms	Cardiac arrest
14	72	M	11	Unknown	Cardiac arrest
15	63	F	3	Unknown	Trauma
16	78	M	7	Unknown	Cardiac Arrest

Tab. 8 Overview of the characteristics of COVID-19+ and COVID-19- subjects included in the study.

Subject ID	Real- Time PCR	VP (n)	VP dimension (mm)
COVID-19 +			
1	Negative	/	/
2	Positive	8	4-5
3	Negative	7	3
4	Positive	7	6
5	Positive	6	5
6	Positive	8	4
7	Negative	9	2-3
8	Negative	8	4-5
COVID-19 -			
9	Negative	11	2-6
10	Negative	6	3
11	Negative	7	4
12	Negative	9	3-4
13	Negative	8	4
14	Negative	7	4
15	Negative	9	2-3
16	Negative	8	4-5

Tab.9 Results of SARS-CoV-2 RNA detection and macroscopic evaluation of VP in both groups.

The macroscopic examination of the tongues showed a great interindividual variability in both groups for morphology, number, and dimension of VP. The COVID-19+ group showed an average number of 6,85± 1,06 papillae with an average dimension of

4,28±1,11 mm. The COVID-19- showed an average number of 8,12±1,55 papillae with a dimension of 3,87±0,99 mm (Tab.9).

Molecular analysis

Nucleic acids were successfully isolated from all 16 samples and PCR analysis revealed the presence of SARS-CoV-2 RNA in filiform, circumvallate papillae in 6 subjects out of 8 diagnosed with COVID-19. All COVID-19- samples were negative.

Morphological analysis: Microscopic evaluation

For each subject filiform, circumvallate foliate papillae were collected, and 48 samples were harvested. Fungiform papillae were not identified in any of the cadavers.

COVID-19+ samples

COVID-19+ samples were characterised by an inflammatory infiltrate more evident than those COVID-19-. The HE sections revealed a well-preserved architecture of the papillae overall, with no dysplastic changes observable (Fig 7. F). At 20X magnification, 62% of the samples (5 out of 8) presented a detached epithelial layer, separated from the basal membrane (Fig. 7B). Some portions presented few, or a single layer of epithelial cells and others had no epithelium at all (12%, 1 out of 8) (Fig. 7D, F). The magnification 40X of the papillary vallum showed a destroyed TB, with disconnection of its components (Fig. 7B).
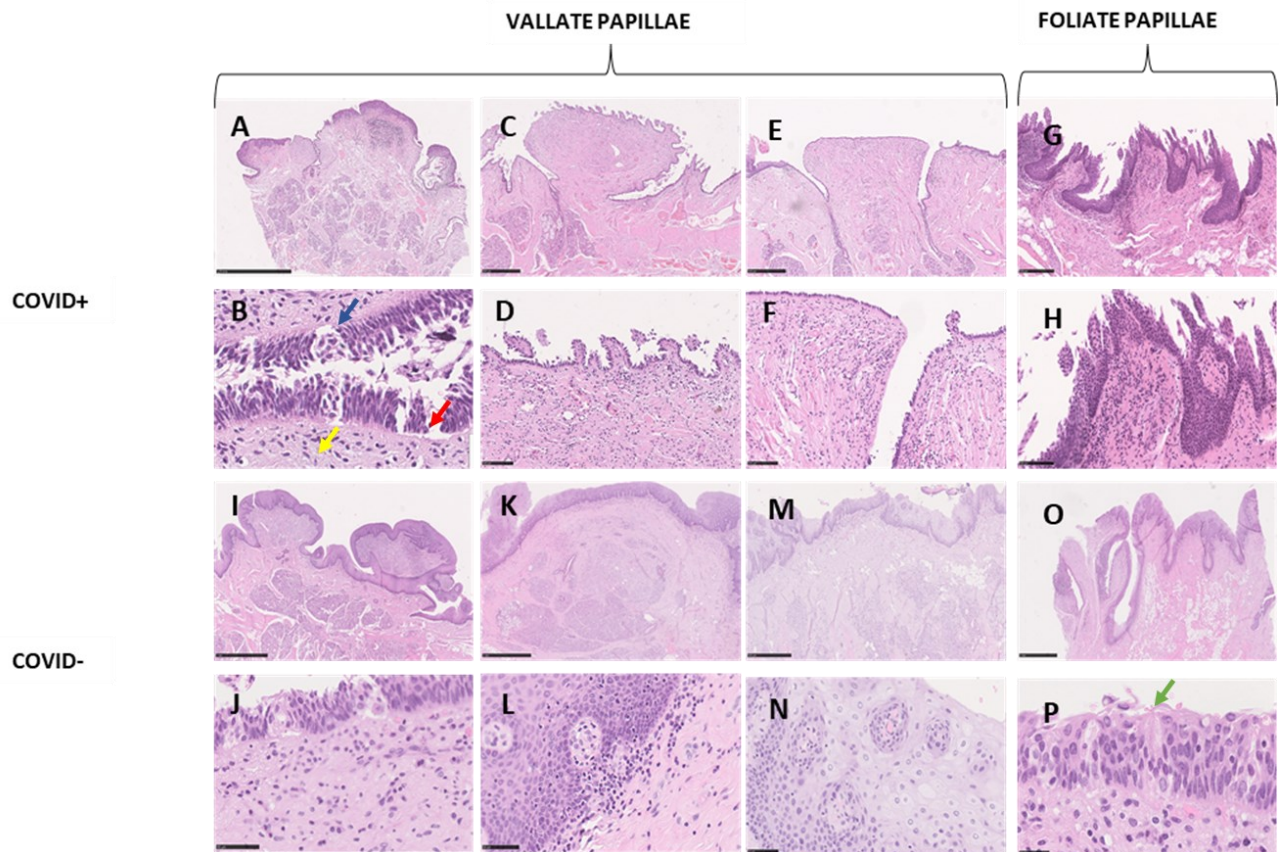
Fig.7 Histological sections of COVID-19+ and Covid- vallate and foliate papillae, haematoxylin-eosin staining. A)C)E)G)I)K)M)O) are samples overviews B)D)F)H)J)L)N)P) are details at different magnifications to show specific details A) Overview of vallata papilla B) 200X magnification of the vallum shows TB disengaged from the epithelium (blue arrow), area of detachment of the epithelium (red arrow), the connective infiltrate presents cells with fibroblastic morphology (yellow arrow) C) overview of the papilla with superficial extroflection D) higher magnification shows de-epithelialization of the papilla with a dense inflammatory infiltrate E) F) vallata papilla with absence in some portions of epithelial layer G) overview of foliate papillae H) higher magnification shows a dense inflammatory infiltrate I) K) overview of vallata papilla J) L) 200X magnification shows well-preserved TB M) O) overview of foliate papilla N) transversal section of taste bud P) 400X magnification of TB, the green arrow point at the taste pit.

The HE staining revealed the presence of stromal fibrosis and inflammatory infiltrate characterised by elongated cells with a fibroblastic morphology in the sub-epithelial layer and of a lymphoid patch rich in lymphocytes deeply in the centre of the VP (100%, 8 out of 8) (Fig. 7. A, B). In one case (ID 5, Fig. 7 C, D) the VP showed epithelial-connective protrusions in the whole profile of the papilla.

FLP showed a well-preserved structure in both COVID-19+ and COVID-19- samples, no signs of disaggregation of the layers were observed, and the epithelium and the

connective tissues did not show signs of alteration of the microstructure of the papilla (Fig.7).

FP showed a preserved architecture, and at high magnification was visible a very dense inflammatory infiltrate with a stromal fibrosis (Fig.8).
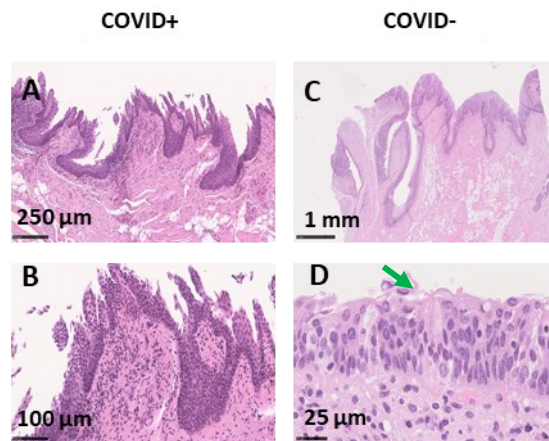

Fig.8 Histological sections of FP, HE staining A) COVID-19 + with a normal structure B) higher magnification shows a dense inflammatory infiltrate and fibrosis. C) Overview of COVID-19- papilla D) A higher magnification shows a TB, the green arrow points at the taste pit.

FLP showed a well-preserved structure in all samples, no signs of disaggregation of the layers were observed, the epithelium and the connective tissue did not show signs of alteration of the microstructure of the papilla (Fig.9). Silver impregnation showed no signs of alteration of the nervous fibres (Fig.10).
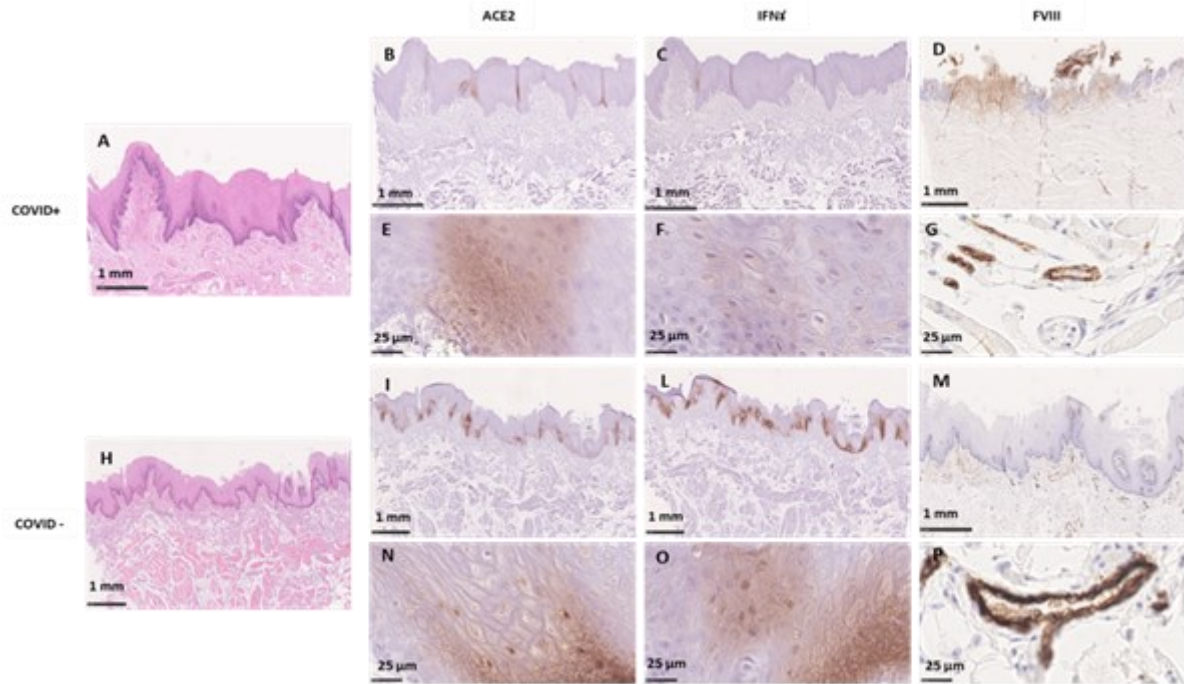
Fig.9 Histological and immunohistochemical sections of a COVID+ papilla (upper panel, A-G). A-D) overviews of the same papilla E-G) high magnification of the immunohistochemical staining. Histological and immunohistochemical sections of a COVID- papilla (lower panel, H-P), H-M) overviews of the same papilla N-P) high magnification of the immunohistochemical signal.

The immunostaining showed the expression of ACE2 (Fig.4) in the nuclei and cytoplasm of the spinous and basal cells in a punctuate pattern in the COVID-19 + tissues. ACE2 signal was observed mainly in COVID-19 + samples in the cells around the blood vessels and Von Ebner glands' duct cells. ACE2 expression was also appreciable in TB cells. The expression of IFNγ (Fig.4) was comparable to ACE2 concerning the localisation and the intensity of the immunohistochemical signal (Fig.4). A strong staining response for Factor VIII antibody was obtained in the cytoplasm of the endothelial cells in all the specimens. A pronounced reaction was evident in both small and large vessels and also in the plasma contained in the vessels.
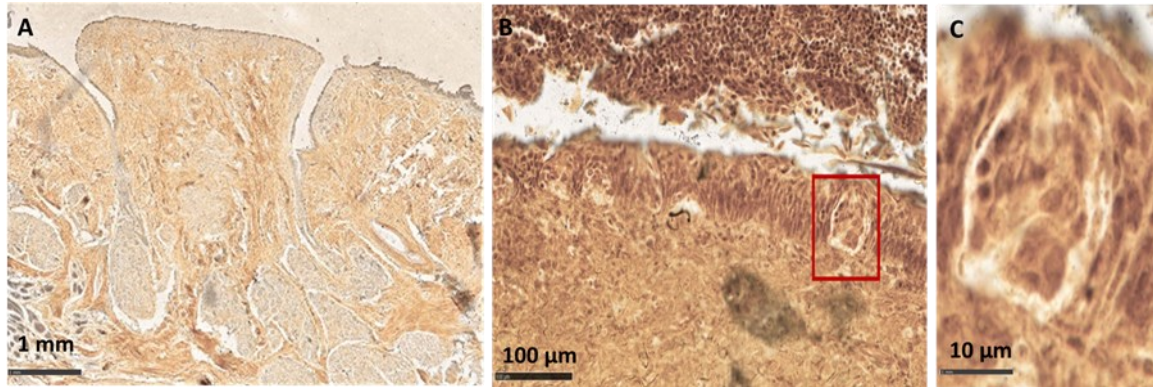
Fig.10 Evaluation of nerve fibres networks in VP and FP, staining with silver impregnation (Bielschowsky method modified by Gless-Marsland). A) Overview of COVID-19 + VP; B and C) details of TB in COVID- FP.

COVID-19 – samples

COVID-19 – samples evidenced a low degree of inflammation. The analysed gustatory papillae, VP and FP, maintained their architecture with no signs of dysplasia or alteration. TBs were appreciable, maintaining the typical bulb shape apically converging in the taste pit (Fig.7). The SI staining showed no signs of nervous fibre alteration for COVID-19 – samples (Fig.8). COVID-19 – samples showed intense staining for ACE2 and IFNγ ex-pressed in the same area as well as COVID-19 + samples, in the granulosum and basal layer of the epithelium (Fig.4). Factor VIII expression was comparable to COVID-19 + samples (Fig.9).

Investigation of the genetical susceptibility to the infection

<u>Evaluation of the distribution of TAS2R38 bitter taste receptor phenotype and haplotypes among COVID-19 patient</u>

Background

Taste receptors, especially the bitter taste receptor, are also expressed extra-orally and seem involved in innate immunity [112,113]. The bitter taste is mediated by 25 functional bitter taste receptors (TAS2Rs), which are G-protein-coupled receptors. One of them, TAS2R38, is highly expressed in the respiratory tract and is implicated in the quorum sensing molecules produced by some pathogens, producing the biocidal nitric oxide, which causes a reduction in viral RNA production and inhibition of the viral replication of SARS-CoV. TAS2R38 affects the fusion between the S protein and ACE2 [114–117]. TAS2R38 presents many variants, with two main haplotypes diffused worldwide, characterised by a different ability to recognise the compound 6-n-propylthiouracil (PROP) chemically. Among the population are distinguishable the taster (PAV= encoding for proline, alanine, vaniline) and the non-taster (AVI= encoding for analine, vaniline, isoleucine)[118]. The association between TAS2R38 haplotype and phenotype is not perfect and still not completely understood. The role of bitter taste receptors in response to pathogens in the respiratory tract raises the possibility that these receptors could be targeted for therapy in COVID-19 diseases.

Some authors investigated the phenotype of TAS2R38 and COVID-19 severity and duration of symptoms, evidencing that non-tasters were significantly more susceptible to infection and hospitalisation than tasters and supertasters[119,120].

Aim

The present study aimed to evaluate the frequency of PAV and AVI alleles in COVID-19 positive individuals with mild or severe symptoms compared to COVID-19 negative subjects to confirm or not the hypothesis that the PAV allele may act as a protecting factor towards SARS-CoV-2 infection and AVI constitutes a risk factor[121].

Methods

The study was conducted according to the principles of the Declaration of Helsinki and was approved by the Università degli Studi di Milano (Italy) ethical committee (number 36/21, 20.04.2021).

Subjects

The enrolment of the participants followed the present inclusion criteria:

- Age> 18
- Caucasian ethnicity (to limit genetic variability)

Exclusion criteria:

- Have pathological lesions of the oral mucosa, including the lingual dorsum.
- Systemic diseases and pharmacological treatments for chronic diseases.

First, a preliminary questionnaire with a general scouting aim was emailed to a target population, including questions about COVID-19 experience. Those who agreed to participate in the study were further skimmed by a second questionnaire, resulting in three categories of participants:

- COVID-19 mild patients (MC): subjects with experience of COVID-19 with mild symptoms or no symptoms at all. Mild cases were considered all the individuals who had any of the following, e.g., fever, cough, sore throat, discomfort, headache, muscle/articular pain, nausea, vomiting, diarrhoea, ageusia, anosmia) but who did not report shortness of breath, dyspnoea, or abnormal chest imaging. Moderate illness referred to individuals who showed evidence of lower respiratory disease during a clinical assessment or imaging and with a saturation of oxygen (SpO2) $\geq$ 94% on room air at sea level.

- COVID-19 severe patients (SC): subjects with previous COVID-19 and experience of severe symptoms; the severity of the illness was defined according to the following criteria: SpO2 < 94% on room air at sea level, a ratio of arterial partial pressure of oxygen to fraction of inspired oxygen (PaO2/FiO2) < 300 mm Hg, respiratory frequency > 30 breaths/min, or lung infiltrates > 50%.

- Healthy COVID-19 close contacts (HC): subjects with no experience of COVID-19 even after an exposition to COVID-19 infected subjects. HC

included non-vaccinated subjects with negative serological tests for SARS-CoV-2

SC and MC groups included subjects with previous COVID-19, healed at the moment of the study, evidenced by PCR analysis.
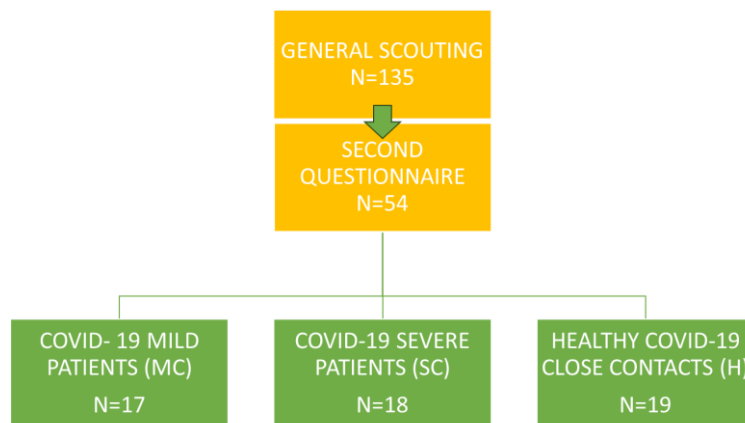

Fig.11 Target population selection process.

DNA collection, extraction and sequencing

Buccal swabs, obtained by scrubbing the oral mucosa for 3 minutes in triplicates, were collected from the participants. The swabs air dried for two hours and were stored at -20°C.

According to the manufacturer's instructions, total DNA was extracted from the swab using the QIAamp DNA Mini kit (Qiagen, Hilden, Germany). Amplification reactions were achieved with AmpliTaq Gold™ 360 (Applied Biosystems™, Thermo Fischer Scientific, Waltham, MA, USA) using primers TAS2R38_For 5′-CCC TCT AAG TTT CCT GCC AGA-3′, TAS2R38_Rev 5′-GCT TTG TGA GGA ATC AGA GTTGT-3′ on a Thermal Cycler 5333 MasterCycler (Eppendorf). Briefly, each sample was treated at 95 °C for 5 min to allow the activation of the DNA polymerase. Then DNAs were amplified by 40 three-step cycles (denaturation at 95 °C for 30 s, annealing at 59 °C for 30 s and extension at 72 °C for 70 s) followed by a final extension step of 10 min at 72 °C. PCR products (1291 bp) were then analysed on a 1.5% agarose gel and treated

with ExoSap (Applied Biosystems™, Thermo Fischer Scientific, Waltham, MA, USA). Applied Biosystems Sequencing was performed with BigDye™ Terminator v1.1 Cycle Sequencing Kit (ThermoFisher Scientific,

Waltham, MA, USA) on a AB3730xl DNA Analyzer™, (ThermoFisher Scientific, Waltham, MA, USA). The used oligonucleotide primers for sequencing were the same as PCR with the addition of these internal primers: TAS2R38_ForInt 5′-CCC AGA TGC TCC TGG GTA -3′ and TAS2R38_RevInt 5′-GAT CTT TAA TCT GCC AGT TGAGC-3′. Sequences obtained were assembled on the reference sequence and then analysed with SeqScape™ Software v3.0 (ThermoFisher Scientific).

PROP phenotype

All participants were asked to put a previously prepared cotton PROP swab in their mouth, dipping in a suprathreshold 50 mM 6-n-propylthiouracil solution (Sigma Aldrich S.r.l.), to assess their PROP-phenotype. Participants were then asked to define the grade of bitterness on the Labeled Magnitude Scale (LMS).

Genetic analysis

Genetic analysis was performed in cooperation with genetic and food experts from the University of Gastronomic Sciences, Pollenzo (Italy) and the Department of Medicine and Life Sciences, Institute of Evolutionary Biology, Barcelona (Spain).

First, the haplotypes for rs10246939, rs1726866 and rs713598 SNPs in each subject in our dataset were reconstructed using the algorithm PHASE. The results showed that each pair of haplotypes in our samples had the highest possible probability, highlighting the accuracy of the analysis. Finally, to facilitate the association of samples with PROP perception-related diplotypes, each haplotype (GCC—ATG) was converted to the relative amino acid sequence present in the TAS2R38 receptor (PAV—AVI). The association between TAS2R38 and PROP perception was tested through PLINK v.1.7 (http:// pngu. mgh. harva rd. edu/ purce ll/ plink/)[118].

Statistical analysis

Statistical support for putative differential apportionment of PROP perception scores

in COVID-19 infection and dysgeusia groups was assessed via ANOVA. It was also tested whether the distribution of each sample's diplotype (PAV/PAV, PAV/AVI or AVI/AVI) was found more (or less) than expected by chance across the different COVID-19 statuses. To do so, in addition to ANOVA, hypotheses testing included Chi-squared test of independence and Fisher exact test.

Results

These results are reported in a scientific publication produced by Risso et al. (2022) [121].

Study population

Fifty-four participants were enrolled in the present study, with a mean age of 46 years (22-90) and 29 were females (54%).

The group consisted of the following (Tab.10):

- H group: 63% females, mean age 44 (24-83)
- MC group: 54% females, mean age 45 (26-90)
- SC group: 44% females, mean age 49 (22-79)

Group	N	Hospitalized	Days at hospital	Temperature> 37 °C	Generic symptoms*	Cough and sore throat	Gastrointestinal symptoms	Pneumonia	Peripheral O2 saturation < 94%	Taste and/ or smell alterations
H	19	0	0	0	0	0	0	0	0	0
MC	17	0	0	16 (94%)	13 (76%)	11 (65%)	5 (29%)	0	0	12 (71%)
SC	18	9 (50%)	34 (5-90)	16 (89%)	16 (89%)	13 (72%)	12 (67%)	10 (56%)	13 (72%)	11 (61%)

Tab.10 Main medical characteristics of the 3 groups. N number. *Including headache, fatigue, generic muscle pain, nausea, diarrhoea, vomiting.

Genetic analysis

All samples exclusively carried the two most common and widespread sequences of alleles, respectively coding for PAV and AVI amino acids. The PROP perception score was recorded, assessed in the taste test, to obtain the binary variables "taster" and "non-taster", thus being able to classify individuals based on their ability to perceive PROP bitterness.

Out of 54 total samples, 21 (39%) were classified as non-taster and 33 (61%) as taster, while, regarding TAS2R38 haplotypes, 9, 25 and 20 (17%, 46%, 37%) individuals carried, respectively, PAV/PAV, PAV/AVI and AVI/AVI diplotypes. Moreover,

PROP status followed the expected distribution across diplotypes, with PAV/PAV, PAV/AVI and AVI/AVI samples (Fig.12) respectively showing tasters frequencies of 0.78, 0.48 and 0.1 and non-tasters frequencies of 0.22, 0.52 and 0.9. Analyses performed with PLINK confirmed the known association between TAS2R38 SNPs and PROP score reported in the test, highlighting how even in a relatively small dataset, this association still holds true. The analyses gave insights into how age, used as a covariate, also contributes to PROP bitter perception, indicating a negative association with PROP scores. It was also tested whether our single nucleotide polymorphisms were significantly related to dysgeusia and COVID-19 infection phenotypes. None of the tests performed provided significant results, highlighting how, at least in our dataset, TAS2R38 genotypes are not responsible for differences in the presence or the severity of COVID-19 infection, and do not influence infection-driven dysgeusia.
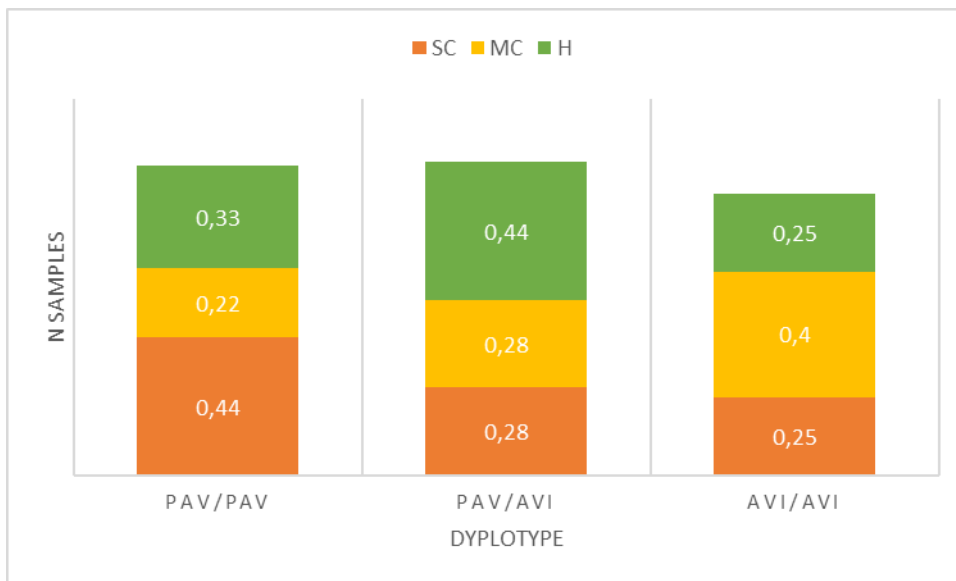

Fig. 12 COVID status distribution among TAS2R38 diplotypes.

Nanomaterials: a potential tool for tissue regeneration

The study conducted by Henin et al. (2022) [111] *highlighted the inflammatory destructive condition of gustatory papillae, most likely compatible with the dysgeusia/ ageusia symptomatology and potential cause of gustatory Long-COVID-19* [122]. *Long-COVID-19 is a condition including a group of long-term complications and consequences of COVID-19 affecting many tissues, such as pulmonary and neural tissues.*

To date, chronic COVID-19 tissue damages are well documented, and constitute challenging issues for many clinicians and patients. Thus, new strategies for the improvement of tissues' regenerative and healing potential are needed with non-invasive, stable and targetable bio-materials. The aim of the present part of the project was to preliminary investigate the applicability of nanomaterials, namely nanofibers and nanoparticles with regenerative purposes[123].

Polyblend Nanofibers to Regenerate Oral Tissues: A Preliminary In Vitro Study

Background

Nanofibers (NF) are fibres synthesised in nano-scale size, from a wide range of materials, with 3D structures and functionalised surface properties. The excellent thermal, mechanical, chemical and morphological properties make nanofibers ideal for biomedical applications: scaffolds for tissue engineering and antimicrobial devices such as mask filters. The 3D nanostructure can be loaded with proteins, enzymes, and drugs to create biologically active devices.

Aim

This preliminary in vitro study aimed to analyse the effects of PCL nanofibers enriched with HA and vitamin E (NFE) vs PCL nanofibers alone (NF) on human gingival fibroblast cultures, being a simple and predictable cellular model largely used in scientific literature. In the present study the morphology, viability, collagen turnover, and mechanosensing were assessed.

Methods

PCL (NF) and PCL enriched with HA and vitamin E (NFE) nanofibers were obtained from a solution of 14% (w/v) of PCL (molecular weight (MWPCL) of 45,000 Dalton)(Sigma-Aldrich, MO, United States) dissolved in chloroform: ethanol (8:2). NFE were produced by adding hyaluronic acid (HA) at 0.002% (Sigma-Aldrich, MO, United States) and vitamin E at 0.0014% (α-Tocopherol; Sigma, St. Louis, MO) to the PCL solution. Concentrations of VitE and HA were defined according to our previous work [124], also considering the maximum resistance without 3D defects of the material to the substances loading. NF and NFE were electrospun by Nanospider TM device (Elmarco, Czech Republic)[125]. The polymer solutions were connected to a high voltage electrocode (56 kV). NF and NFE were placed on a grounded collector electrode.

NF and NFE were spun as 50x50 cm sheets, at room temperature (24°C) and a relative humidity of approximately 50%.

- NF and NFE were characterised using attenuated total reflection Fourier transform infrared spectroscopy (ATR-FTIR), recording at T =298 K, under a nitrogen atmosphere, in a 550–4,000 cm−1 wavelength range using an Agilent Cary 640-IR infrared spectrometer (Agilent Technologies, Santa Clara, CA, United States) equipped with a single bounce ZnSe ATR accessory. All the spectra were recorded in triplicate.

- Mechanical properties of five 0.5×2 cm^2 sheet pieces were preconditioned in PBS for 10 min, and then evaluated by a dynamic mechanical analyser (DMA) (TA, Q800). The DMA strain rate was 0.02 min^{-1}; a tensile test was performed with a preload of 1 mN at room temperature.

- Biodegradability test was performed by a stereomicroscope (SZX Olympus instruments), leaving nanofibers for 28 days in a phosphate buffer saline (PBS) solution.

- Morphological analysis was effectuated by scanning electron microscope (SEM) (Tescan Vega 3, Brno, Czech Republic) to verify the nanofiber's diameter and largest pore size by means of image analysis software (Vega3 SB, Tescan a.s).

Cell Cultures of Primary Gingival Fibroblasts (HGF)

Gingival biopsies were collected during appointments for impacted wisdom teeth extractions. The study followed the principles of the Declaration of Helsinki and was conducted according to the local Ethics Committee of Università degli Studi di Milano, Milan (29/18 of the 28 June 2018).

After PBS wash, gingival samples were cut into small fragments and digested in collagenase I 4 mg/ml (Millipore,United States). Cell suspension was filtered and plated in a T25 flask. Human gingival fibroblasts (HGF) were cultured at 37°C in a 5% CO2 humidified incubator in a medium containing 89% Dulbecco's Modified Eagle Medium, 10% heat-inactivated fetal bovine serum (GIBCO), 1% L-Glutamine. Cells were seeded on plastic or nanofibers in 6- or 24-well multi-well plates at the concentration of 1.5×104. After 4 passages, cells at 80% confluence, were cultured for 72 hours on NF, NFE and plastic (Control). Primary HGF were tested for viability and adhesion. Two replicate experiments for both NF and NFE were performed. A technical triplicate was applied and conducted at 37°C in a 5% CO2 humidified incubator in each experiment.

Viability Test by alamarBlue

Cell viability was tested using alamarBlue® (Thermo Fisher Scientific), to measure viability quantitatively. 7×10^3 cells were seeded on NF and NFE in 24-well multi-well plates. Cell viability was tested at 3 different time points (24, 48, and 72 h from seeding). The colourimetric variation of the essay was read by a spectrophotometer (Glo Max Discover, Promega Corporation, United States).

The proliferation curve, the percentage of cell proliferation (compared to CT) were obtained for each experimental group, through an algorithm according to the manufacturer instructions.

Morphological Analysis

Samples were fixed with 2.5% glutaraldehyde, postfixed in osmium tetroxide, dehydrated through an increasing scale of alcohol, infiltrated with hexamethyldisilane, and dried. Samples were mounted on stubs and covered with a thin layer of gold. Samples were then observed with SEM, pictures were acquired at a total magnification until 1,000x by means of a Jeol Neoscope Electron Microscope (JCM-6000; Nikon, Tokyo, Japan).

Real-time PCR

After cells were harvested, the total RNA was isolated through Tri Reagent (Sigma, Italy). One µg of RNA was reverse transcribed in a 20 µL if reaction mix (Bio-Rad, Italy). mRNA levels for long type I collagen (COL-I), lysyl hydroxylase 2 (LH2b), and tissue inhibitor of matrix metalloproteinase 1 (TIMP-1) were analysed by real-time RT-PCR in samples run in triplicate. Glyceraldehyde 3-phosphate dehydrogenase (GAPDH) was used as a housekeeping gene to normalise the differences in the amount of total RNA in each sample. The primers sequences were the following:

GAPDH: sense CCCTTCATTGACCTCAACTACATG, antisense TGG GATTTCCATTGATGACAAGC;

LH2b: sense GGGAAACATTCCAAATGCTCAG, antisense GCCAGAGGTCATTGTTATAATGGG;

TIMP-1: sense GGCTTCTGGCATCCTGTTGTTG, antisense AAGGTGGTCTGGTTGACTTCTGG;

PAX: sense CAGCAGACACGCATCTCG, antisense GAGCTGCTCCCTGTCTTCC;

VNC: sense GGAGGTGATTAACCAGCCAAT, antisense AATGATGTCATTGCCCTTGC.

Each sample was analysed in triplicate in a Bioer LineGene 9600 thermal cycler (Bioer, China). The cycle threshold (Ct) was determined and gene expression levels relative to that of GAPDH were calculated using the ΔCT method.

Slot Blot

Slot blot analysis was performed in serum-free cell culture supernatants. Cell culture media protein content was determined by a standardised colorimetric assay (DC Protein Assay, Bio- Rad, Italy); 100 µg of total protein per sample in a final volume of 200 µL of Tris buffer saline (TBS) was spotted into a nitrocellulose membrane in a Bio-Dot SF apparatus (Bio-Rad, Italy). Membranes were blocked for 1 h with 5% skimmed milk in TBST (TBS containing 0.05% Tween-20), pH 8, and incubated for 1 h at room temperature in a monoclonal antibody to COL-I (1:1,000 in TBST) (Sigma-Aldrich, Milan, Italy) and MMP-1 (1 µg/ml in TBST, Millipore, Milan, Italy).

After washing, membranes were incubated in HRP-conjugated rabbit antimouse serum (1:6,000 in TBST to detect COL-I; 1:20,000 in TBST to detect MMP-1) (Sigma, Italy) for 1 h. Immunoreactive bands were revealed by the Opti-4CN substrate or Amplified Opti-4CN substrate (Bio-Rad, Italy) and scanned densitometrically (UVBand, Eppendorf, Italy).

Statistical Analysis

Descriptive analysis was performed and mean and standard deviation (SD) of the values obtained from the two experimental technical triplicates were computed for both NF and NFE samples in all performed tests. A nonparametric statistical analysis by Wilcoxon rank-sum test was used to compare the results of the mechanical characterisation of NF and NFE, and a p value < 0.05 was considered significant (GraphPad Software Inc., San Diego). Comparisons between NF and NFE mean values were performed at each time point of the viability test by means of a paired t-test with a level of significance of p < 0.05 (GraphPad Software Inc., San Diego, CA 92108, United States). Differences associated with p values lower than 5% were to be considered statistically significant.

Results

The present work is described by Canciani et al. (2021) [126].

Nanofibers Characterization

The ATR-FTIR spectra of NFE, NF and VITE and HA showed a signal of NF compatible with PCL signal (Fig.13). NFE presented a signal similar to NF, however the presence of a breaded peak at about 3,400 cm−1, typical of O–H stretching vibrations, the broadening of the signal at 1,176 cm−1, and the growth of the peak at 1,103 cm−1 suggest the proper loading of HA and vitamin E in the samples NFE. HA presence influences the spectrum from 500 to 700 cm−1 by increasing the values in NFE compared with NF as illustrated in figure B (Fig. 13B). Furthermore, considering vitamin E, a peak around 3,008 cm-1 was evidenced, confirming its incorporation in NFE sample (Fig. 13C).
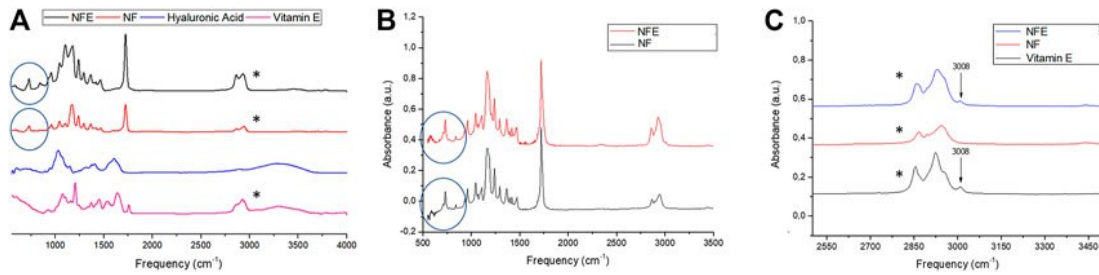
Fig. 13 Panel shows (A) ATR-FTIR spectra of samples NFE, NF, and of vitamin E and hyaluronic acid. (B) Spectra highlights hyaluronic acid peak (blue circles) and (C) the peak relative to vitamin E (black asterisks).

Concerning the stress break, NF presented a higher value than NFE (1.47 ± 0.34 MPa vs 1.06 ± 0.25 MPa, p >0.05). In contrast, deformation at break was significantly higher in NF than in NFE ($31.52 \pm 5.08\%$ vs. $14.11 \pm 4.64\%$, $p < 0.01$). Strain resulted statistically significant between NF and NFE for p value < 0.01. Biodegradability observation showed that after 28 days, the nanofibers had maintained their structure.

At SEM observation, NF and NFE were organised in mesh and resulted in fibers of different sizes and organisation (Fig.14). The fibres diameter ranged between 0.2 and 0.4 μm for both groups with a normal distribution.
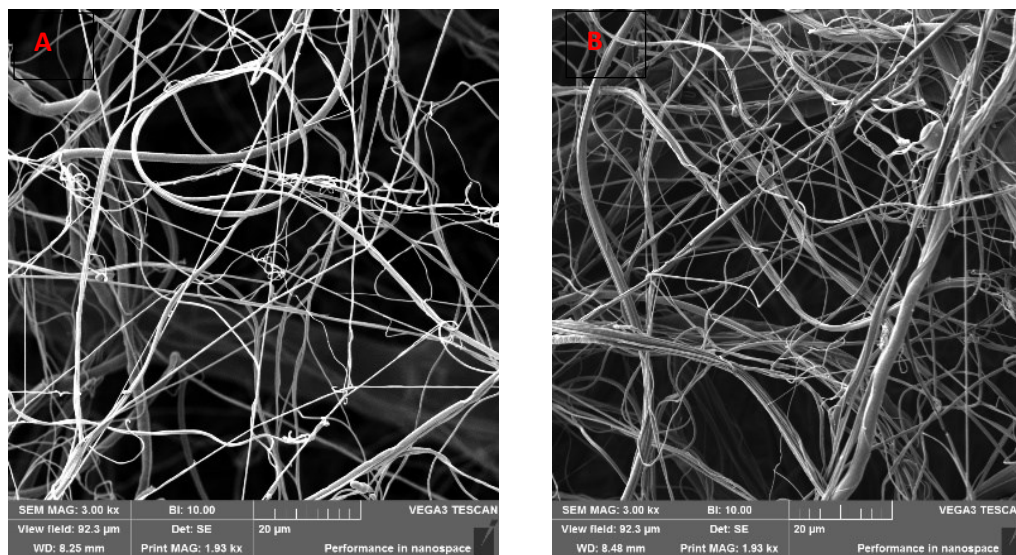

Fig.14 SEM micrographs of the nanofibers A) NF and B) NFE.

Fibroblasts Morphology and Adhesion on NF and NFE

After seeding, HGF grew adhering on nanofibers. HGF through SEM observation showed to be resident on the surface of NF and NFE (Fig.15). Cells on both samples

evidenced cytoplasmatic protrusions extended on nanofibers, tending to create cellular bridges through the pores of the electrospun tissue.
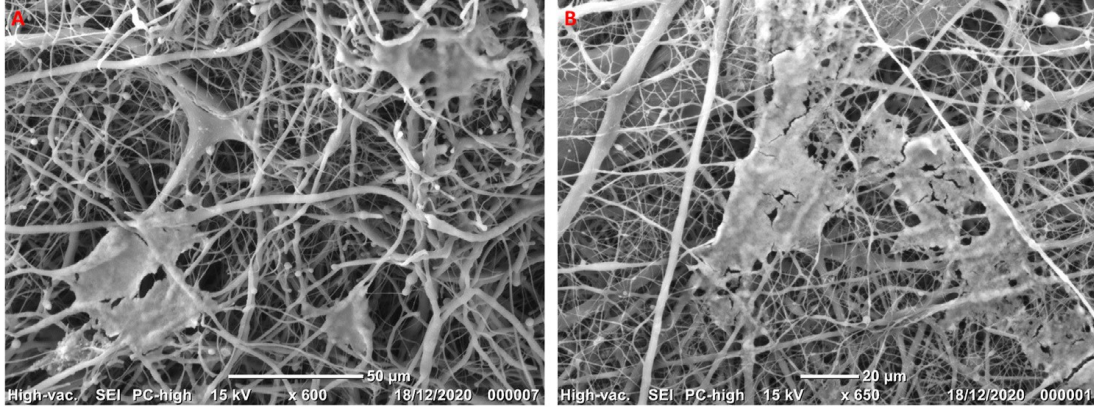

Fig.15 SEM Micrographs showing HGF cultured on NF (A) and NFE (B)

Viability of HGF on NF and NFE

AlamarBlue® test evaluation showed a similar curve of cell cultured on NF (NFc) and NFE (NFEc) metabolic activities. The viability trend of both groups showed a slight decrease at 24h and 48h compared to the Control. At 72 h from seeding, NFc and NFEc showed values over Control threshold (Fig. 16).
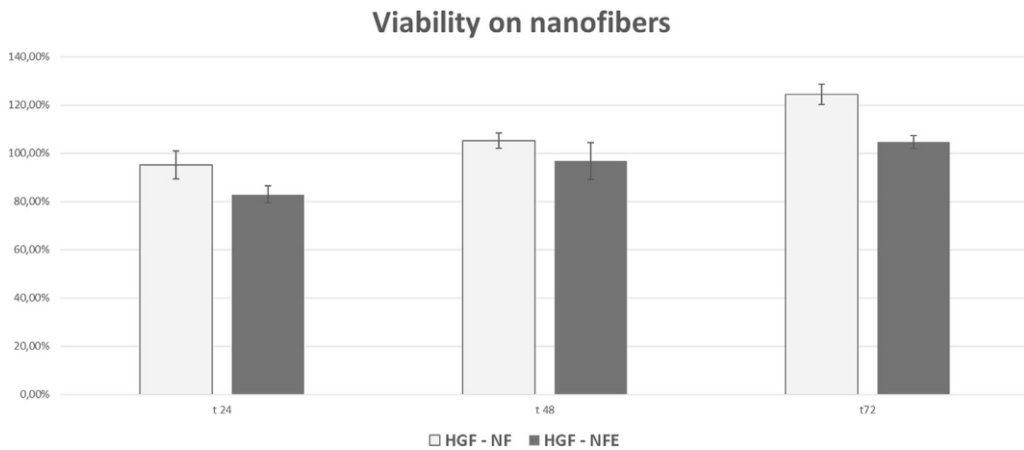

Fig.16 Bar graphs showing cell viability and proliferation of HGF expressed as a % relative to CT (considered as the 100%). At all the considered time points and experimental conditions, cell viability was higher than 80%, suggesting that nanofibers do not elicit any evident cytotoxicity.

Expression of Genes and Proteins Related to Collagen Turnover

Collagen I (COL-1)

COL-1 mRNA levels, assessed by Real-Time PCR, were increased in cells cultured on NFc and downregulated on NFEc (respectively +45% vs CT and -66% vs Control).

COL-1 protein secretion, evaluated through slot blot, was decreased in NFc (-39%) vs NFEc (-75%) (Fig.17).

Collagen maturation

Collagen maturation was evaluated by analysing mRNA levels for LH2b, using Real-Time PCR, resulting downregulated in NFc and upregulated in NFc. The LH2b mRNA/COL-1 mRNA and LH2b mRNA7COL-1 protein ratios showed a high value in NFEc, suggesting an increased collagen cross-linking (Fig.17).

Collagen degradation

MMP-1 level in cell cultures supernatant, analysed using slot blot was downregulated on NFEc compared to NFc and Control.

TIMP-1 mRNA level resulted decrease in NFc and unchanged compared to Control in NFEc (Fig.17).

Expression of Mechanosensors (PAX, VCN, and YAP)

These components of the adhesion plaque act as mechanosensors and were analysed to understand whether NF has any mechanical effect of collagen turnover pathway. The analysed mechanosensors mRNA resulted upregulated on NFc and downregulated on NFEc (Fig.17).
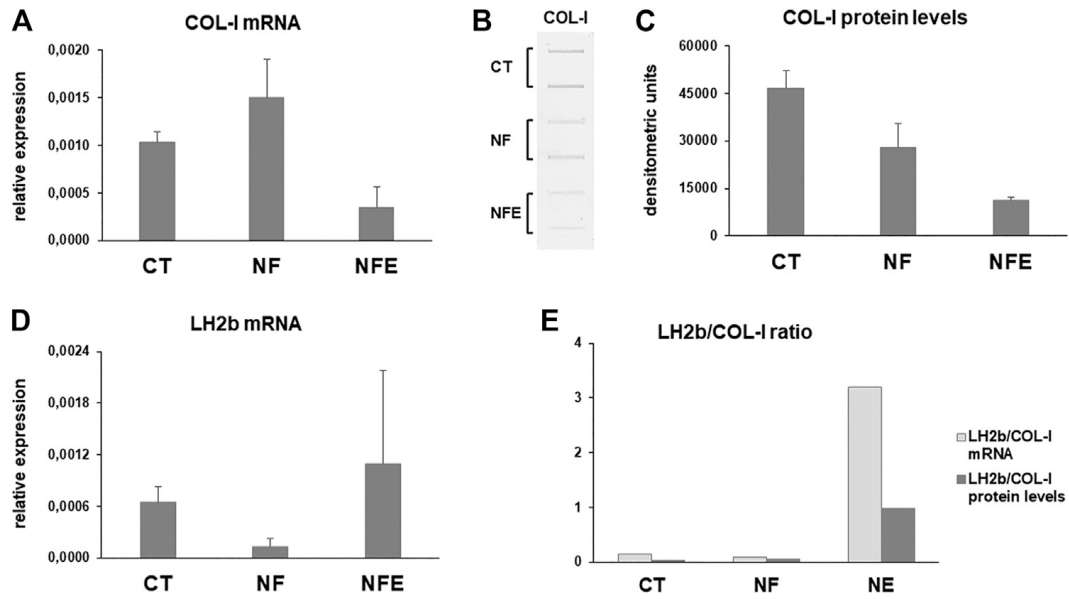
Fig. 17 (A) Bar graphs showing COL-I mRNA levels in HGF cultured on NF and NFE. (B) Representative slot blot and bar graphs showing COL-I protein levels (C) secreted in cell culture supernatant of HGF cultured on NF and NFE assayed by slot blot after densitometric scanning of immunoreactive bands in the considered experimental conditions. Data are expressed as mean ± SD of two independent experiments. (D) mRNA levels for long lysyl hydroxylase 2 (LH2b) in CT and cells grown on NF and NFE. Data were normalized on GAPDH gene expression and are expressed as mean ± SD for at least two independent experiments. (E) Bar graphs showing the LH2b mRNA/COL-I mRNA and LH2b mRNA/COL-I protein ratio in the different experimental conditions.

Evaluation of the biological response to MIP nanoparticle: preliminary in vitro study

Background

The new frontiers of drug delivery are orientating towards a selecting and efficient targeting carrier system. Molecularly imprinted polymers (MIP) represent promising polymeric vehicles since they can recognize specific target molecules.

Aim

This study explored a novel targeted drug delivery system born from the conjugation of synthetic antibodies (MIP NPs) to polymersomes.

Methods

All the phases of the study were performed in the Division of Biomaterials and Tissue Engineering (Eastman Dental Institute, Royal Free Hospital, UCL Medical school, Rowland Hill Street, London, NW3 2PF, United Kingdom).

MIP NPs production

Molecularly imprinted nanoparticles (NPs MIP) were produced in the chemistry laboratory of the Division of Biomaterials and Tissue Engineering[127]

MIP NPs were synthesised adapting a protocol from Canfarotta et al. (2018)[127] .

Four distinct groups of MIP NPs were produced targeted against four epitopes: EGFR, HER2 linear, HER2 conformational and HA5, receptor overexpressed in breast cancers, in order to promote active targeting of human cancer breast cells.

Cell cultures

Human breast cancer cell lines were used for these experiments. MDA-MB-468 cells over-expressing EGFR receptor and Sk-BR-3 cells overexpressing HER2 receptor, were purchased from ATCC. MDA-MB-468 were cultured in Leibovits's L-15 Medium (1X) (GIBCO) supplemented with 10% fetal bovine serum (FBS) and incubated in a HERA cell VIOS 150i air free incubator, in absence of CO_2. MDA-MB-468 were passaged 4-6 times.

SK-BR-3 were cultured in DMEM High Glucose (Dulbecco's Modified Eagle Medium) supplemented with 10% fetal bovine serum (FBS) and 1% L-glutamine respectively and incubated at 37°C with 5% CO_2 prior to usage (Thermo Scientific,UK). SK-BR-3 were used at passage number 18-26.

Morphological evaluation

MIP NPs were characterised using Transmission Electron Microscopy (Philips CM20). After sonication, MIP NP solutions were filtered using a PTFE syringe filter (0.45 μm) (Fisher Scientific, UK). Five μL of MIP NP were placed into a copper grid (400 mesh, from EM Resolutions, UK) and left overnight to dry at room temperature.After 24h under a UV lamp, other 5 μL of sonicated MIP NPs were deposited onto the grid and finally blotted with filter paper and treated with phosphotungstic acid staining agent 0.75% (w/v) (pH 7.4) for 5 s for all samples and 1s for HER2 conformational samples, blotting away the excess using filter paper.

Binding Affinity of MIP NPs

The binding affinity with MIP NPs, both cell lines were seeded onto 96-well plates (Cellstar UK) at 105 cells/mL concentration. After sonication of MIP NPs to obtain a homogenous sample, were added to cell cultures with increasing concentrations (18.75 to 300 ng/mL). After 20 min and 1h of incubation at 37°C, supernatants was collected and placed in black well to read fluorescence intensity by means of a spectrofluorometer (Infinite® 200 PRO, UK) at 20°C, with a wavelengths for excitation and emission set at 540 nm and 600 nm, respectively. Control wells were incubated with equivalent volumes of PBS, PBS and cells.

Results

MIP NPS Morphological characterization

TEM was used to characterise the morphology and size of the synthesised MIP NPs. The solid phase synthesis technique resulted in spheroidal MIP NPs of regular sizes when measured in the dry state using TEM (Fig. 18).
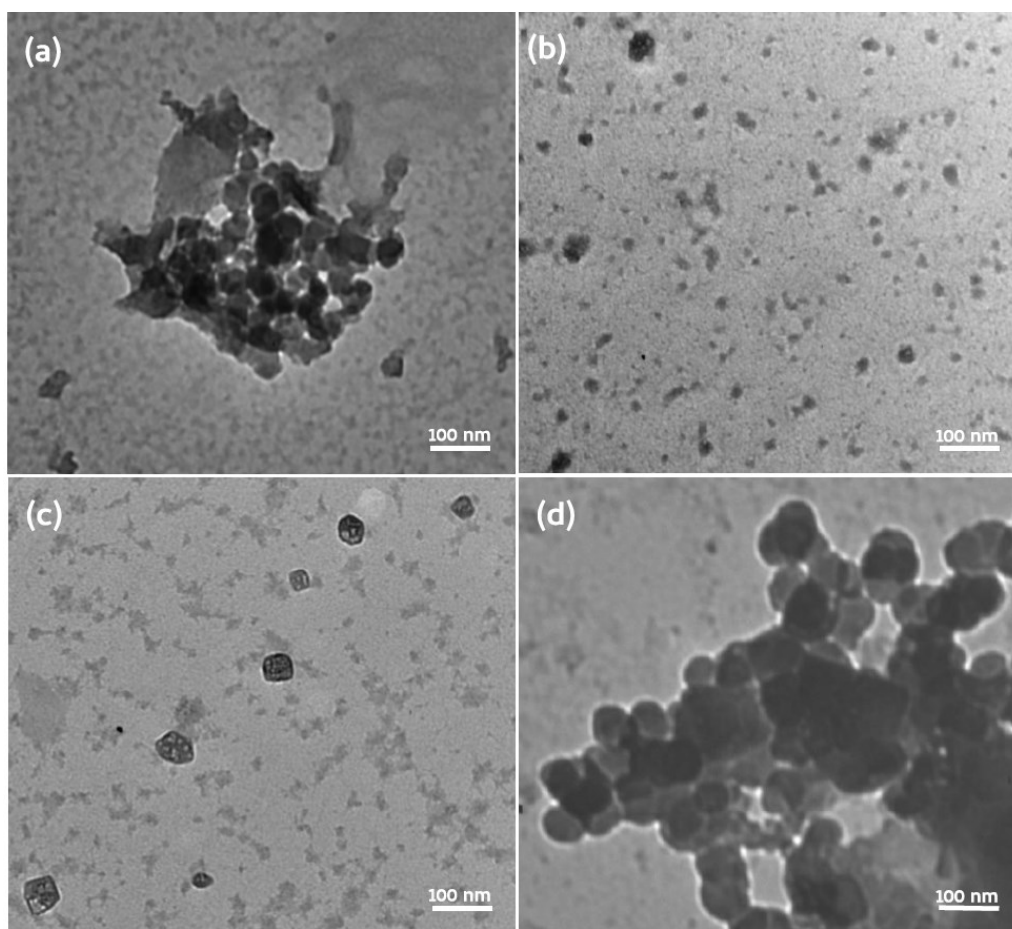
.

Fig. 18 TEM images of a) EGFR MIP NPs b) HER2 linear MIP NPs c) HER2 conformational MIP NPs d) HA5 MIP NPs. The scale bars all equal to 100 nm.

The size distribution of all the MIP NPs was determined using NTA at room temperature; the average hydrodynamic particle sizes obtained for the imprinted MIP NPs are as follows; (EGFR 135 ± 1 nm, HER2 Linear 130 ± 4 nm, HER2 conformational 140 ± 7 nm, HA5 185 ± 32 nm) (Figure 12). The various peptide templates are within a similar size range, suggesting that the peptides used to imprint the MIP NPs did not significantly influence the size (p-value = 0.430).

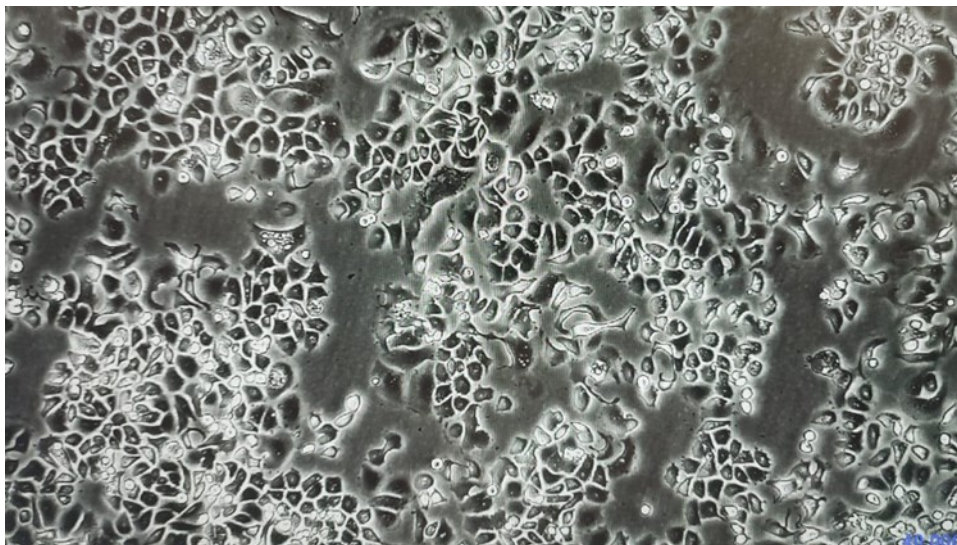*Binding affinity of MIP NPs to MDA-MB-468 and SK-BR-3 cancer cells*

Fig.19 Exemplificative Micrograph at the optical microscope, showing SK-BR-3 cells at 80% confluence**.**

The binding affinities presented demonstrate the percentage of bound fluorescent MIP NPs with increasing concentrations to SK-BR-3 (Fig.19) and MDA-MB-468 cancer cells, measured using a spectrofluorometer.
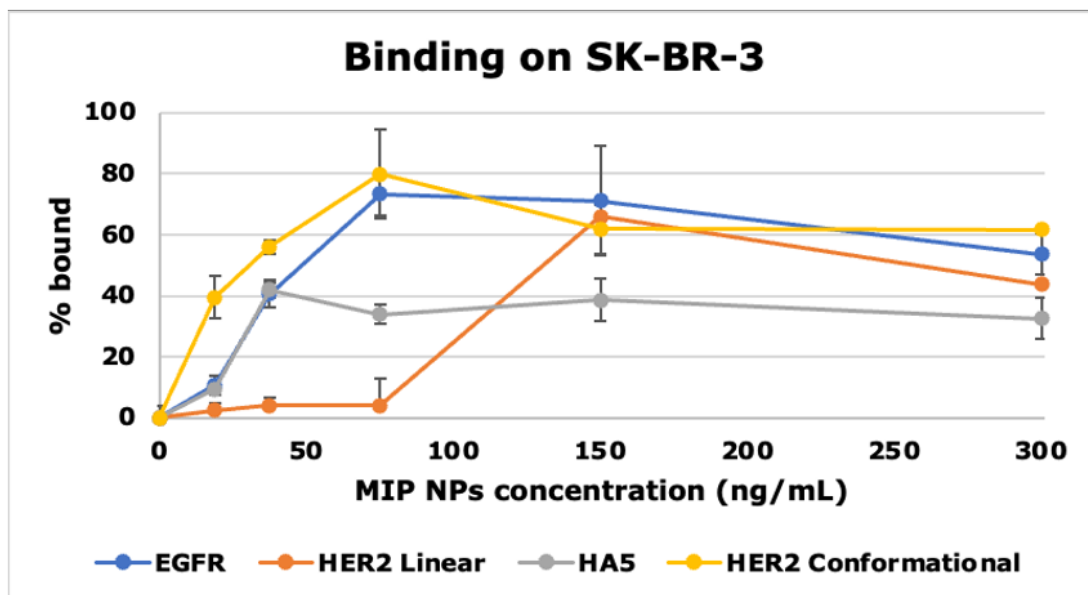
Binding on SK-BR-3

Fig.20 Binding curves of increasing concentrations of bound MIP NPs (EGFR, HER2 linear, HER2 conformational and HA5) SK-BR-3 cancer cells (over-expression of HER2) expressed as a percentage.

Concerning SK-BR-3 cancer cells, as the concentration of HER2 conformational MIP NPs increases, a rapid increase can be seen in the number of MIP NPs bound, with 80% bound at 37.5 ng/mL, in comparison to MDA-MB-468 cancer cells where they were bound the least out of all tested MIP NPs (Fig.18). Furthermore, amongst the highest concentration of MIP NPs in SK-BR-3 cells (300 ng/mL), HER2 conformational MIP NPs have the highest amount bound (~60%) in comparison to other MIP NPs such as the control group (~30%). HER2 linear MIP NPs bound more highly at higher concentrations (150 ng/mL) however, they still do not bind as strongly as the conformational epitope of the same protein. EGFR MIP NPs bound similarly to HER2 conformational MIP NPs with a similar binding profile even at higher concentrations. On the other hand, the amount of HA5 bound increased as the concentration increased, reaching a peak of approximately 40% bound at 37.5 ng/mL before reaching a plateau of around 30-40% bound at higher concentrations (Fig.20.

Binding on MDA-MB-468

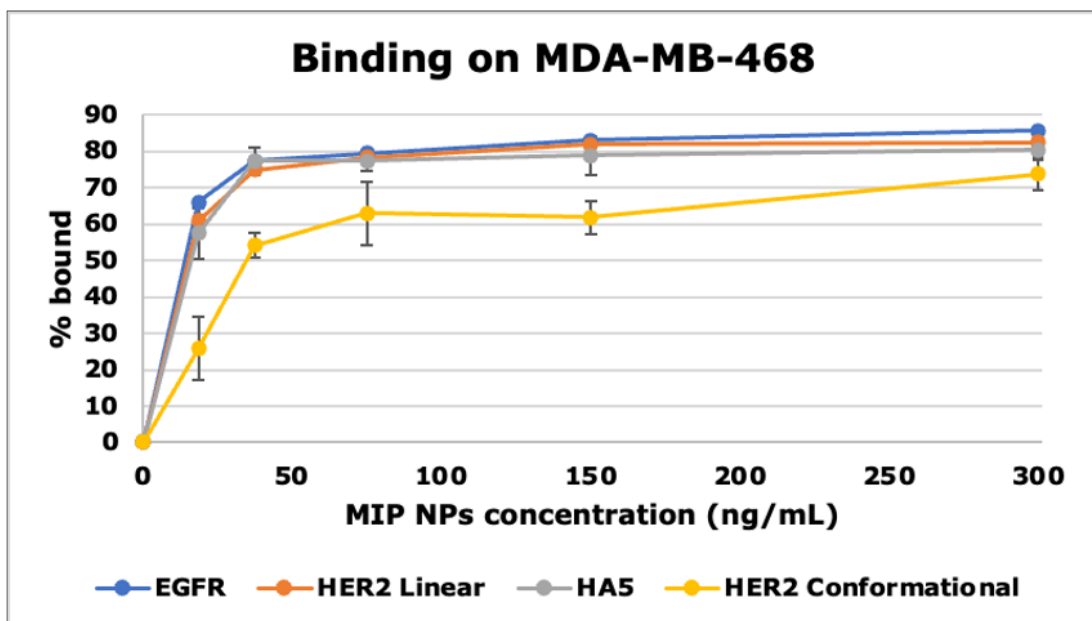**Fig.21** Binding curves of increasing concentrations of bound MIP NPs (EGFR, HER2 linear, HER2 conformational and HA5) MDA-MB-468 cancer cells (over-expression of HER2) expressed as a percentage.

On the MDA-MB-468 cancer cell lines concentration-dependent binding can be seen whereby the increase in MIP NP concentration is proportional to the amount bound to the BC cells before plateauing at 75 ng/mL (Fig.21). EGFR MIP NPs are the most

highly bound at the highest concentration of 300 ng/mL (80%). At the lowest concentration of MIP NPs (18.75 ng/mL), EGFR MIP NPs were also the highest bound at 70%. The lowest bound at both lower and high concentrations are the HER2 conformational and HA5 (control) MIP NPs which suggests that they do not have as high an affinity towards cancer cells overexpressing EGFR. The HER2 linear MIP NPs appear to bind as strongly as the EGFR MIP NPs with similar binding affinity.

Discussion

The COVID-19 pandemic has been a sudden and urgent global issue for which the healthcare system and governments were not ready. Researchers from all fields quickly started working on different aspects of this vast emergency. Being both a clinician and an anatomist, I could address whether SARS-CoV-2 was effectively present and infectious in the oral cavity, from different points of view. Thus, I could participate in different studies which evolved with the changes happening during the pandemic.

The rationale of the present thesis project was to investigate the presence and the action of the virus in the oral cavity in tissues and fluids, in order to use the salivary sample for a non-invasive diagnostic sample applicable also in the screening and surveillance field and finally starting to use new technologies such as the nanomaterials for possible regenerative application.

One of the first studies, started in 2020, was performed on cadavers aiming at detecting the viral RNA in the lingual tissues and analysing the characteristics of lingual tissues in COVID-19+ samples compared to negative ones.

This study highlighted the traceability of the virus RNA in the lingual tissue even after death. In fact, previous studies reported the presence of SARS-CoV-2 RNA in alive subjects from FFPE lingual and gland tissues, but at the time the literature was lacking concerning lingual tissues formalin-fixed sampled from cadavers. Six COVID-19+ subjects resulted positive to Real-Time RT-PCR investigation, while two resulted negative. One of the two negative samples belonged to subject ID1, who died after traumatic injuries and whose tongue was not analysed macroscopically because of the un-preserved morphology. The COVID-19 diagnosis was revealed during routine hospital tests, but according to the clinical file, the subject had no symptoms. This could suggest that subject ID1 could have been asymptomatic and that the virus might not harbour the oral tissues since the very early phases of the disease. The penetration capacity of the virus inside the tissues in asymptomatic subjects or in the early stages of the disease is very controversial [128], despite SARS-CoV-2 has been detected in the saliva in the early stages of the disease [11,108,109]. Also ID3 resulted negative to Real-Time RT-PCR investigation. However, ID3 resulted positive for IgG anti-

77

SARS-CoV-2 test and any clinical information did not support this datum. The VPs of the subject were characterised by a very thin layer of epithelial cells, absent in some portions of the papilla (Fig.7 E,F and 8A), with an infiltrate of fibroblastic-like cells, signs that could suggest chronic damage of the papillae, evidently in a case of previous infection of the subject.

The microscopic observation showed a high degree of inflammation and destruction of TB in COVID-19+ subjects. In fact, SARS-CoV-2 was reported to compromise the infected cells with extensive vacuolisation and apoptosis, in an ex vivo study on airway epithelium[129]. In the same way, gustatory cells could be damaged. TB damage can cause taste impairment with a variable recovery time. One of the most common symptoms in the chronic manifestations of COVID-19, the "Long Covid" is dysgeusia. Boscolo-Rizzo et al. (2023) described in a prospective study performed on 403 respondents that 66,3% of participants reported impairment of taste and smell, and 21% of those still reported the same problem after 3 years[130]. Yao et al. (2023), biopsied 16 patients after 6 weeks from positive NPS, and after 6-month finding persistence of SARS-CoV-2 in taste papillae, especially in the epithelial layer (basal and suprabasal) and lamina propria, also evidencing disruption of neurites in the lamina propria and misshapen taste buds in fungiform papillae [122]. However, according to Okada et al. (2021), 90% of the patients regain taste function within 4-15 days, a time-lapse compatible with the life span of gustatory sensory cells (15-20 days) [131,132].

As confirmed by other authors, ACE2 expression was observed in the nuclei and cytoplasm of the stratum granulosum of the lingual tissues[32,133]. However, the present study showed a lower ACE2 detection in COVID-19+ subjects compared to the negative ones. Many studies indeed confirmed the downregulation of ACE2 induced by SARS-CoV-2 [134]. ACE2 is a type-I transmembrane protein expressed in many tissues. Its function as a negative regulator of the renin-angiotensin system catalysing the hydrolysis of angiotensin II into Angiotensin (1-7), a peptide reducing lung inflammation, fibrosis, and pulmonary arterial hypertension. Therefore, ACE2 plays a protective role in preventing tissue injuries, and before the pandemic, the downregulation of ACE2 showed pulmonary oedema, acute respiratory distress

syndrome and tissue damage to other organs[135]. Lu et al. (2022) reported downregulation of ACE2 due to SARS-CoV-2 infection as well[136].

Concerning IFN ɤ, the signalling of this antimicrobial cytokine is reported to be increased in COVID-19 disease, locally and systemically and also plays a crucial role in the response to infection also in TB[137]. Wang et al. (2007) reported a TB damage induced by IFNs due to bacterial and viral infection in a study in mice.

Taste impairment is known to be related to viral/bacterial infection or inflammatory conditions since dysgeusia seems to be associated with an infection-induced inflammation that because of the cytokine pathways can affect the taste receptors [138].

Regarding Factor VIII, our study did not highlight any difference between positive and negative samples. Thrombo-inflammation and hypercoagulability have been documented as the primary cause of morbidity and mortality in SARS-CoV-2 infection. The virus, in fact, has a direct and indirect effect on platelets and endothelium, promoting inflammation and coagulopathy, which provoke thrombi and emboli formation and haemorrhagic events. In a study by Wichmann et al. (2020), it was observed that massive pulmonary embolisms originating from deep vein thrombosis in the lower extremities were the direct cause of death in four out of twelve COVID-19-positive autopsies [139]. Increased levels of prothrombotic molecules, which are typically increased during inflammatory responses, have been documented in COVID-19 patients [140]. In our study, factor VIII distribution within lingual tissues exhibited a similar pattern in both COVID-19-positive and COVID-19-negative samples.

Other researchers have examined factor VIII presence in lung tissues from COVID-19+ and COVID-19- cadavers and have observed an increased expression of Factor VIII in the COVID-19+ samples [50]. Nonetheless, pulmonary endothelium is known to produce factor VIII locally, representing an extrahepatic site for its synthesis. it is an extrahepatic site of its production, which might explain the difference between these results[141,142].

Among the limitations of the present study are the small sample size and the limited clinical knowledge about the subjects examined.

Among taste receptors, TAS2R38, one of the bitter receptors, has been evidenced to be abundantly expressed in the respiratory tract and to be able to respond to quorum-sensing molecules produced by pathogens, stimulating a biocidal activity and a reduction in viral replication, inhibiting SARS-CoV. Akerstrom, et al. reported that nitric oxide produced by TAS2R38 reduces the initial viral replication, inhibiting the spike protein. A retrospective, cross-sectional study evidenced on 100 adults that all the 21 requiring hospitalisations were non-tasters (AVI/AVI) while the others were classified as tasters (PAV/AVI) and supertasters (PAV/PAV)[119]. Our study performed in 2021 on 54 individuals categorised in Mild COVID-19 (MC), Severe COVID-19 (SC) and healthy COVID-19 close contacts (H) [143], evidenced that all the samples carried out the most common sequences of alleles, coding for PAV and AVI amino acids. No significant differences between the groups were evidenced concerning the role of TAS2R38 genotypes in the severity of COVID-19 infection. Including only Caucasian individuals in the sample could help narrow down haplotype heterogeneity, since only the two most common haplotypes have been found. However, our analysis confirmed the relationship between TAS2R38 diplotypes and PROP perception. Concerning, the COVID-19 gravity related to the phenotype taster/non taster our study excluded an association. However, those results are applicable to healthy individuals and not under pharmacological treatment.

In parallel to the first study, in 2020, our research group, in collaboration with the Microbiology Division, ASST Santi Paolo e Carlo, Milano (Italy) tested the reliability of Molecular Salivary Test compared with Naso Pharyngeal Swab[108]. The results showed a concordance of 0.85 in symptomatic adults. Those who were not concordant, having a positive NPS and negative MST, two subjects already developed IgG antibodies against the virus. Among the differing results in the paediatric sample, in one case, the saliva tested negative vs NPS positive and in 6 cases, MTS was positive vs NPS negative. In two cases, saliva resulted in positive two days before NPS, suggesting the oropharynx as the first site to be colonised. A limitation of MST is related to the fact that in the presence of sputum, RT-PCR can be altered. However, Yokota et al. (2021) support the use of MST as a more sensitive tool for contact-tracing,

since is more effective in discovering asymptomatic cases. However, MST can overcome some NPS limitations being a test self-performable but still maintains all the limitation of a laboratory test, needing facilities and specialized figures to be dedicated and requiring at least 24 hours for the results[144]. Thus, in emergency cases is preferable the use of tools such as the rapid antigenic test to screen huge numbers of people and maintaining low economic cost. MST seems to be specifically suitable for small communities needed to be controlled through a careful monitoring, such as school [109].

The present thesis followed subsequently the application of MST as a surveillance tool, first only on children of two primary schools (November 2020) and, one year later, after the mandatory vaccine, (April 2021) surveilling a school staff also evaluating their immunological profile. In particular, we focused our attention on school setting being one of the most fragile communities at the time, needing to non-invasive and friendly test to maintain the school open. These studies confirmed that MST can be a well-tolerated, precise, simple, cheap and useful tool for the diagnosis of infection in children and for active school monitoring. The first surveillance period, started in November 2020, corresponded to one of the peaks periods of COVID-19 waves and indeed we could detect the virus in the samples of five asymptomatic children (Fig.20),
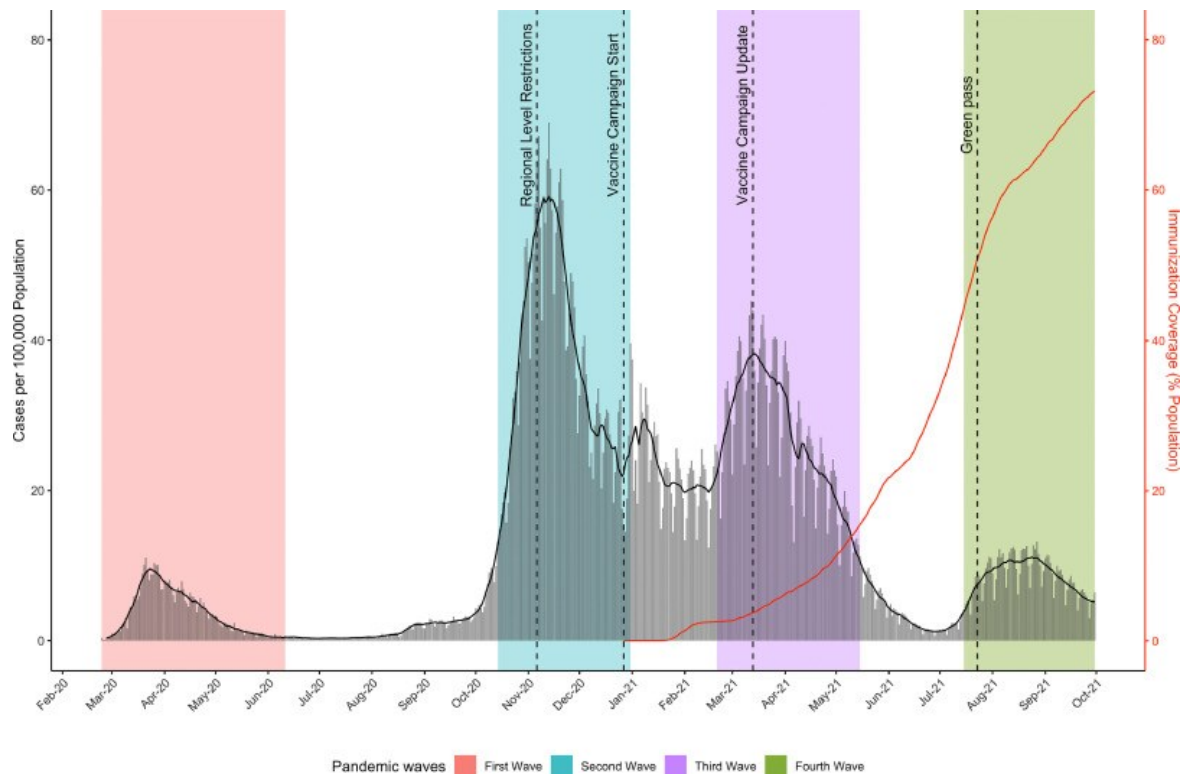
promptly and quickly quarantining their classes before the infection could spread, proving the ability of MST to detect SARS-CoV-2 even in cases with low viral load.

Fig.20 Graphic representation of the infection cases in Italy during COVID-19 waves compared to health policies: blue) Regional Level Restriction violet) vaccine campaign green) green pass. [145].

The second study set from April 2021 to June 2022 had the different aim to follow the immunological profile of a school personnel group after vaccination, employing MST as an active infection control in case of abnormalities in the antibody titre. MST in those cases could prove if the abnormality is due to active infection. In the first phase, surveillance occurred weekly between the first and second vaccine doses to quickly identify positive COVID-19 cases, as full immunity was expected after the second dose. In the second phase, the intervals between time points were extended to monitor participants' antibody responses throughout the school year, with assessments at 1, 4, 7, and 13 months after the second dose. This scheduling was partly determined by logistical requirements, as there was limited robust evidence on antibody response dynamics before the study, and current literature still lacks consensus on the ideal time frame for assessing antibody levels post-vaccination.

In this work, serologic test results revealed that 75% of subjects tested positive for SARS-CoV-2 antibodies one month after their first vaccine dose, and 100% tested positive one month after their second dose. Three months after the second dose, there was a slight decline in antibody response, but at six months, an increase was observed, likely due to some participant receiving a third vaccine dose. The booster dose significantly boosted the immune system, with none of the triple-immunized subjects showing an antibody decline. These findings are consistent with a study by Firinu et al. (2022) showing higher anti-SARS-CoV-2 IgG levels after a heterologous booster dose[146].

A quantitative ELISA test was conducted on 33 subjects, confirming the overall trend of antibody response observed through semiquantitative analysis. However, the limited sample size and lack of data at all time points prevented a comprehensive assessment of the antibody curve. Notably, the absence of samples before the initial vaccine dose made it impossible to evaluate the vaccine's direct impact on the antibody response.

Furthermore, an ELISA test targeting IgG against the NCP of SARS-CoV-2 showed that only two subjects contracted SARS-CoV-2 during the study period. It is possible that these infections occurred before the collection of samples and were asymptomatic. Amjadi et al. (2021) suggests that IgGs against the N protein peak approximately three weeks after the onset of symptoms or infection. These findings highlight the importance of periodic surveillance in identifying active COVID-19 cases, as it can be more reliable than self-reported infections[146].

All MSTs (molecular swab tests) conducted at various time points in the study yielded negative results, possibly reflecting the overall decrease in new COVID-19 cases and hospitalisations in Italy between April and September 2021.

This second surveillance program, presented positive aspects, as already mentioned [147,148]. Patient self-collection of samples is both convenient and readily accepted, reducing the need for direct interactions between healthcare providers and patients, thereby minimising the risk of infection among healthcare personnel involved in testing. Molecular tests conducted using a salivary swab exhibit a sensitivity level comparable to nasopharyngeal swabs [149,150]. Dried blood spot (DBS) testing has proven effective in simplifying the logistics of serological testing, including sample collection, transportation, and storage, with an impressive 96% overall concordance with quantitative tests [90] Some limitations were the low adhesion and compliance of participants. When planning surveillance programs, attention should be paid to making the target population aware of the importance to adhere in community studies and instructions should be provided regularly. Moreover, the study's design and the schedule for collecting samples were impacted by dynamic elements tied to the emergency, including the emergence of novel variants, the introduction of various treatments and vaccines, and the implementation of stay-at-home measures. These variables could potentially be foreseen and managed in a comparable future scenario when devising a research plan.

As a matter of fact, such studies helped in understanding some aspects that could be useful in case of a future emergency. In future, should a new pandemic occur, it might be useful to be cautious about the closure of some settings, especially schools. Developing reliable and friendly procedures, and instruments to screen the population, like the ones described in the present study, could be useful to limit restrictions with their dramatic, numerous and various consequences.

As oral healthcare workers, we confirmed that the oral cavity acts as a reservoir for viruses, including SARS-CoV-2. The dental care procedures dealing with body fluids and aerosol-generating have always been considered exposure-prone. Oral healthcare workers, indeed, are used to practising using PPE and adopting infection control measures, also before COVID-19[151] . Carmagnola et al. (2022), in a retrospective analysis of the Italian board of Physicians and Dentists database, evidenced that both categories were similarly affected by COVID-19 [152]. However, the number of deaths among GPs was threefold higher than among dentists, suggesting that dentists had a greater ability to use PPE. However, even after the resolution of the emergency, some of the measures adopted during the pandemic in order to maintain a safe dental practice for patients and operators have been maintained by many professionals.

Nanomaterials were revealed to be promising materials in the field of regenerative medicine. Concerning nanofibers, our research group evaluated the biological response of Human gingival fibroblasts to these polyblend materials. NF exhibit a texture similar to the native Extra Cellular Matrix (ECM) and can be loaded to stimulate resident cells. In this part of the project, NF were loaded with Vitamin E (VitE) and Hyaluronic Acid (HA), in order to characterise the effect on ECM deposition and turnover. Several studies proposed the use of nanofibers to regenerate [125,153] different tissues [154,155] however, only few preliminary published articles are available in oral fields [156,157].

NFE showed a stable fibrillar structure organised in mesh, similar to ECM. However, adding VitE and HA increased the fiber's diameter and reduced its

mechanical properties. Gunn et al. (2010) suggested that these characteristics should promote cell guidance during adhesion and proliferation, water-binding increasing volume in situ and the reserve of substances able to influence the quality of ECM [158]. The cellular response was assessed evaluating proliferation, adhesion and collagen turnover pathways. SEM observation revealed a different behaviour of HGF in contact with NF and NFE. NF seemed to promote cell motility wile NFE the cellular interconnection. Collagen I (COL-1) is the main component of gingival ECM and HGF finely control its synthesis, maturation and degradation. A nonsynchronous regulation of COL-1 gene and protein expression was shown on NFc. NFEc evidenced both COL-1 gene and protein levels decreased, compared to NF and CT. However, the analysis of LH2b, key element in the collagen maturation, showed to be increased in NFEc, suggesting that NFE seem able to stimulate COL-1 maturation, by cross linking to improve its stability and favouring its deposition.

Concerning the analysis of COL-1 degradation, MMP-1 responsible for the interstitial collagen breakdown and TIMP-1 the inhibitor of MMP-1, were analysed. MMP-1 was downregulated in NFEc and normally expressed in CT and NF, indicating that NFE are likely able to decrease COL-1 degradation, strengthened by downregulation of TIMP-1. The mechanosensors expression (PAX, VCN and YAP) showed PAX and VCN expressed at a lower extent in NFEc, suggesting that HA could be able to reduce the mechanoresponsivity of HGF, resulting similarly regulated in NFc and CT. To explain this effect, we can hypothesize that HA interaction with its CD44 receptor could likely modulate fibroblast adhesion to the substrate, thus influencing fibroblast behavior [159].

Considered as a whole, these preliminary in vitro findings suggest that PCL-enriched nanofibers (NFE) could represent a device to enhance HGF proliferation and biosynthetic phenotype, likely favouring collagen deposition in the gingival connective tissue. However, further experiments are needed to confirm these results and the mechanism responsible of NFE biological activity

on a higher number of samples, in order to understand if NFE could represent the basis to build a new biomaterial for oral soft tissue regeneration.

Regarding nanoparticle production with therapeutical aims, MIP NPs showed to be a versatile material concerning its targeting and its handling. MIP NPs were produced with different epitopes targeting human breast cancer cells and the Binding Affinity experiment evidenced their ability to bind the proper target. This experiment opened new possibilities for the conjugation of MIP NPs as a therapeutic tool for the non-invasive regeneration of injured tissues after SARS-CoV-2 infection. Despite the pandemic emergency seems to be solved at the moment, the long-term effect of the virus can still be evident. Long COVID or Post-COVID Conditions are known as long-term effects of COVID-19 experienced by about 65 million people, affecting people of all ages, including children. Long COVID is known to be a multisystemic condition characterised often by severe symptoms following a mild or severe SARS-CoV-2 infection. Long-COVID includes cardiovascular, thrombotic and cerebrovascular disease, type 2 diabetes, myalgic encephalomyelitis, chronic fatigue syndrome and postural orthostatic tachycardia syndrome [123]. Among the neurological complications, brain fog, memory deficits, headache, ageusia, anosmia, anxiety and depression can last several months[160]. Akanchise et al. (2023) proposed the Nanomedicine based on nanoparticles carrying antioxidant and neuroprotective agents as a potential strategy for the neurological recovery [160]. Moon et al. (2012) explored the application of nanoparticles in responses to malaria antigen for the humoral response modulation[161]. Skwarek et al. (2023) proposed nanoparticles for the immunomodulation in SARS-CoV-2 infection, in those cases of frequent infection, with a immunostimulant effect [162]. To conclude, nanomaterials are promising and innovative strategies for targeted non-invasive therapy, being specifically directed against cellular markers and possessing drug-realising properties. Further studies will continue

to investigate their applicability in also different field, such as the prevention, therapy and regeneration.

Conclusions

The present project confirmed that the Oral cavity may act as a reservoir for SARS-CoV-2, being lingual and salivary samples positive for viral detection. The presence of SARS-CoV-2 in saliva allowed us to optimise the Molecular Salivary Test for diagnostic and surveillance purposes. The morphological analysis of lingual tissues showed inflammation and disruption of taste buds in COVID-19 positive subjects, allowing us to hypothesise that dysgeusia could be due to a local inflammatory mechanism. Among taste receptors, bitter taste receptor TAS2R38 was revealed to not correlate with the severity of COVID-19 symptoms in a phenotypic and genetic analysis.

Nanofibers and nanoparticles were shown to be promising materials in the field of regeneration for their mechanical, chemical, and morphological features and concerning their properties as drug delivery and targetable systems.

These findings opened many new fields of investigation, such as the characterisation of the long-term consequences of COVID-19, known as Long-COVID and the strategies to manage it, including tissue regeneration. Some of these topics are currently under investigation. However, taking advantage of previous studies and the past pandemic is crucial to prepare guidelines and strategies to deal promptly with future emergencies.

References

International outbreak of novel SARS-CoV-2 coronavirus infection. [cited 16 Oct 2023]. Available: https://www.epicentro.iss.it/en/coronavirus/sars-cov-2-international-outbreak

2   Ke R, Sanche S, Romero-Severson E, Hengartner N. Fast spread of COVID-19 in Europe and the US suggests the necessity of early, strong and comprehensive interventions. medRxiv. 2020 [cited 16 Oct 2023]. Medline:32511619 doi:10.1101/2020.04.04.20050427

3   Sanche S, Lin YT, Xu C, Romero-Severson E, Hengartner N, Ke R. High Contagiousness and Rapid Spread of Severe Acute Respiratory Syndrome Coronavirus 2 - Volume 26, Number 7—July 2020 - Emerging Infectious Diseases journal - CDC. Emerg Infect Dis. 2020;26:1470–7. Medline:32255761 doi:10.3201/EID2607.200282

4   Gatto M, Bertuzzo E, Mari L, Miccoli S, Carraro L, Casagrandi R, et al. Spread and dynamics of the COVID-19 epidemic in Italy: Effects of emergency containment measures. Proc Natl Acad Sci U S A. 2020;117:10484–91. Medline:32327608 doi:10.1073/PNAS.2004978117/SUPPL_FILE/PNAS.2004978117.SM02.GIF

5   Amendola A, Bianchi S, Gori M, Colzani D, Canuti M, Borghi E, et al. Evidence of SARS-CoV-2 RNA in an Oropharyngeal Swab Specimen, Milan, Italy, Early December 2019. Emerg Infect Dis. 2021;27:648–50. Medline:33292923 doi:10.3201/EID2702.204632

6   Remuzzi A, Remuzzi G. COVID-19 and Italy: what next? Lancet. 2020;395:1225–8. Medline:32178769 doi:10.1016/S0140-6736(20)30627-9

7   Onder G, Rezza G, Brusaferro S. Case-Fatality Rate and Characteristics of Patients Dying in Relation to COVID-19 in Italy. JAMA. 2020;323:1775–6. Medline:32203977 doi:10.1001/JAMA.2020.4683

8   COVID-19 Strategy update. [cited 16 Oct 2023]. Available: https://www.who.int/publications/m/item/covid-19-strategy-update

9   Isolation, quarantine and close contacts: what they are and what you should do - ISS (EN) - ISS. [cited 19 Oct 2023]. Available: https://www.iss.it/web/iss-en/at-home-isolation-quarantine-and-close-contacts/-/asset_publisher/dIL47HGZFgWh/content/isolation-quarantine-and-close-contacts-what-they-are-and-what-you-should-do

10   Bchetnia M, Girard C, Duchaine C, Laprise C. The outbreak of the novel severe acute respiratory syndrome coronavirus 2 (SARS-CoV-2): A review of the current global status. J Infect Public Health. 2020;13:1601–10. Medline:32778421 doi:10.1016/J.JIPH.2020.07.011

11   Carmagnola D, Henin D, Pellegrini G, Canciani E, Perrotta M, Sangiorgio A, et al. Diagnostic testing for sars-cov-2: State of the art and perspectives of molecular salivary testing. Dent Cadmos. 2021;89:264–76. doi:10.19256/D.CADMOS.04.2021.05

12 Trova Norme & Concorsi - Normativa Sanitaria. [cited 16 Oct 2023]. Available: https://www.trovanorme.salute.gov.it/norme/dettaglioAtto?id=86394.%20Accessed:%2022%20March%202023

13 O'Connor DB, Aggleton JP, Chakrabarti B, Cooper CL, Creswell C, Dunsmuir S, et al. Research priorities for the COVID-19 pandemic and beyond: A call to action for psychological science. Br J Psychol. 2020;111:603–29. Medline:32683689 doi:10.1111/BJOP.12468

14 Infografica web - Dati della Sorveglianza integrata COVID-19 in Italia. [cited 16 Oct 2023]. Available: https://www.epicentro.iss.it/coronavirus/sars-cov-2-dashboard

15 Viner RM, Russell SJ, Croker H, Packer J, Ward J, Stansfield C, et al. School closure and management practices during coronavirus outbreaks including COVID-19: a rapid systematic review. Lancet Child Adolesc Health. 2020;4:397–404. Medline:32272089 doi:10.1016/S2352-4642(20)30095-X

16 M M, AM N, S B, S B, M R, R M, et al. [The impact of COVID-19 pandemic on children and adolescents. The contribution of epidemiology for a safe reopening of schools in Italy]. Epidemiol Prev. 2021;45:239–44. Medline:34549565 doi:10.19191/EP21.4.P239.079

17 Kuiken T, Fouchier RAM, Schutten M, Rimmelzwaan GF, Van Amerongen G, Van Riel D, et al. Newly discovered coronavirus as the primary cause of severe acute respiratory syndrome. The Lancet. 2003;362:263–70. Medline:12892955 doi:10.1016/S0140-6736(03)13967-0

18 Beyerstedt S, Barbosa Casaro E, Bevilaqua Rangel É. COVID-19: angiotensin-converting enzyme 2 (ACE2) expression and tissue susceptibility to SARS-CoV-2 infection. [cited 16 Oct 2023]. doi:10.1007/s10096-020-04138-6/Published

19 Murray E, Tomaszewski M, Guzik TJ. Binding of SARS-CoV-2 and angiotensin-converting enzyme 2: clinical implications. Cardiovasc Res. 2020;116:E87–9. Medline:32301968 doi:10.1093/CVR/CVAA096

20 Wrapp D, Wang N, Corbett KS, Goldsmith JA, Hsieh C-L, Abiona O, et al. Cryo-EM Structure of the 2019-nCoV Spike in the Prefusion Conformation. bioRxiv. 2020 [cited 19 Oct 2023]. Medline:32511295 doi:10.1101/2020.02.11.944462

21 Glowacka I, Bertram S, Herzog P, Pfefferle S, Steffen I, Muench MO, et al. Differential downregulation of ACE2 by the spike proteins of severe acute respiratory syndrome coronavirus and human coronavirus NL63. J Virol. 2010;84:1198–205. Medline:19864379 doi:10.1128/JVI.01248-09

22 Vaduganathan M, Vardeny O, Michel T, McMurray JJV, Pfeffer MA, Solomon SD. Renin-Angiotensin-Aldosterone System Inhibitors in Patients with Covid-19. N Engl J Med. 2020;382:1653–9. Medline:32227760 doi:10.1056/NEJMSR2005760

23 Tikellis C, Bernardi S, Burns WC. Angiotensin-converting enzyme 2 is a key modulator of the renin-angiotensin system in cardiovascular and renal disease. Curr Opin Nephrol Hypertens. 2011;20:62–8. Medline:21099686 doi:10.1097/MNH.0B013E328341164A

24   Chen J, Jiang Q, Xia X, Liu K, Yu Z, Tao W, et al. Individual variation of the SARS-CoV-2 receptor ACE2 gene expression and regulation. Aging Cell. 2020;19. Medline:32558150 doi:10.1111/ACEL.13168

25   Xu H, Zhong L, Deng J, Peng J, Dan H, Zeng X, et al. High expression of ACE2 receptor of 2019-nCoV on the epithelial cells of oral mucosa. International Journal of Oral Science 2020 12:1. 2020;12:1–5. Medline:32094336 doi:10.1038/s41368-020-0074-x

26   Su H, Yang M, Wan C, Yi LX, Tang F, Zhu HY, et al. Renal histopathological analysis of 26 postmortem findings of patients with COVID-19 in China. Kidney Int. 2020;98:219–27. Medline:32327202 doi:10.1016/J.KINT.2020.04.003

27   Liu F, Long X, Zou W, Fang M, Wu W, Li W, et al. Highly ACE2 Expression in Pancreas May Cause Pancreas Damage After SARS-CoV-2 Infection. medRxiv. 2020;2020.02.28.20029181. doi:10.1101/2020.02.28.20029181

28   Qi F, Qian S, Zhang S, Zhang Z. Single cell RNA sequencing of 13 human tissues identify cell types and receptors of human coronaviruses. Biochem Biophys Res Commun. 2020;526:135–40. Medline:32199615 doi:10.1016/J.BBRC.2020.03.044

29   Li M, Chen L, Zhang J, Xiong C, Li X. The SARS-CoV-2 receptor ACE2 expression of maternal-fetal interface and fetal organs by single-cell transcriptome study. PLoS One. 2020;15:e0230295. Medline:32298273 doi:10.1371/JOURNAL.PONE.0230295

30   Zou X, Chen K, Zou J, Han P, Hao J, Han Z. Single-cell RNA-seq data analysis on the receptor ACE2 expression reveals the potential risk of different human organs vulnerable to 2019-nCoV infection. Front Med. 2020;14:185–92. Medline:32170560 doi:10.1007/S11684-020-0754-0

31   Qi F, Qian S, Zhang S, Zhang Z. Single cell RNA sequencing of 13 human tissues identify cell types and receptors of human coronaviruses. Biochem Biophys Res Commun. 2020;526:135–40. Medline:32199615 doi:10.1016/J.BBRC.2020.03.044

32   Sawa Y, Ibaragi S, Okui T, Yamashita J, Ikebe T, Harada H. Expression of SARS-CoV-2 entry factors in human oral tissue. J Anat. 2021;238:1341–54. Medline:33421967 doi:10.1111/JOA.13391

33   SARS-CoV-2 variants of concern as of 06 October 2023. [cited 17 Oct 2023]. Available: https://www.ecdc.europa.eu/en/covid-19/variants-concern

34   O'Toole Á, Pybus OG, Abram ME, Kelly EJ, Rambaut A. Pango lineage designation and assignment using SARS-CoV-2 spike gene nucleotide sequences. BMC Genomics. 2022;23. Medline:35148677 doi:10.1186/s12864-022-08358-2

35   SARS-CoV-2 variants of concern as of 9 March 2023.

36   Emerging Variants of SARS-CoV-2 And Novel Therapeutics Against Coronavirus (COVID-19).

37   Perico N, Cortinovis M, Suter F, Remuzzi G. Home as the new frontier for the treatment of COVID-19: the case for anti-inflammatory agents. Lancet Infect Dis. 2022. doi:10.1016/s1473-3099(22)00433-9

38   Watson OJ, Barnsley G, Toor J, Hogan AB, Winskill P, Ghani AC. Global impact of the first year of COVID-19 vaccination: a mathematical modelling study. Lancet Infect Dis. 2022;22:1293–302. Medline:35753318 doi:10.1016/S1473-3099(22)00320-6

39   Wang MY, Zhao R, Gao LJ, Gao XF, Wang DP, Cao JM. SARS-CoV-2: Structure, Biology, and Structure-Based Therapeutics Development. Front Cell Infect Microbiol. 2020;10:587269. Medline:33324574 doi:10.3389/FCIMB.2020.587269/BIBTEX

40   Chan JFW, Yuan S, Kok KH, To KKW, Chu H, Yang J, et al. A familial cluster of pneumonia associated with the 2019 novel coronavirus indicating person-to-person transmission: a study of a family cluster. The Lancet. 2020;395:514–23. Medline:31986261 doi:10.1016/S0140-6736(20)30154-9

41   Meselson M. Droplets and Aerosols in the Transmission of SARS-CoV-2. New England Journal of Medicine. 2020;382:2063–2063. Medline:32294374 doi:10.1056/NEJMC2009324/SUPPL_FILE/NEJMC2009324_DISCLOSURES.PDF

42   Morawska L, Cao J. Airborne transmission of SARS-CoV-2: The world should face the reality. Environ Int. 2020;139. Medline:32294574 doi:10.1016/J.ENVINT.2020.105730

43   Sommerstein R, Fux CA, Vuichard-Gysin D, Abbas M, Marschall J, Balmelli C, et al. Risk of SARS-CoV-2 transmission by aerosols, the rational use of masks, and protection of healthcare workers from COVID-19. Antimicrob Resist Infect Control. 2020;9:1–8. Medline:32631450 doi:10.1186/S13756-020-00763-0/TABLES/3

44   Tang S, Mao Y, Jones RM, Tan Q, Ji JS, Li N, et al. Aerosol transmission of SARS-CoV-2? Evidence, prevention and control. Environ Int. 2020;144. Medline:32822927 doi:10.1016/J.ENVINT.2020.106039

45   van Doremalen N, Bushmaker T, Morris DH, Holbrook MG, Gamble A, Williamson BN, et al. Aerosol and Surface Stability of SARS-CoV-2 as Compared with SARS-CoV-1. New England Journal of Medicine. 2020;382:1564–7. Medline:32182409 doi:10.1056/NEJMC2004973/SUPPL_FILE/NEJMC2004973_DISCLOSURES.PDF

46   Zhang R, Li Y, Zhang AL, Wang Y, Molina MJ. Identifying airborne transmission as the dominant route for the spread of COVID-19. Proc Natl Acad Sci U S A. 2020;117:14857–63. Medline:32527856 doi:10.1073/PNAS.2009637117

47   Coronavirus disease (COVID-19): How is it transmitted? [cited 17 Oct 2023]. Available: https://www.who.int/news-room/questions-and-answers/item/coronavirus-disease-covid-19-how-is-it-transmitted

48   Yang S, Lee GWM, Chen CM, Wu CC, Yu KP. The size and concentration of droplets generated by coughing in human subjects. J Aerosol Med. 2007;20:484–94. Medline:18158720 doi:10.1089/JAM.2007.0610

49   Asadi S, Bouvier N, Wexler AS, Ristenpart WD. The coronavirus pandemic and aerosols: Does COVID-19 transmit via expiratory particles? Aerosol Science and Technology. 2020;54:635–8. doi:10.1080/02786826.2020.1749229

50   Riley EC, Murphy G, Riley RL. Airborne spread of measles in a suburban elementary school. Am J Epidemiol. 1978;107:421–32. Medline:665658 doi:10.1093/OXFORDJOURNALS.AJE.A112560

51   da Rosa Mesquita R, Francelino Silva Junior LC, Santos Santana FM, Farias de Oliveira T, Campos Alcântara R, Monteiro Arnozo G, et al. Clinical manifestations of COVID-19 in the general population: systematic review. Wien Klin Wochenschr. 2021;133:377. Medline:33242148 doi:10.1007/S00508-020-01760-4

52   Guan W, Ni Z, Hu Y, Liang W, Ou C, He J, et al. Clinical Characteristics of Coronavirus Disease 2019 in China. New England Journal of Medicine. 2020;382:1708–20. Medline:32109013 doi:10.1056/NEJMOA2002032/SUPPL_FILE/NEJMOA2002032_DISCLOSURES.PDF

53   Coronavirus disease (COVID-19). [cited 17 Oct 2023]. Available: https://www.who.int/news-room/fact-sheets/detail/coronavirus-disease-(covid-19)

54   Mason RJ. Pathogenesis of COVID-19 from a cell biology perspective. Eur Respir J. 2020;55. Medline:32269085 doi:10.1183/13993003.00607-2020

55   Wise J. Covid-19: Symptomatic infection with omicron variant is milder and shorter than with delta, study reports. [cited 23 Oct 2023]. doi:10.1016/S0140-6736(22)00327-0

56   Meyerowitz EA, Richterman A, Bogoch II, Low N, Cevik M. Towards an accurate and systematic characterisation of persistently asymptomatic infection with SARS-CoV-2. Lancet Infect Dis. 2021;21:e163–9. Medline:33301725 doi:10.1016/S1473-3099(20)30837-9

57   Stone LM, Tan SS, Tam PPL, Finger TE. Analysis of Cell Lineage Relationships in Taste Buds. Journal of Neuroscience. 2002;22. doi:10.1523/jneurosci.22-11-04522.2002

58   Suzuki T. Cellular mechanisms in taste buds. The Bulletin of Tokyo Dental College. 2007. doi:10.2209/tdcpublication.48.151

59   Okada Y, Yoshimura K, Toya S, Tsuchimochi M. Pathogenesis of taste impairment and salivary dysfunction in COVID-19 patients. Japanese Dental Science Review. 2021. doi:10.1016/j.jdsr.2021.07.001

60   Arey LB, Tremaine MJ, Monzingo FL. The numerical and topographical relations of taste buds to human circumv allate papillae throughout the life span. Anat Rec. 1935;64:9–25. doi:10.1002/ar.1090640103

61   Ghannam MG, Singh P. Anatomy, Head and Neck, Salivary Glands. StatPearls. 2023 [cited 20 Oct 2023]. Medline:30855909

62   MANDEL ID. Salivary Diagnosis: Promises, Promises. Ann N Y Acad Sci. 1993;694:1–10. Medline:8215047 doi:10.1111/J.1749-6632.1993.TB18336.X

63   Cui Y, Yang M, Zhu J, Zhang H, Duan Z, Wang S, et al. Developments in diagnostic applications of saliva in human organ diseases. Med Nov Technol Devices. 2022;13:100115. doi:10.1016/J.MEDNTD.2022.100115

64   Huang N, Pérez P, Kato T, Mikami Y, Okuda K, Gilmore RC, et al. SARS-CoV-2 infection of the oral cavity and saliva. Nat Med. [cited 17 Oct 2023]. doi:10.1038/s41591-021-01296-8

65 Marchesan JT, Warner BM, Byrd KM. The "oral" history of COVID-19: Primary infection, salivary transmission, and post-acute implications. J Periodontol. 2021;92:1357–67. Medline:34390597 doi:10.1002/JPER.21-0277

66 Offenbacher S, Salvi GE. Induction of Prostaglandin Release from Macrophages by Bacterial Endotoxin. Clinical Infectious Diseases. 1999;28:505–13. Medline:10194068 doi:10.1086/515177

67 Hawkes CH, Lang GA. Smell and taste disorders. GMS Curr Top Otorhinolaryngol Head Neck Surg. 2011;10:1–418. Medline:22558054 doi:10.3205/CTO000077

68 Mutiawati E, Fahriani M, Mamada SS, Fajar JK, Frediansyah A, Maliga HA, et al. Anosmia and dysgeusia in SARS-CoV-2 infection: incidence and effects on COVID-19 severity and mortality, and the possible pathobiology mechanisms - a systematic review and meta-analysis. F1000Research 2021 10:40. 2021;10:40. Medline:33824716 doi:10.12688/f1000research.28393.1

69 Generoso JS, de Quevedo JLB, Cattani M, Lodetti BF, Sousa L, Collodel A, et al. Neurobiology of COVID-19: how can the virus affect the brain? Braz J Psychiatry. 2021;43:650–64. Medline:33605367 doi:10.1590/1516-4446-2020-1488

70 Baig AM, Khaleeq A, Ali U, Syeda H. Evidence of the COVID-19 Virus Targeting the CNS: Tissue Distribution, Host-Virus Interaction, and Proposed Neurotropic Mechanisms. ACS Chem Neurosci. 2020;11:995–8. Medline:32167747 doi:10.1021/ACSCHEMNEURO.0C00122

71 Elmakaty I, Ferih K, Karen O, Ouda A, Elsabagh A, Amarah A, et al. Clinical Implications of COVID-19 Presence in CSF: Systematic Review of Case Reports. Cells. 2022;11. Medline:36291083 doi:10.3390/CELLS11203212

72 Mehraeen E, Behnezhad F, Salehi MA, Noori T, Harandi H, SeyedAlinaghi SA. Olfactory and gustatory dysfunctions due to the coronavirus disease (COVID-19): a review of current evidence. Eur Arch Otorhinolaryngol. 2021;278:307–12. Medline:32556781 doi:10.1007/S00405-020-06120-6

73 Wang C, Wu H, Ding X, Ji H, Jiao P, Song H, et al. Does infection of 2019 novel coronavirus cause acute and/or chronic sialadenitis? Med Hypotheses. 2020;140. Medline:32361098 doi:10.1016/J.MEHY.2020.109789

74 Chen L, Zhao J, Peng J, Li X, Deng X, Geng Z, et al. Detection of SARS-CoV-2 in saliva and characterization of oral symptoms in COVID-19 patients. Cell Prolif. 2020;53. Medline:33073910 doi:10.1111/CPR.12923

75 Biadsee A, Biadsee A, Kassem F, Dagan O, Masarwa S, Ormianer Z. Olfactory and Oral Manifestations of COVID-19: Sex-Related Symptoms-A Potential Pathway to Early Diagnosis. Otolaryngol Head Neck Surg. 2020;163:722–8. Medline:32539587 doi:10.1177/0194599820934380

76 Eghbali Zarch R, Hosseinzadeh P. COVID-19 from the perspective of dentists: A case report and brief review of more than 170 cases. Dermatol Ther. 2021;34. Medline:33368888 doi:10.1111/DTH.14717

77 Lechien JR, Chiesa-Estomba CM, De Siati DR, Horoi M, Le Bon SD, Rodriguez A, et al. Olfactory and gustatory dysfunctions as a clinical presentation of mild-to-moderate

forms of the coronavirus disease (COVID-19): a multicenter European study. Eur Arch Otorhinolaryngol. 2020;277:2251–61. Medline:32253535 doi:10.1007/S00405-020-05965-1

78   Capaccio P, Pignataro L, Corbellino M, Popescu-Dutruit S, Torretta S. Acute Parotitis: A Possible Precocious Clinical Manifestation of SARS-CoV-2 Infection? Otolaryngol Head Neck Surg. 2020;163:182–3. Medline:32369434 doi:10.1177/0194599820926992

79   Fisher A, Roberts A, Mckinlay AR, Fancourt D, Burton A. The impact of the COVID-19 pandemic on mental health and well-being of people living with a long-term physical health condition: a qualitative study. [cited 19 Oct 2023]. doi:10.1186/s12889-021-11751-3

80   Iranmanesh B, Khalili M, Amiri R, Zartab H, Aflatoonian M. Oral manifestations of COVID-19 disease: A review article. Dermatol Ther. 2021;34:e14578. Medline:33236823 doi:10.1111/DTH.14578

81   Cruz Tapia RO, Peraza Labrador AJ, Guimaraes DM, Matos Valdez LH. Oral mucosal lesions in patients with SARS-CoV-2 infection. Report of four cases. Are they a true sign of COVID-19 disease? Special Care in Dentistry. 2020;40:555–60. Medline:32882068 doi:10.1111/SCD.12520

82   Trevethan R. Sensitivity, Specificity, and Predictive Values: Foundations, Pliabilities, and Pitfalls in Research and Practice. Front Public Health. 2017;5. Medline:29209603 doi:10.3389/FPUBH.2017.00307

83   Testing strategies for SARS-CoV-2. [cited 19 Oct 2023]. Available: https://www.ecdc.europa.eu/en/covid-19/surveillance/testing-strategies

84   Jayamohan H, Lambert CJ, Sant HJ, Jafek A, Patel D, Feng H, et al. SARS-CoV-2 pandemic: a review of molecular diagnostic tools including sample collection and commercial response with associated advantages and limitations. Anal Bioanal Chem. 2021;413:49–71. Medline:33073312 doi:10.1007/S00216-020-02958-1

85   COVID-19 Testing: What You Need to Know | CDC. [cited 23 Oct 2023]. Available: https://www.cdc.gov/coronavirus/2019-ncov/symptoms-testing/testing.html

86   Kucirka LM, Lauer SA, Laeyendecker O, Boon D, Lessler J. Variation in False-Negative Rate of Reverse Transcriptase Polymerase Chain Reaction-Based SARS-CoV-2 Tests by Time Since Exposure. Ann Intern Med. 2020;173:262–8. Medline:32422057 doi:10.7326/M20-1495

87   Vogels CBF, Watkins AE, Harden CA, Brackney DE, Shafer J, Wang J, et al. SalivaDirect: A simplified and flexible platform to enhance SARS-CoV-2 testing capacity. medRxiv. 2020;2020.08.03.20167791. doi:10.1101/2020.08.03.20167791

88   At-Home COVID-19 Antigen Tests-Take Steps to Reduce Your Risk of False Negative Results: FDA Safety Communication | FDA. [cited 23 Oct 2023]. Available: https://www.fda.gov/medical-devices/safety-communications/home-covid-19-antigen-tests-take-steps-reduce-your-risk-false-negative-results-fda-safety

89   Antigen-detection in the diagnosis of SARS-CoV-2 infection. [cited 17 Oct 2023]. Available: https://www.who.int/publications/i/item/antigen-detection-in-the-diagnosis-of-sars-cov-2infection-using-rapid-immunoassays

90   Amendola A, Bianchi S, Gori M, Barcellini L, Colzani D, Canuti M, et al. Back to school: use of Dried Blood Spot for the detection of SARS-CoV-2-specific immunoglobulin G (IgG) among schoolchildren in Milan, Italy. medRxiv. 2020;2020.07.29.20164186. doi:10.1101/2020.07.29.20164186

91   Morley GL, Taylor S, Jossi S, Perez-Toledo M, Faustini SE, Marcial-Juarez E, et al. Sensitive Detection of SARS-CoV-2–Specific Antibodies in Dried Blood Spot Samples. Emerg Infect Dis. 2020;26:2970. Medline:32969788 doi:10.3201/EID2612.203309

92   I vaccini anti COVID-19. [cited 21 Mar 2023]. Available: https://www.epicentro.iss.it/vaccini/covid-19

93   Overview of COVID-19 Vaccines | CDC. [cited 20 Oct 2023]. Available: https://www.cdc.gov/coronavirus/2019-ncov/vaccines/different-vaccines/overview-COVID-19-vaccines.html

94   Monforte AD, Tavelli A, De Benedittis S, Bai F, Tincati C, Gazzola L, et al. Real World Estimate of Vaccination Protection in Individuals Hospitalized for COVID-19. Vaccines (Basel). 2022;10:550. doi:10.3390/VACCINES10040550/S1

95   Maestri G, Boemo RL, Soares L do A, de Souza AAU, Immich APS. Development of drug reservoirs based on nanofibers and capsules for epistaxis treatment. J Drug Deliv Sci Technol. 2020;55:101398. doi:10.1016/J.JDDST.2019.101398

96   Jiffrin R, Razak SIA, Jamaludin MI, Hamzah ASA, Mazian MA, Jaya MAT, et al. Electrospun Nanofiber Composites for Drug Delivery: A Review on Current Progresses. Polymers 2022, Vol 14, Page 3725. 2022;14:3725. doi:10.3390/POLYM14183725

97   Quirós J, Borges JP, Boltes K, Rodea-Palomares I, Rosal R. Antimicrobial electrospun silver-, copper- and zinc-doped polyvinylpyrrolidone nanofibers. J Hazard Mater. 2015;299:298–305. Medline:26142159 doi:10.1016/J.JHAZMAT.2015.06.028

98   Stojanov S, Berlec A. Electrospun Nanofibers as Carriers of Microorganisms, Stem Cells, Proteins, and Nucleic Acids in Therapeutic and Other Applications. Front Bioeng Biotechnol. 2020;8. Medline:32158751 doi:10.3389/FBIOE.2020.00130

99   Liu R, Poma A. Advances in Molecularly Imprinted Polymers as Drug Delivery Systems. Molecules 2021, Vol 26, Page 3589. 2021;26:3589. Medline:34208380 doi:10.3390/MOLECULES26123589

100   Haupt K, Rangel PXM, Tse B, Bui S. Molecularly Imprinted Polymers: Antibody Mimics for Bioimaging and Therapy. 2020 [cited 20 Oct 2023]. doi:10.1021/acs.chemrev.0c00428

101   Lala NL, Ramaseshan R, Bojun L, Sundarrajan S, Barhate RS, Liu YJ, et al. Fabrication of nanofibers with antimicrobial functionality used as filters: protection against bacterial contaminants. Biotechnol Bioeng. 2007;97:1357–65. Medline:17274060 doi:10.1002/BIT.21351

102 Muniz NO, Gabut S, Maton M, Odou P, Vialette M, Pinon A, et al. Electrospun Filtering Membrane Designed as Component of Self-Decontaminating Protective Masks. Nanomaterials. 2023;13. doi:10.3390/NANO13010009/S1

103 Jackman JA, Yoon BK, Ouyang L, Wang N, Ferhan AR, Kim J, et al. Biomimetic Nanomaterial Strategies for Virus Targeting: Antiviral Therapies and Vaccines. Adv Funct Mater. 2021;31:2008352. doi:10.1002/ADFM.202008352

104 Sigl C, Willner EM, Engelen W, Kretzmann JA, Sachenbacher K, Liedl A, et al. Programmable icosahedral shell system for virus trapping. Nature Materials 2021 20:9. 2021;20:1281–9. Medline:34127822 doi:10.1038/s41563-021-01020-4

105 Zhang Q, Honko A, Zhou J, Gong H, Downs SN, Vasquez JH, et al. Cellular Nanosponges Inhibit SARS-CoV-2 Infectivity. Nano Lett. 2020;20:5570–4. Medline:32551679 doi:10.1021/ACS.NANOLETT.0C02278/ASSET/IMAGES/LARGE/NL0C02278_0003.JPEG

106 Parisi OI, Dattilo M, Patitucci F, Malivindi R, Delbue S, Ferrante P, et al. Design and development of plastic antibodies against SARS-CoV-2 RBD based on molecularly imprinted polymers that inhibit in vitro virus infection. Nanoscale. 2021;13:16885–99. Medline:34528987 doi:10.1039/D1NR03727G

107 2019-novel coronavirus (2019-nCoV) real-time rRT-PCR panel primers and probes. 2020. Available: https://stacks.cdc.gov/view/cdc/84525

108 Borghi E, Massa V, Carmagnola D, Dellavia C, Parodi C, Ottaviano E, et al. Saliva sampling for chasing SARS-CoV-2: A Game-changing strategy. Pharmacological Research. 2021. doi:10.1016/j.phrs.2020.105380

109 Carmagnola D, Pellegrini G, Canciani E, Henin D, Perrotta M, Forlanini F, et al. Saliva molecular testing for sars-cov-2 surveillance in two italian primary schools. Children. 2021;8. doi:10.3390/children8070544

110 CDC 2019-Novel Coronavirus (2019-nCoV) Real-Time RT-PCR Diagnostic Panel For Emergency Use Only Instructions for Use.

111 Henin D, Pellegrini G, Carmagnola D, Lanza Attisano GC, Lopez G, Ferrero S, et al. Morphological and Immunopathological Aspects of Lingual Tissues in COVID-19. Cells. 2022;11. Medline:35406811 doi:10.3390/CELLS11071248

112 Tizzano M, Gulbransen BD, Vandenbeuch A, Clapp TR, Herman JP, Sibhatu HM, et al. Nasal chemosensory cells use bitter taste signaling to detect irritants and bacterial signals. Proc Natl Acad Sci U S A. 2010;107:3210–5. Medline:20133764 doi:10.1073/PNAS.0911934107

113 Lee RJ, Cohen NA. Taste receptors in innate immunity. Cell Mol Life Sci. 2015;72:217–36. Medline:25323130 doi:10.1007/S00018-014-1736-7

114 Lee RJ, Xiong G, Kofonow JM, Chen B, Lysenko A, Jiang P, et al. T2R38 taste receptor polymorphisms underlie susceptibility to upper respiratory infection. J Clin Invest. 2012;122:4145–59. Medline:23041624 doi:10.1172/JCI64240

115   Viswanathan VK. Sensing bacteria, without bitterness? Gut Microbes. 2013;4:91–3. Medline:23380647 doi:10.4161/GMIC.23776

116   Åkerström S, Gunalan V, Keng CT, Tan YJ, Mirazimi A. Dual effect of nitric oxide on SARS-CoV replication: viral RNA production and palmitoylation of the S protein are affected.   Virology.   2009;395:1–9.   Medline:19800091 doi:10.1016/J.VIROL.2009.09.007

117   Åkerström S, Mousavi-Jazi M, Klingström J, Leijon M, Lundkvist Å, Mirazimi A. Nitric oxide inhibits the replication cycle of severe acute respiratory syndrome coronavirus. J Virol. 2005;79:1966–9. Medline:15650225 doi:10.1128/JVI.79.3.1966-1969.2005

118   Risso DS, Mezzavilla M, Pagani L, Robino A, Morini G, Tofanelli S, et al. Global diversity in the TAS2R38 bitter taste receptor: revisiting a classic evolutionary PROPosal. Sci Rep. 2016;6. Medline:27138342 doi:10.1038/SREP25506

119   Barham HP, Taha MA, Hall CA. Does phenotypic expression of bitter taste receptor T2R38 show association with COVID-19 severity? Int Forum Allergy Rhinol. 2020;10:1255–7. Medline:32856411 doi:10.1002/ALR.22692

120   Barham HP, Taha MA, Broyles ST, Stevenson MM, Zito BA, Hall CA. Association Between Bitter Taste Receptor Phenotype and Clinical Outcomes Among Patients With COVID-19.   JAMA   Netw   Open.   2021;4.   Medline:34032852 doi:10.1001/JAMANETWORKOPEN.2021.11410

121   Risso D, Carmagnola D, Morini G, Pellegrini G, Canciani E, Antinucci M, et al. Distribution of TAS2R38 bitter taste receptor phenotype and haplotypes among COVID-19 patients. Sci Rep. 2022;12. Medline:35513681 doi:10.1038/S41598-022-10747-2

122   Yao Q, Doyle E, Liu Q-R, Appleton A, O'connell JF, Weng N-P, et al. Long-Term Dysfunction of Taste Papillae in SARS-CoV-2. 2023. doi:10.1056/EVIDoa2300046

123   Davis HE, McCorkell L, Vogel JM, Topol EJ. Long COVID: major findings, mechanisms and recommendations. Nature Reviews Microbiology 2023 21:3. 2023;21:133–46. Medline:36639608 doi:10.1038/s41579-022-00846-2

124   Canciani E, Sirello R, Pellegrini G, Henin D, Perrotta M, Toma M, et al. Effects of vitamin and amino acid-enriched hyaluronic acid gel on the healing of oral mucosa: In vivo   and   in   vitro   study.   Medicina   (Lithuania).   2021;57. doi:10.3390/medicina57030285

125   Amler E, Filová E, Buzgo M, Prosecká E, Rampichová M, Nečas A, et al. Functionalized nanofibers as drug-delivery systems for osteochondral regeneration. Nanomedicine (Lond). 2014;9:1083–94. Medline:24978465 doi:10.2217/NNM.14.57

126   Canciani E, Gagliano N, Paino F, Amler E, Divin R, Denti L, et al. Polyblend Nanofibers to Regenerate Gingival Tissue: A Preliminary In Vitro Study. Front Mater. 2021;8:670010. doi:10.3389/FMATS.2021.670010/BIBTEX

127   Canfarotta F, Lezina L, Guerreiro A, Czulak J, Petukhov A, Daks A, et al. Specific Drug Delivery to Cancer Cells with Double-Imprinted Nanoparticles against Epidermal

Growth Factor Receptor. Nano Lett. 2018;18:4641–6. Medline:29969563 doi:10.1021/ACS.NANOLETT.7B03206

128　Bradley BT, Maioli H, Johnston R, Chaudhry I, Fink SL, Xu H, et al. Histopathology and ultrastructural findings of fatal COVID-19 infections in Washington State: a case series. The Lancet. 2020;396. doi:10.1016/S0140-6736(20)31305-2

129　Borczuk AC, Salvatore SP, Seshan S V., Patel SS, Bussel JB, Mostyka M, et al. COVID-19 pulmonary pathology: a multi-institutional autopsy cohort from Italy and New York City. Mod Pathol. 2020;33:2156–68. Medline:32879413 doi:10.1038/S41379-020-00661-1

130　Boscolo-Rizzo P, Spinato G, Hopkins C, Marzolino R, Cavicchia A, Zucchini S, et al. Evaluating long-term smell or taste dysfunction in mildly symptomatic COVID-19 patients: a 3-year follow-up study. Eur Arch Otorhinolaryngol. 2023 [cited 20 Oct 2023]. Medline:37715807 doi:10.1007/S00405-023-08227-Y

131　Breslin PAS, Huang L. Human Taste: Peripheral Anatomy, Taste Transduction, and Coding Human Taste. Adv Otorhinolaryngol Basel, Karger. 2006.

132　Okada Y, Yoshimura K, Toya S, Tsuchimochi M. Pathogenesis of taste impairment and salivary dysfunction in COVID-19 patients. Japanese Dental Science Review. 2021;57:111–22. doi:10.1016/J.JDSR.2021.07.001

133　Sakaguchi W, Kubota N, Shimizu T, Saruta J, Fuchida S, Kawata A, et al. Existence of SARS-CoV-2 entry molecules in the oral cavity. Int J Mol Sci. 2020;21:1–16. Medline:32825469 doi:10.3390/ijms21176000

134　Haga S, Yamamoto N, Nakai-Murakami C, Osawa Y, Tokunaga K, Sata T, et al. Modulation of TNF-α-converting enzyme by the spike protein of SARS-CoV and ACE2 induces TNF-α production and facilitates viral entry. Proc Natl Acad Sci U S A. 2008;105. doi:10.1073/pnas.0711241105

135　Santos RAS, Sampaio WO, Alzamora AC, Motta-Santos D, Alenina N, Bader M, et al. The ACE2/Angiotensin-(1-7)/MAS Axis of the Renin-Angiotensin System: Focus on Angiotensin-(1-7). Physiol Rev. 2018;98:505–53. Medline:29351514 doi:10.1152/PHYSREV.00023.2016

136　Lu Y, Zhu Q, Fox DM, Gao C, Stanley SA, Luo K. SARS-CoV-2 down-regulates ACE2 through lysosomal degradation. Mol Biol Cell. 2022;33. Medline:36287912 doi:10.1091/MBC.E22-02-0045/ASSET/IMAGES/LARGE/MBC-33-AR147-G007.JPEG

137　Kuba K, Imai Y, Rao S, Gao H, Guo F, Guan B, et al. A crucial role of angiotensin converting enzyme 2 (ACE2) in SARS coronavirus-induced lung injury. Nat Med. 2005;11. doi:10.1038/nm1267

138　Wang H, Zhou M, Brand J, Huang L. Inflammation activates the interferon signaling pathways in taste bud cells. Journal of Neuroscience. 2007;27:10703–13. Medline:17913904 doi:10.1523/JNEUROSCI.3102-07.2007

139　Wichmann D, Sperhake JP, Lütgehetmann M, Steurer S, Edler C, Heinemann A, et al. Autopsy Findings and Venous Thromboembolism in Patients With COVID-19: A

Prospective Cohort Study. Ann Intern Med. 2020;173:268–77. Medline:32374815 doi:10.7326/M20-2003

140 Rapkiewicz A V., Mai X, Carsons SE, Pittaluga S, Kleiner DE, Berger JS, et al. Megakaryocytes and platelet-fibrin thrombi characterize multi-organ thrombosis at autopsy in COVID-19: A case series. EClinicalMedicine. 2020;24. doi:10.1016/j.eclinm.2020.100434

141 Jacquemin M, Neyrinck A, Hermanns MI, Lavend'homme R, Rega F, Saint-Remy JM, et al. FVIII production by human lung microvascular endothelial cells. Blood. 2006;108. doi:10.1182/blood-2005-11-4571

142 Gu SX, Tyagi T, Jain K, Gu VW, Lee SH, Hwa JM, et al. Thrombocytopathy and endotheliopathy: crucial contributors to COVID-19 thromboinflammation. Nature Reviews Cardiology. 2021. doi:10.1038/s41569-020-00469-1

143 COVID-19 Treatment Guidelines. [cited 20 Oct 2023]. Available: https://www.covid19treatmentguidelines.nih.gov/

144 Yokota I, Shane PY, Okada K, Unoki Y, Yang Y, Inao T, et al. Mass Screening of Asymptomatic Persons for Severe Acute Respiratory Syndrome Coronavirus 2 Using Saliva. Clin Infect Dis. 2021;73:E559–65. Medline:32976596 doi:10.1093/CID/CIAA1388

145 Reno C, Sanmarchi F, Stoto MA, Fantini MP, Lenzi J, Golinelli D. The impact of health policies and vaccine rollout on the COVID-19 pandemic waves in Italy. Health Policy Technol. 2022;11:100604. doi:10.1016/J.HLPT.2022.100604

146 Amjadi MF, O'Connell SE, Armbrust T, Mergaert AM, Narpala SR, Halfmann PJ, et al. Specific COVID-19 Symptoms Correlate with High Antibody Levels against SARS-CoV-2. Immunohorizons. 2021;5:466–76. Medline:34398806 doi:10.4049/IMMUNOHORIZONS.2100022

147 Gandini S, Rainisio M, Iannuzzo ML, Bellerba F, Cecconi F, Scorrano L. A cross-sectional and prospective cohort study of the role of schools in the SARS-CoV-2 second wave in Italy. The Lancet Regional Health - Europe. 2021;5. doi:10.1016/j.lanepe.2021.100092

148 Raimondi S, Gandini S, Rubio Quintanares GH, Abecasis A, Lopalco PL, D'Ecclesiis O, et al. Correction: European Cohorts of patients and schools to Advance Response to Epidemics (EuCARE): a cluster randomised interventional and observational study protocol to investigate the relationship between schools and SARS-CoV-2 infection. BMC Infect Dis. 2023;23:96. Medline:36797690 doi:10.1186/S12879-023-08065-7

149 Johnson AJ, Zhou S, Hoops SL, Hillmann B, Schomaker M, Kincaid R, et al. Saliva Testing Is Accurate for Early-Stage and Presymptomatic COVID-19. Microbiol Spectr. 2021;9. Medline:34259552 doi:10.1128/SPECTRUM.00086-21

150 Tan SH, Allicock O, Armstrong-Hough M, Wyllie AL. Saliva as a gold-standard sample for SARS-CoV-2 detection. Lancet Respir Med. 2021;9:562–4. Medline:33887248 doi:10.1016/S2213-2600(21)00178-8

151   Patil S, Moafa IH, Bhandi S, Jafer MA, Khan SS, Khan S, et al. Dental care and personal protective measures for dentists and non-dental health care workers. Disease-a-Month. 2020;66. Medline:32741545 doi:10.1016/j.disamonth.2020.101056

152   Carmagnola D, Toma M, Henin D, Perrotta M, Pellegrini G, Dellavia C. Personal Protection Equipment and Infection Control Procedures among Health Workers during the COVID-19 Pandemic. Healthcare (Basel). 2022;10. Medline:35628080 doi:10.3390/HEALTHCARE10050944

153   Ahadian S, Finbloom JA, Mofidfar M, Diltemiz SE, Nasrollahi F, Davoodi E, et al. Micro and nanoscale technologies in oral drug delivery. Adv Drug Deliv Rev. 2020;157:37. Medline:32707147 doi:10.1016/J.ADDR.2020.07.012

154   Beznoska J, Uhlík J, Kestlerová A, Královič M, Divín R, Fedačko J, et al. PVA and PCL nanofibers are suitable for tissue covering and regeneration. Physiol Res. 2019;68:S501–8. Medline:32118482 doi:10.33549/PHYSIOLRES.934389

155   Wang M, Roy AK, Webster TJ. Development of Chitosan/Poly(Vinyl Alcohol) Electrospun Nanofibers for Infection Related Wound Healing. Front Physiol. 2017;7. Medline:28123370 doi:10.3389/FPHYS.2016.00683

156   Mohandesnezhad S, Pilehvar-Soltanahmadi Y, Alizadeh E, Goodarzi A, Davaran S, Khatamian M, et al. In vitro evaluation of Zeolite-nHA blended PCL/PLA nanofibers for dental tissue engineering. Mater Chem Phys. 2020;252:123152. doi:10.1016/J.MATCHEMPHYS.2020.123152

157   Bonilla-Represa V, Abalos-Labruzzi C, Herrera-Martinez M, Guerrero-Pérez MO. Nanomaterials in Dentistry: State of the Art and Future Challenges. Nanomaterials (Basel). 2020;10:1–27. Medline:32906829 doi:10.3390/NANO10091770

158   Gunn J, Zhang M. Polyblend nanofibers for biomedical applications: perspectives and challenges. doi:10.1016/j.tibtech.2009.12.006

159   Price RD, Myers S, Leigh IM, Navsaria HA. The Role of Hyaluronic Acid in Wound Healing. American Journal of Clinical Dermatology 2005 6:6. 2012;6:393–402. Medline:16343027 doi:10.2165/00128071-200506060-00006

160   Lautenschlager S, Gomes Daré R, Akanchise T, Angelova A. Potential of Nano-Antioxidants and Nanomedicine for Recovery from Neurological Disorders Linked to Long COVID Syndrome. Antioxidants 2023, Vol 12, Page 393. 2023;12:393. doi:10.3390/ANTIOX12020393

161   Moon JJ, Suh H, Li A V., Ockenhouse CF, Yadava A, Irvine DJ. Enhancing humoral responses to a malaria antigen with nanoparticle vaccines that expand Tfh cells and promote germinal center induction. Proc Natl Acad Sci U S A. 2012;109:1080–5. Medline:22247289 doi:10.1073/PNAS.1112648109

162   Skwarek A, Gąsecka A, Jaguszewski MJ, Szarpak Ł, Dzieciątkowski T, Filipiak KJ. Nanoparticles: a breakthrough in COVID-19 prevention, diagnosis and treatment. Archives of Medical Science. 2023;19:1410–20. doi:10.5114/AOMS/142103